محاكاة التفاعلات الكهروكيمياوية في خلايا الطلاء الكهروكيمياوي

أطروحة

مقدمة الى كلية الهندسة في جامعة بابل كجزء من متطلبات نيل
درجة ماجستير علوم في هندسة المواد

من قبل

كاظم خيون كحلول

بكالوريوس ١٩٨٦

تشرين الاول ٢٠٠٥

وما يُلقّيها إلا الّذينَ صَبَروا وَما يُلقّ

إلا ذوحَظٍ عَظِيمٍ

صدق الله العلي العظيم

فصلت الآية (٣٥)

SIMULATION OF ELECTROCHEMICAL REACTIONS IN ELECTROPLATING CELLS

A THESIS
SUBMITTED TO THE COLLEGE OF ENGINEERING OF THE UNIVERSITY OF BABYLON IN PARTIAL FULFILMENT OF THE REQUIREMENTS FOR THE DEGREE OF MASTER OF SCIENCE IN MATERIALS ENGINEERING

BY

KADHIM KUION KAHLOL
(B.SC.,١٩٨٦)

October ٢٠٠٥

"EXAMINING COMMITTEE CERTIFICATE"

We certify that we have read this thesis entitled " **Simulation of electrochemical reaction in electroplating cells "** and as an examining committee, examined the student " **Kadhim kuion kahlol "** in its contents and that in our opinion it meets the standards of a thesis of the degree of Master of Science in Materials Engineering**.**

Signature:
Name: Chief Researchers
Dr. Jaleel K.Ahmed
(chairman)
Date: / / ٢٠٠٦

Signature:
Name: Prof
Dr. Dakhil N.Taha
(Member)
Date: / / ٢٠٠٦

Signature:
Name: Lecturer
Dr. Kadhim F.AL-Sultani
(Member)
Date: / / ٢٠٠٦

Signature:
Name: Asst. Prof
Dr.Tahseen A.AL-Hattab
Date: / / ٢٠٠٦

Signature:
Name: Ass. Prof.
Dr. Haydar A.Hussain
Date: / / ٢٠٠٦

Approval of the Materials Engineering Department.
Head of the Materials Engineering Department.

Signature:
Name: Asst. Prof
Dr. Fadhil M.Hassoun
Date: / / ٢٠٠٦

Approval of the College of Engineering.
Dean of the College of Engineering.

Signature:
Name: Prof
Dr. Abd Al-Wahid k.Rajih
Date: / / ٢٠٠٦

ACKNOWLEDGMENTS

First of all thanks are due to **ALLAH** who enabled me to achieve this research work.

I wish to express my deepest gratitude and sincere thanks to my supervisors **Dr. Tahseen A.AL-Hattab** and **Dr. Haydar A.Hussain** for their guidance , invaluable recommendations and constructive comments which greatly improved the structure and presentation of the thesis.

My great appreciation is expressed to the Dean of the college of Engineering **Dr. Abd Al-Wahid K.Rajih** and to the head of the Materials Engineering department **Dr. Fadhil M. Hassoun** for the encouragements and supports.

Sincere thanks are also expressed to the staff of the Materials Engineering department and to the staff of advanced computer laboratory for the facilities they proved during my work.

I record my sincere gratituds to my family for their encouragement and support during the period of preparing this work.

Finally, I am grateful to all that have helped me in carrying out this research.

kadhim
٢٠٠٥

"CERTIFICATION"

We certify that this thesis entitled " **Simulation of electrochemical reactions in electroplating cells**" was prepared by **kadhim kuion kahlol** under our supervision at **BABYLON UNIVERSITY** in partial fulfilment of the requirements for the degree of Master of Science in Materials Engineering**.**

Signature:
Name:**Asst. prof**
Dr. Tahseen A.AL-Hattab
Date: ٥ /١٠ / ٢٠٠٥

Signature:
Name:**Ass. Prof.**
Dr. Haydar A.Hussain
Date: ٥ /١٠ / ٢٠٠٥

"CERTIFICATION"

We certify that this thesis entitled " **Simulation of electrochemical reactions in electroplating cells**" was prepared by **kadhim kuion kahlol** under our supervision at **BABYLON UNIVERSITY** in partial fulfilment of the requirements for the degree of Master of Science in Materials Engineering**.**

Signature:
Name:**Asst. prof**
Dr. Tahseen A.AL-Hattab
Date: ٥ /١٠ / ٢٠٠٥

Signature:
Name:**Ass. Prof.**
Dr. Haydar A.Hussain
Date: ٥ /١٠ / ٢٠٠٥

الخلاصة

ان الاهتمام المتزايد بالظاهرة الكهروكيمياوية اصبح واضحا ومتزايدا من خلال تواجدها اليومي في اقتصاديات الصناعه ككل والامثله على ذلك كثيرة فمنها الموجودة في البطاريات ، خلايا الوقود او المتسعات ، السيارات الكهربائيه ، الاجهزه المحمولة او الانتاج الصناعي الكيمياوي ؛ انتاج الكلور، الصودا ، الالمنيوم؛ الطلاء الكهروكيمياوي ، المكائن الكهربائية ، التنقيه بالتحليل الكهربائي ؛ والتأكل .

يعد اسلوب محاكاة الخلايا الكهروكيمياوية خلال عملية الطلاء الكهروكيمياوي من الاساليب الحديثه والجديدة في الوقت الحاضر . قد تم التطرق في هذه الدراسة الى معرفة حركيات التفاعلات الكيمياوية و الكهروكيمياوية من خلال فهم ونمذجة التفاعلات الكهروكيمياوية الاساسية و التفاعلات الكيمياوية المرافقة لها اثناء عملية الطلاء الكهروكيمياوي وتأثير الظروف المختلفه على حركية وسرعة التفاعلات .

من اجل تطبيق هذا الاسلوب تم الاعتماد على معادلات متوسط المجال الحركي ومعادلة بوزون المستعمله لنموذج شبكي مشحون ، وباستعمال نوعين من الخلايا باتجاه واحد لاغراض الجانب النظري في هذه الدراسة وهما (نصف الخليه ، والخلية الكاملة) ذات الحجم (100) تحت تاثير جهد مسلط مقداره ($2KT/e$) او عدمه . مع العرض بأن الخلية تحتوي على قطبين متماثلين سمك كل واحد منهما (10) .

ولاجل اظهار نتائج هذه الدراسة بشكلها المطلوب تم بناء برنامج حاسوبي بلغة فيجوال بيسك لحساب التراكيز وهي (الذرات المعدنية ، الايونات الموجبه ، الايونات السالبه ، المذيب ، الفراغات ، الالكترونات) ، توزيع الشحنات والجهد الكهربائي عبر المواقع . فقد استعملت طريقتين لحساب تيار الانتشار ، التي يعتمد عليها بشكل رئيسي في معادلات متوسط المجال الحركي وهي ؛ الاولى احلال الايونات بدلا من المذيب ؛ والثانيه التدرج بالجهد الكيمياوي . وفي كلتا الطريقتين فقد اظهرت النتائج خلال الفترات الزمنية الثلاثه ($t = (1,3,5)\times 10^5$) على النحو التالي:-

في حالة تسليط جهد عبر الخلية فأنه يزداد استمرارية الترسيب لفترات زمنية طويلة جدا ومن ثم يتوقف عند أنهيار قطب الأنود ، ومن الملاحظ ان الترسيب يزداد عندما تزداد مساحة توزيع الشحنات عند قطب الكاثود هذا من جهه ، ومن جهه اخرى فأن النمو

الايوني الموجب يكون على شكل قمة عند قطب الكاثود ويكون متدرج بين قطبي الانود والكاثود ، ويحصل العكس بالنسبه للنمو الايوني السالب ، وفي الوقت نفسه فأن توزيع الجهد الكهربائي عبر المواقع عندما يكون عالي يؤدي بالنتيجه الى زيادة الترسيب .

أما في الحالة الاخرى التي لم يتم تسليط جهد عبر الخلية فأن الترسيب سوف يبدأ ومن ثم يتوقف عند زمن ($t = 10^6$) ويعزى ذلك الى توقف التفاعلات الكهروكيمياوية عند هذا الزمن .

ومن خلال استعمال الطريقتين آنفة الذكر تمت المقارنه بينهما عند زمن ($t = 5\times10^5$) فوجد ان الترسيب للطريقه الاولى (بتيارالانتشار) اكثر كمية (تركيز للذرات المعدنية) لنصف الخلية من الطريقة الثانية (بتيارالانتشار) ، ويجري العكس في حالة الخلية الكامله .

كما وتم التعرف في هذه الدراسة على تأثير الظروف المختلفه على عملية الترسيب و هي (التراكيز ، فرق الجهد ، طاقة Fermi ، المسافه بين الاقطاب) عند زمن($t = 0.5\times10^5$) فوجد أن الزيادة في تراكيزالايونات الموجبه و السالبه في المحلول ، فرق الجهد عبر الاقطاب ، طاقة Fermi يؤدي بالنتيجة الى زيادة في الترسيب فيما يكون العكس عند زيادة المسافة بين الاقطاب .

ABSTRACT

The increasing interest of the electrochemical phenomenon becomes clearer due to the major contribution of which in the whole industry economics. Examples are found in batteries, fuel cells or capacitors, for electric vehicles, portable devices or industrial productions of chemicals; in the production of chlorine, caustic soda, aluminium; in electroplating, electromachining, and electrorefining; and in corrosion.

The simulation manner of electrochemical cells through the electrochemical plating is recently considered one of the most modern ones . In this study , it is acquainted with the kinetics of the chemical and electrochemical reactions by modeling and understanding of the essential and secondary (conjugate) chemical and electrochemical reactions during plating process . In addition , the effects of various conditions on the speed and kinetic of those reactions is also considered.

In order to apply this manner , the mean-field kinetic equations and poisson equation for charged lattice model are adopted using two types of one-dimensional cells for theortical part of this study , namely (half and full cell) of size (100) with and without an applied potential of ($2KT/e$) . provided that the cell should contain two identical electrodes of thickness (10) .

A computer program in visual basic is specially constructed to show the results of this study as it should be . Through this program the concentrations are determined including (metallic atoms, cations, anions, solvents, vacancies and electrons) , the charges distribution and electrical potential across the sites.

Two methods are used to determine the diffusion current , on which , the mean-field kinetic equations mainly depend .They are :-

١. Ions replacement instead of the solvent.

٢. The gradient of the chemical potential .

In both methods , during the three periods ($t = (1,3,5)\times 10^5$) , the results showed that under potential application across the cell , the deposition continues for long time then it is suppressed when the anode reaches failure limit , and it is observed that the deposition increases with the extension of space charges at the cathode , from the other hand , the ionic evolution (cation) will take a peak shape at the cathode , then it has a certain gradient between anode and cathode. A reversed situation occurs for the anions evolution . At the same time, electric potential distribution across the sites becomes higher resulting in deposition increasing .

Without potential application across the cell ,the deposition starts and then stopped at time ($t = 10^6$) due to suppression of electrochemical reactions at this time .

Comparing the two methods mentioned above at time ($t = 5\times 10^5$) , it is found that the deposition in the first method by diffusion current is larger in quantity (for the metallic atoms concentration for the half cell) than the second method. The reverse is occurred for the full cell .

It is found in this study that the deposition at ($t = 0.5\times 10^5$) is directely proportional to each of ionic concentration(cation and anion) in the electrolyte , potential difference and Fermi energy and inversely proportional to electrodes spacing.

LIST OF CONTENTS

CHAPTER THREE: THEORETICAL ANALYSIS OF MEAN-FIELD KINETIC AND POISSON EQUATIONS

CHAPTER FOUR: COMPUTER PROGRAM

CHAPTER FIVE: RESULTS AND DISCUSSIONS

CHAPTER SIX: CONCLUSIONS AND RECOMENDATIONS

CHAPTER ONE

INTRODUCTION

١.١ General

Electrochemical phenomena are ubiquitous in nature as well as in industry . Application includes for example batteries , fuel cells , catalysis processes , aluminum or magnesium electrolytic production , corrosion problems , electrodeposition and electroplating [١].

In ١٨٠٠, Volta built his first Voltaic pile. Thirty years later, Faraday established that the amount of chemical change is proportional to the quantity of electricity passed through the electrolysis. He introduced the terms cathode, anode, electrode, ion, cation, anion, and electrolyte. Later in ١٩٠١, Thomas A. Edison and Waldemar Jungner invented the first alkaline rechargeable batteries. Finally, in ١٩٧٧, Alan MacDiarmid and Alan Heeger discovered the electrical conductance of polyacetylene, leading to the construction with David MacInnes in ١٩٨١ of the first battery with no metallic constituents [٢,٣].

The above preceding can be summarized as scheme below describing the electrochemical processes[٤]:-

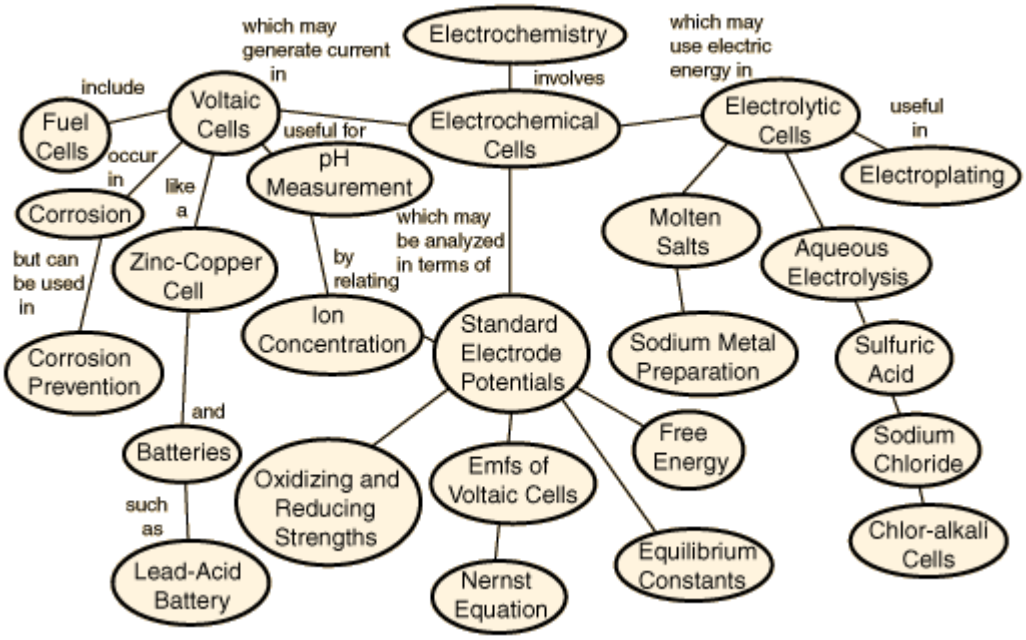

١.٢ Electric Double Layers

Whenever two pieces of material (two phases) are brought into contact a potential difference is set up between them. This occurs through a flow of charge, taking place until the potential difference, $\Delta\phi$, built up by the flow of equalizing charges compensates for the difference of the chemical potentials, $\Delta\mu_i$, of individual entities in the two phases. Then , at equilibrium:

$$\Delta\mu_i + z_i F\Delta\phi = 0 \qquad (١.١)$$

where:

F : the Faraday constant.

z_i : valency of ion .

equation(١.١) can be put in the form:

$$\Delta\tilde{\mu}_i = \Delta(\mu_i + z_i F\Delta\phi) = 0 \qquad (١.١`)$$

where:

$$\tilde{\mu}_i = \mu_i + z_i F\phi \qquad (١.٢)$$

is called the electrochemical potential of the species, i . Thus , at equilibrium:

$$(\tilde{\mu}_i)_{phase1} = (\tilde{\mu}_i)_{phase2} \qquad (١.٣)$$

for each species, i .

It is not necessary to devise specific examples of electric double layers, because wherever there is a junction between two pieces of material, involving a layer of moisture or an actual solution, there is an electrochemical double layer. Thus it is virtually impossible for the electrochemical potential of an entity in one phase to be the same as it is in another phase, before the phases are brought into contact ; and if the electrochemical potentials are not equal, a current will flow until they become equal , thus developing a potential difference[٥].

It will be helpfull if it is proceeded gradually towards a model of the double layer which is nowadays considered to agree with the experimental observations. Historically , the first model was that of Helmholtz and Perrin (figure ١.١) . It regards the double layer simply as a plane layer of charges

(excess adsorbed ions) in the solution, confronting a plane layer of charges of opposite sign on the electrode.

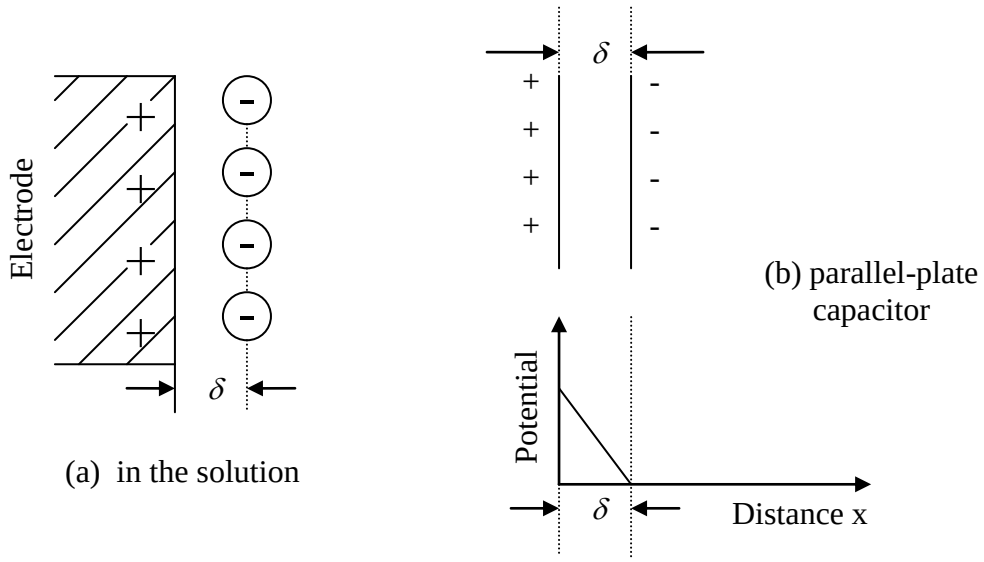

Figure (١.١) The Helmholtz model .

It was from this simple idea that the name 'double layer' developed .

Helmholtz model is much oversimplified .A strict and rigid distribution of ions on a simple plane seems unlikely . There must be thermal agitation of the ions on the solution side and they are not confined to one single sheet at ٠.٥nm or so from the metal , but distributed over a much greater distance into the bulk of the solution[٥].

This idea of the distribution of charge on the solution side was the main point of another theory, the Gouy-Chapman theory of the diffuse layer. It resembles, in respect of this distribution, the Debye-Huckel theory of the ionic atmosphere, which it preceded historically. The interplay of thermal and electrical forces near a charged electrode builds up an ionic cloud of effective thickness κ^{-1}.

$$\kappa^{-1} = 1/B\sqrt{c} = 1/[(N_A e_o^2 / 500\varepsilon_r\varepsilon_o \mathrm{KT})^{1/2}\sqrt{c}] \qquad (١.٤)$$

where:

B: the value which is dependent on the temperature and the electrolyte permittivity.

c : the bulk concentration of the ١,١-valent electrolyte in mol dm^{-3}.

N_A : the Avogadro constant=٦.٠٢٢١٤$\times$١٠^{23} mol^{-1}.

e_o : the charge of electron .

$\varepsilon_r\varepsilon_o$: permittivity{the ion relative permittivity in solvent and in vacuum respectively}.

K : Boltzmann constant=١.٣٨٠٦٥٨$\times$١٠$^{-23}$ J K^{-1} mol^{-1}.

T : temperature=٢٩٨ K .

The concentration profiles within the diffuse layer are given by the following exponential relationships:

$$c_+ = c\exp[-(e_o\psi_x/\mathrm{KT})] \qquad (١.٥)$$

$$c_- = c\exp[+(e_o\psi_x/\mathrm{KT})] \qquad (١.٥`)$$

where c_+ and c_- are the concentrations of cations and anions at a distance x from the electrode ,respectively, and ψ_x the potential at distance x from the electrode, and it is given by:

$$\psi_x = \psi_o \exp(-\kappa x) \qquad (١.٦)$$

where:

ψ_o : the potential at the electrode surface .

Figure (١.٢) shows the concentration profiles within the diffuse layer.

The principal conclusions of the Gouy-Chapman theory are summarized in figure (١.٣) .

The Gouy-Chapman theory gives an overestimate , with too much stress on distribution, which means physical (coulombic) adsorption, and not enough stress upon the sticking of the ions on to the electrode on the solution side[٥].

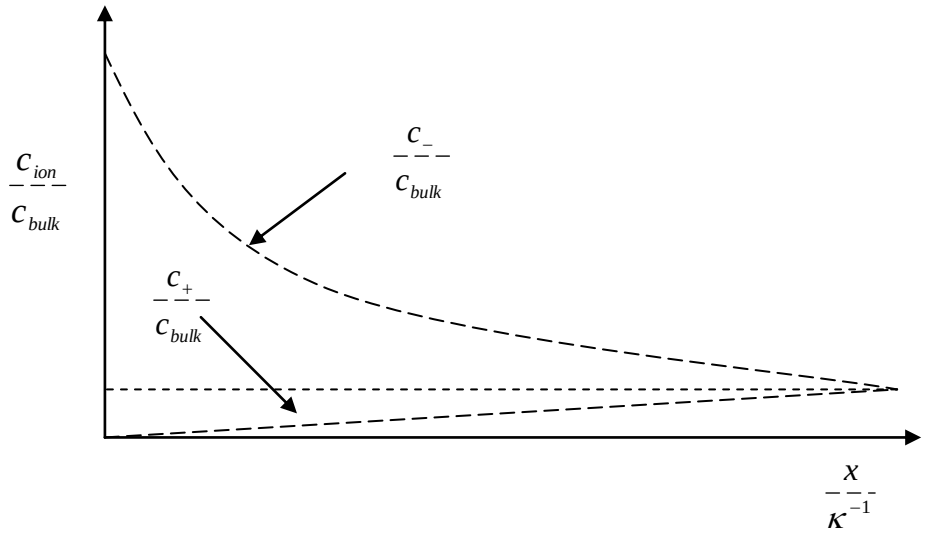

Figure (١.٢) The concentration profiles within the diffuse layer at a metal/NaF interphase.

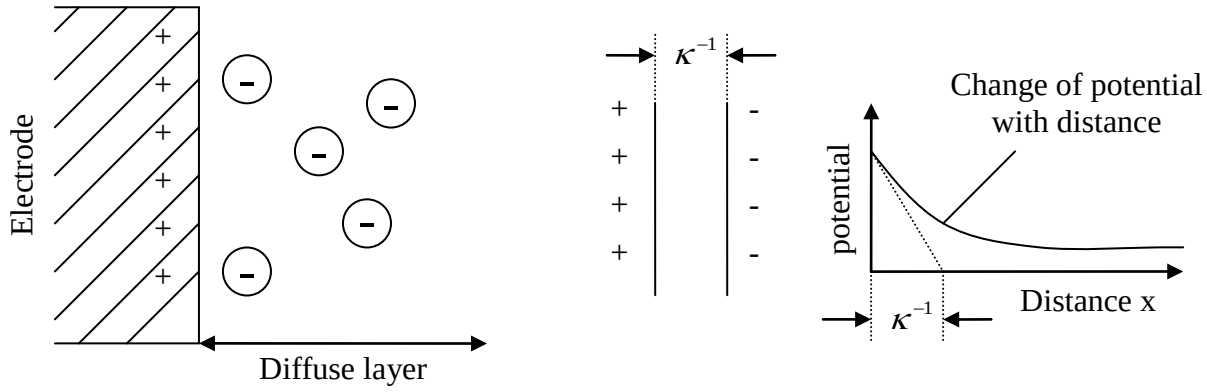

(a) in the solution

(b) parallel –plate capacitor

Figure (١.٣) The Gouy-Chapman model.

A third and better model of the situation in the double layer is that of Stern model , in which the ideas of Helmholtz and of Gouy-Chapman were combined . According to Stern, some of the charge on the solution lies in a plane called 'the plane of closest approach' , and the remainder is spread out in the solution (in Gouy-Chapman style) . The plane of closest approach of the ions to the electrode divides the solution side into two regions:a Helmholtz and Perrin region, and a Gouy-Chapman region . Each of these two regions

can be simulated by a parallel plate capacitor, and therefore the double layer is equivalent for two capacitors in series. The variation of potential with distance is linear in the first region and exponential in the second region (figure ١.٤)[٥].

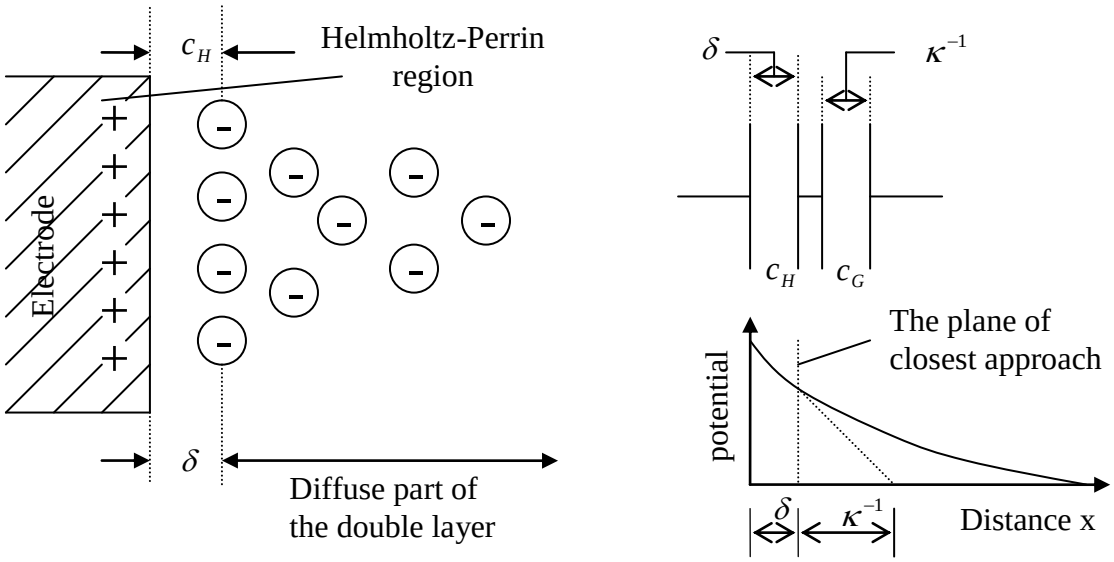

Figure (١.٤) The Stern model .

The total capacitance of the double layer is therefore given by:

$$1/\ c = 1/\ c_H + 1/\ c_G \qquad (١.٧)$$

where c_H and c_G are the capacitances of the two equivalent capacitors.

Let $\psi_{x=0}$ be the potential of the electrode with respect to that of the bulk of the solution; and consider the case when ψ_o (the potential of the Helmholtz plane) is sufficiently small. Then (equation ١.٦) the potential variation can be described by:

$$\psi = \psi_{(x=0)} \frac{x}{\delta} \quad \text{for} \quad x < \delta$$

$$\psi = \psi_o \exp[-\kappa(x-\delta)] \quad \text{for } x > \delta \qquad (١.٨)$$

The fact that water molecules in contact with the electrode will no longer have the same structure as water in the bulk of the solution , but will be oriented as dipoles on to the electrode (thus contributing to the potential

difference across it), was neglected until the ١٩٦٠'s. A scheme which takes this important factor into account is shown in figure (١.٥).

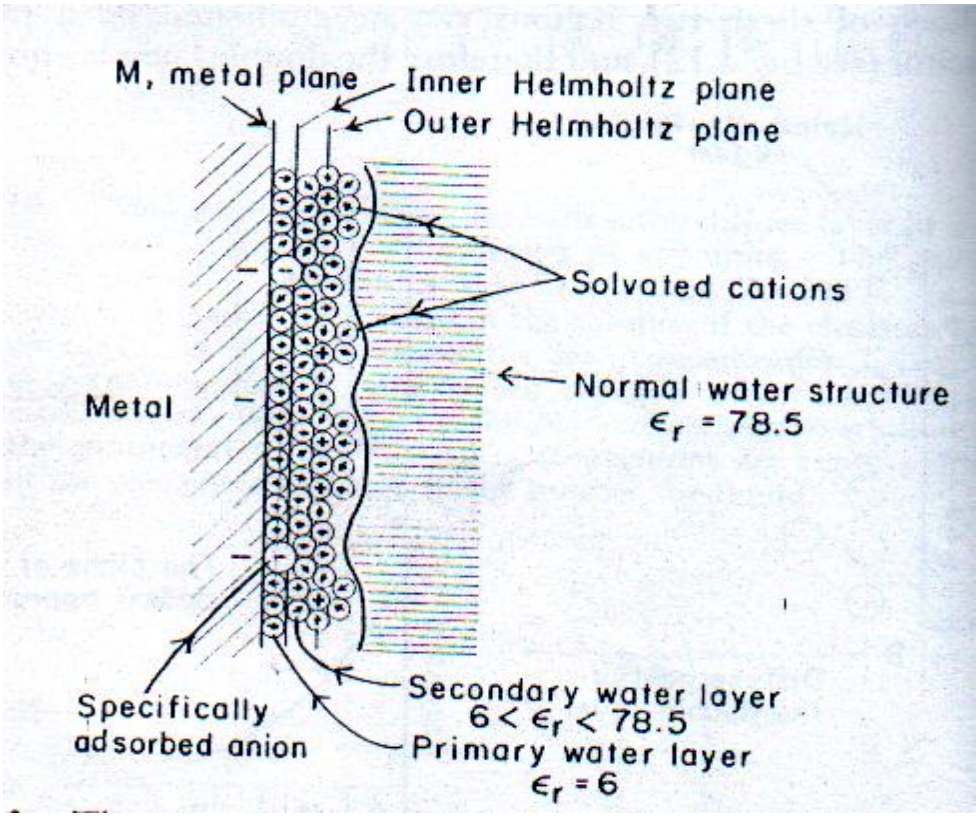

Figure (١.٥) The structure of the double layer according to Bockris,Devanathan and Muller .

As it is seen there , a distinction is made between contact-adsorbed ions and the solvated cations which are adsorbed out of direct contact with the electrode . The plane passing through the centres of contact-adsorbed anions is called the 'inner Helmholtz plane ' and that passing through the centres of solvated ions, the 'outer Helmholtz plane' . In fact , there are two outer Helmholtz plane , one for the cations and the other for the anions, but in our first-approximation discussion it was assumed that these two planes were identical . Thus, three regions must be distinguished in the structure of the solution side at an electrified interface .The water layer in the first region is stressed by the force exerted on it by the electrode field , and thus the relative permittivity of this 'primary water layer ' with fully oriented water molecules is much less than the permittivity of water in bulk, and ε_r =about ٦.(This is the

relative permittivity of water molecules when they are dielectrically saturated, as they will be at the high field strenghth attained in double layers).

The water molecules in layers further from the electrode than the first are oriented by the electrode filed, but are also partly disoriented by thermal and hydrogen-bonding influences. The relative permittivity of this secondary water layer rises with increasing distance from the electrode ,from about ٦ to the bulk value of ٧٨.٥ at ٢٩٨K.

This is the model of the double layer that will be used (figure ١.٥) ,but when making rough and ready calculations, the model may be considered in a simple Helmholtzian way (figure ١.١)[٥].

١.٣ The Kinetics of Electronic Charge Transfer

In this section , the act of charge transfer is described and the rate of that transfer is related to the potential difference in the interface.

To explain the physico-chemical view point of the charge transfer, the formula of the probability P_E is reviewed , where an energy level E in a metal will be populated by electrons is known as the Fermi-Dirac distribution function:

$$p_E = \frac{1}{\exp[(E - E_F)/\mathrm{KT}] + 1} \qquad (١.٩)$$

where E_F is known as the Fermi energy.

If $E = E_F$ in equation (١.٩) , then the exponential term becomes $e^0 = 1$ and $P_E = \frac{1}{2}$, so the Fermi level is that energy level which is half- populated by electrons at T>٠ K. When $P_E = 1$, the energy level of energy E is full, and the electrons find no states available to move into in the metal. Levels which are full will not conduct electricity because they have no empty sites into which moving electrons can pass. Thus, electron levels which are full cannot act as source or sink for electrons and cannot take part in an electrode reaction[٥].

Correspondingly, when P_E tends to zero, there are not enough electrons present to act as a source of electrons in charge transfer.

If an electron is considered to be emitted from a metal into a vacuum. As the electron tries to enter the vacuum a positive image charge is induced on the metal, and the electron experiences a force pulling it back. Thus, the electron encounters an energy barrier of finite height and width.

It should be expected, using classical mechanics, that the electron would have to have an energy greater than the energy of the barrier to leap over it and escape from the metal .Only a very small fraction of the electrons inside the metal has an energy greater than or equal to that corresponding to the top of the barrier. Consequently, the emission current by such a classical path is very small. By raising the temperature, the exponential $\exp(-\Delta E/\mathrm{KT})$ (where ΔE is the barrier height) increases, and an increasing number of electrons pass over the barrier. This is what happens when a hot wire emits electrons, as in a classical diode[٥].

The theory of this kind of emission current was given long ago. It is easy to show that ,for electrochemical situations, current densities arising in this way at electrodes would be $<١٠^{-16}\,\mathrm{Am}^{-2}$, where as the normal order of electrode currents is about $١٠\,\mathrm{Am}^{-2}$.

Thus , the classical over the barrier calculation gives results quite remote from currents observed experimentally, and one must conclude that classical mechanics cannot apply to the transfer of electrons from a metal in solution to neighbouring ions. This means that common sense (based on understanding of the way big objects behave) does not apply to the electron-level events which occur at electrodes . What does apply is quantum mechanics, the physics of the not-so-common- sense behaviour of very small particles. The laws of quantum- mechanical 'tunnelling' will govern when an electron can leave a metal and go to the solution. And quantum - mechanical tunneling will determine the probability that an electron can leave the solution and enter the metal[٥].

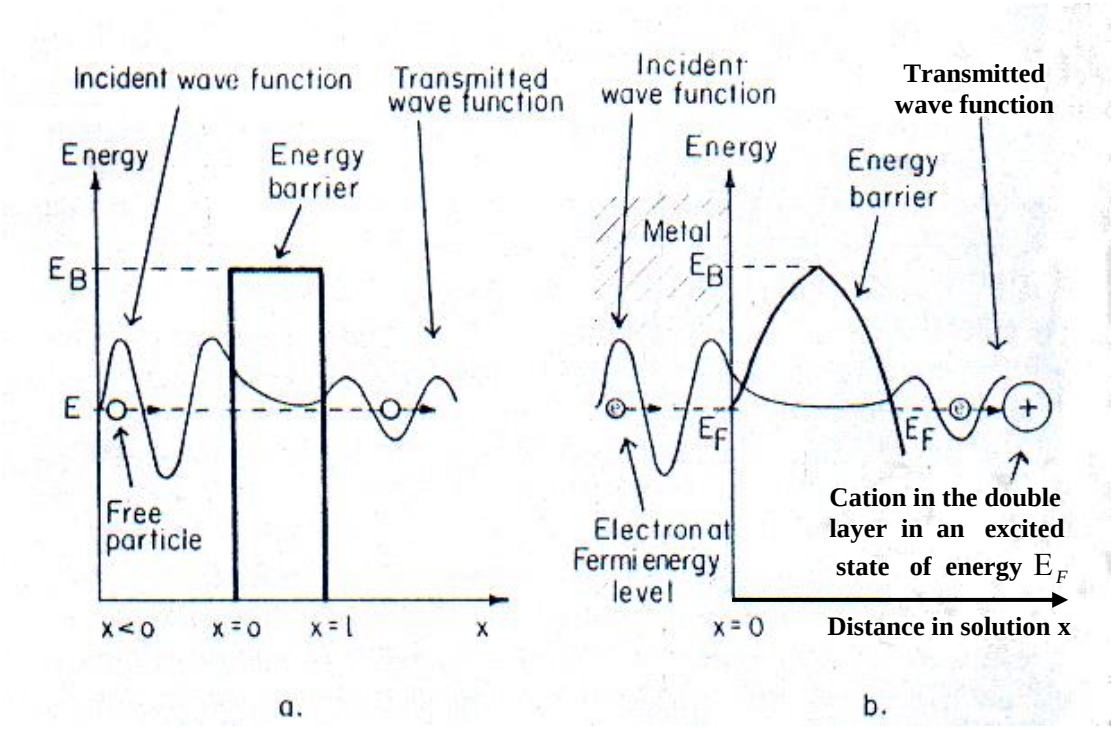

Figure (١.٦) Pictures the quantum – mechanical tunneling (a) of a free particle through a rectangular energy barrier in vacuum , and (b) of an electron through a metal – electrolyte interface .

Figure ١.٦ (a) illustrates quantum-mechanical tunnel transfer through a barrier. According to classical mechanics, a free particle of energy E smaller than the energy E_B of the barrier could never escape to the region $x > l$. In quantum mechanics , there is some probability that the particle will get to the other side of the barrier, because the behaviour of the particle is described by a wave-function[٥].

In figure ١.٦ (a) the wave function of the system is superimposed on the energy diagram and the whole picture is intended to be interpreted qualitatively. The behaviour of particle can be predicted in quantum mechanics if the behaviour of the wave function is known.In the first region, $x < 0$, and beyond the barrier the wave function varies periodically with distance, x. In the second region $(0 < x < l)$ the wave function varies in non-periodic way. There is a formula for the ratio between the number of particle penetrating the barrier at $x > l$, and the number of particles striking the barrier at $x < 0$. The essential part of this formula is the exponential term :

$$\exp\{-4\pi l h^{-1}[2m(E_B - E)^{1/2}]\} \qquad (١.١٠)$$

where m is the mass of the particle. Hence, the transmission coefficient will not be zero unless at least one of the quantities E_B, l , or m has the value infinity. For a given $(E_B - E)$ and l, the transmission coefficient increases as the mass of the particle decreases. Thus ,electron tunnel more easily than atoms .But it is electrons which have to cross the barrier.

It is easy to show ,from equation (١.٩) , that if E is about ٠.١ eV above the Fermi energy the probability (at ٢٩٨ K) of the level containing an electron is $<١٠^{-2}$, and if it is ٠.١ eV below the Fermi level ,the probability that the level will be full is ٠.٩٩. A level above the Fermi level 'empty' and a level below the Fermi level 'full' shall therefore be called.

Thus,for energy levels around the Fermi level , there are many electrons available to react with materials in solution. For levels below the Fermi level, there are no empty states and no mobility , so that electron transfer is not possible. It assumed that all the electrons involved in the electric current do have energies of E_F.

Figure ١.٦ (b) illustrates tunneling at a metal-electrolyte interface. The shape of the barrier varies with distance in a smooth fashion. Nevertheless, the barrier is qualitatively similar to the rectangular barrier shown in figure ١.٦(a) , and for the purpose of this present argument it is safely to work in terms of the simpler square barrier.

The tunneling of an electron (of energy E_F) from a metal to a particle in the solution takes place only if another energy condition is fulfilled. There must be a level in that particle which is available (empty) and which is at the same energy , E_F , as the electron in the metal .No energy change is observed during electron transfer, so that electron must pass from metal to solution, and vice versa, without loss of energy. Hence, it is interested in the probability of excitation of energy levels in the solution particles (example H_3O^+) to the level of the metal's Fermi level. Between these levels , and the corresponding

levels in the metal , transfer will occur. In the electronation reaction , $H_3O^+ + e \rightarrow H_{ads} + H_2O$, the $H-O$ bonds are excited, and may be longer than bonds in the unexcited state[٥].

Chemically , the rate of interfacial reactions are expressed in mol $m^{-2}s^{-1}$, but in electrochemistry ,they are expressed in Am^{-2}(to display the current density). The two expressions are related. According to Faraday's laws of electrolysis, When ٩٦٤٩٦C(=F) are passed across an interface, one mole of material is liberated if the charge on the ionic species involved is e , and $1/z$ moles if the charge is ze.

For current density i in Am^{-2} (=C $s^{-1}m^{-2}$) the number of moles discharged per $(metre)^2$ per second is i/zF . So the reaction rate is

$$v = i/zF \qquad (١.١١)$$

Since i is proportional to v , current-density is mentioned in electrochemistry it is really to think of the rate of an electrode reaction. A high current density means a high electrochemical reaction rate.

A typical reaction rate is ١٠ mA cm^{-2}=١٠٠ Am^{-2}; when the actual calculated value of v will be ١٠٠/٩٦٤٩٦$\cong$١٠$^{-3}$ mol $m^{-2}s^{-1}$ for ions of one unit charge[٥].

When the electrode is made more negative, electrons are expelled to the solution ; and when it is made more positive, they are attracted. However , at any condition of the electrode, there is some emission of electrons and some acceptance of them. It depends upon whether the electron-ejecting or the electron-accepting current is greater. A net electrochemical reaction rate is therefore written as:

$$i_{net,cathode} = i_- - i_+ \qquad (١.١٢)$$

This equation means: ' the net cathode current density observed in an outside circuit is the difference of the cathodic (electron emitting) current density and the anodic (electron accepting) current density '.

There must be an analogous equation for the net anode current (when the electrode is positive enough to make the partial anodic current predominate), and this will be :

$$i_{net,anode} = i_+ - i_- \qquad (١.١٢`)$$

This equation would read: ' the net anode current density is the difference of the actual anodic current density, and the corresponding cathodic current density ' .

Figure (١.٧) illustrates the physical meaning of these two current densities. When the cathodic current is greater than the anodic current a net cathodic current, corresponding to $M^+ + e \rightarrow M(e)$, flows through the interface; when the anodic current predominates a net anodic current, corresponding to $M(e) \rightarrow M^+ + e$, flows through the interface[٥] .

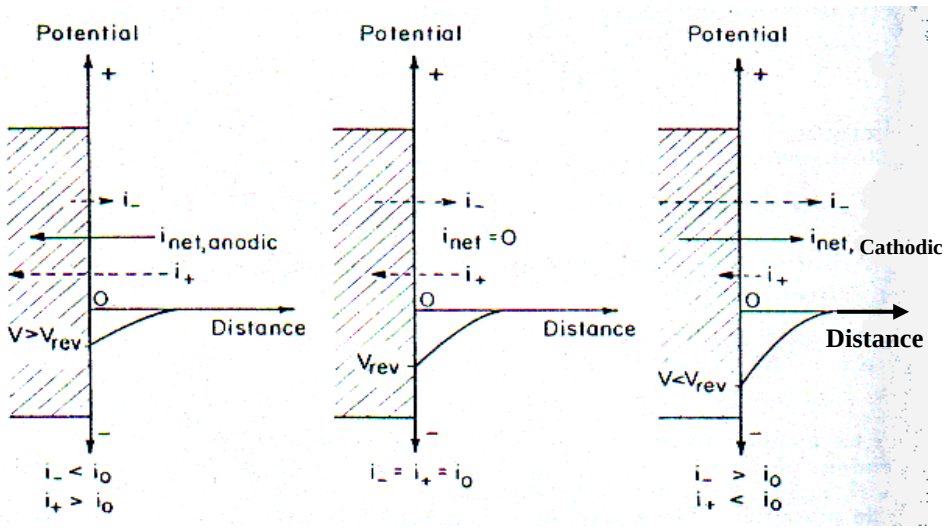

Figure (١.٧) The meaning of the exchange current density i_o . The arrows indicate the electron flows through the interface . The reversible potential difference across the double layer is supposed to be negative .

If a net anodic current density is considered as a positive quantity and a net cathodic current density as a negative quantity, then the following equations (١.١٢) and (١.١٢`) can be used instead of :

$$i_{net} = i_+ - i_- \qquad (١.١٣)$$

When $i_+ > i_-$, $i_{net} = i_{net,anodic} > 0$ and when $i_+ < i_-$, $i_{net} = i_{net,cathodic} < 0$.

Expressing i_+ and i_- in terms of the potential difference, V, across the double layer, yields the following relation between the net current density and the potential difference V:

$$i_{net} = (i_+)_{V=0} \exp[(1-\beta)FV/RT] - (i_-)_{V=0} \exp(-\beta FV/RT) \qquad (١.١٤)$$

where:

R: the gas constant=٨.٣١٤ $JK^{-1}mol^{-1}$.

β: symmetry factor.

The relationship which has been deduced is that between the current and the potential of an electrode. One basic aspect of the relation has not yet been brought out. If there is a net anodic current when the electrode is sufficiently positive and a net cathodic current when the electrode is sufficiently negative, then there must exist a potential at which there is no net current, i.e. equilibrium in the electrode reaction would exist. Hence[٥]:

$$i_{net} = 0 \quad \text{when} \quad i_- = i_+ \qquad (١.١٥)$$

This means that the rates of electron ejection (emission) and injection (acceptance)would be equal and the current zero.

This special potential at which the rates are equal is called by several names the equilibrium potential, the reversible potential, or the thermodynamic potential . From now onwards, it shall be refered to as V_{rev}. Thus, $i_{net} = 0$ when $V = V_{rev}$ (١.١٥`)

and from equation (١.١٤) it follows that:

$$i_o = (i_+)_{V=0} \exp[(1-\beta)FV_{rev}/RT] = (i_-)_{V=0} \exp(-\beta FV_{rev}/RT) \qquad (١.١٦)$$

i_o is called the exchange current density.

Figure (١.٧) illustrates also the meaning of exchange current density: at equilibrium (i.e., when $V = V_{rev}$), the partial anodic and cathodic current densities (positive equilibrium) are equal , and $i_o = (i_+)_{rev} + (i_-)_{rev}$. When V is more positive than V_{rev} , $i_- < i_o$, $i_+ > i_o$, and a net anodic current (electrons from solution to metal) flows through the interface. When V is more negative

than V_{rev} , $i_- > i_o$, $i_+ < i_o$, and a net cathodic current flows through the interface.

Equation (١.١٤) can be written in terms of V_{rev} :

$$i = (i_+)_{V=0} \exp[(1-\beta)FV_{rev}/RT]\exp[(1-\beta)F(V-V_{rev})/RT]$$
$$-(i_-)_{V=0}\exp(-\beta FV_{rev}/RT)\exp(-\beta F(V-V_{rev})/RT) \qquad (١.١٤`)$$

Then , using the expressions of i_o (equation (١.١٦)) :

$$i = i_o\{\exp[(1-\beta)F(V-V_{rev})/RT]-\exp(-\beta F(V-V_{rev})/RT)\} \qquad (١.١٧)$$

The difference $$\eta = V - V_{rev} \qquad (١.١٨)$$

expresses how far away from the equilibrium (or reversible) potential the current state is, and is called the over potential of the electrode reaction.

The over potential η is the extra potential that must be applied to an electrode reaction to make it occur at a certain net velocity. When $\eta = 0$, the electrode is at its reversible position and no net current passes. The cathodic and anodic partial reactions are still occurring , but $i_{net} = 0$ (i.e. $(i_-)_{rev} = (i_+)_{rev} = i_o$) . If $\eta > 0$ (i.e. $V > V_{rev}$), $i_- < i_o$ and $i_+ > i_o$; a net anodic current flows through the interface . If $\eta < 0$ (i.e. $V < V_{rev}$), $i_- > i_o$ and $i_+ < i_o$; a net cathodic current flows through the interface (see also Figure ١.٧).

If it is returned to equation (١.١٧) and replaced $V - V_{rev}$ by η :

$$i = i_o\{\exp[(1-\beta)F\eta/RT]-\exp(-\beta F\eta/RT)\} \qquad (١.١٩)$$

This is the Butler-Volmer equation, and relates the net current density of the electrochemical reaction to the overpotential. The Butler-Volmer equation shows that:

At positive (anodic) overpotentials , i is positive , so that the net current is anodic, and at negative (cathodic) overpotentials, i is negative , so that the net current is cathodic.

If more electrons are put into electrodes, or more are taken out , the level of the Fermi electrons is being altered . Hence, the change in the Fermi level in the metal from the value it had at equilibrium measures the

overpotential , and both correspond to the net reaction rate (or current density) to which they give rise[٥] .

An important aspect of electrochemical is dendritic growth that taking place at cathode electrode and leading to branched structures resulted from mass transfer in the electrolyte and at the electrodes of electrochemical cells.For this reason , the study of electrochemical growth is necessary for prediction or determination of the growth speed, branch thickness and overall structures. The efficiency of the cell is highly dependent on the distribution of chemical reactants in the vicinity of these electrodes. One difficulty is to predict the distributions of concentrations in electrolytes. The calculation of concentration in electrochemical cell is achieved depending on mean-field kinetic equations derived using charge microscopic model.

١.٤ The Important aspect of Electrochemical Process

The important aspect of electrochemical process are dendritic growth(densely branches, shapes and branch thickness),electrochemical reactions that happen inside the cell represented by oxidation-reduction processes at surface of anode and cathode , lattice model and mean-field kinetic equations(to calculate local concentrations inside the cell to simulate growth and dissolution).

١.٤.١ Electrochemical Growth (Dendritic Growth)

Electrochemical growth may lead to the formation of complex and highly branched structures that can be fractals (like in diffusion limited aggregation(DLA)) or densely branched, depending on the experimental conditions[٦,٧].Figure (١.٨) shows an example of dendrites. Dendritic growth is one of the most remarkable phenomena observable in the dynamics of phase transitions. The term ‘dendritic structure’ has come to embrace a wealth of different tree-like structures formed during aggregation or solidification

processes. Probably the most well-known dendritic structure is the snowflake;however, the description of snowflake formation is particularly diffcult due to the complicated crystal growth dynamics [٨]. Roughly, dendritic shapes can be divided into two categories: very irregular, fractal shapes produced for example in electrodeposition and the more regular shapes produced during the solidification of a crystal from an undercooled or supersaturated liquid [٩,١٠].

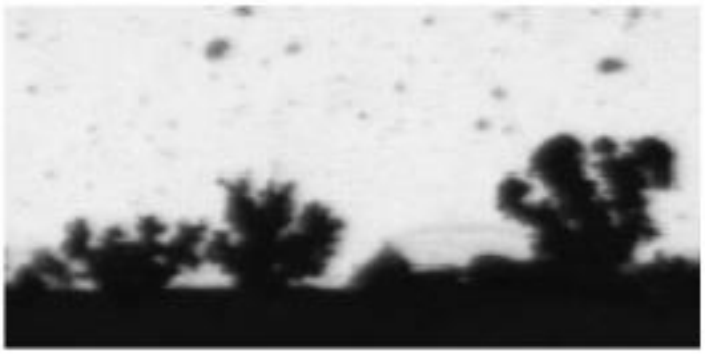

Figure (١.٨) Dendritic growth at the interface between a lithium and a polymer electrolyte[٧] .

١.٤.٢ Electrochemical Reactions

Electrochemical reactions take place , namely reduction and electrodeposition on the cathode , oxidation and dissolution on the anode .In addition to the charged double layers at the metal-solution interface , ionic transport in the electrolyte may lead to the formation of extended space-charge regions,which makes it necessary to include Poisson equation[١١]. Diffusion , migration and convection are the main transport mechanisms through the electrolyte(see figures ١.٩ and ١.١٠).

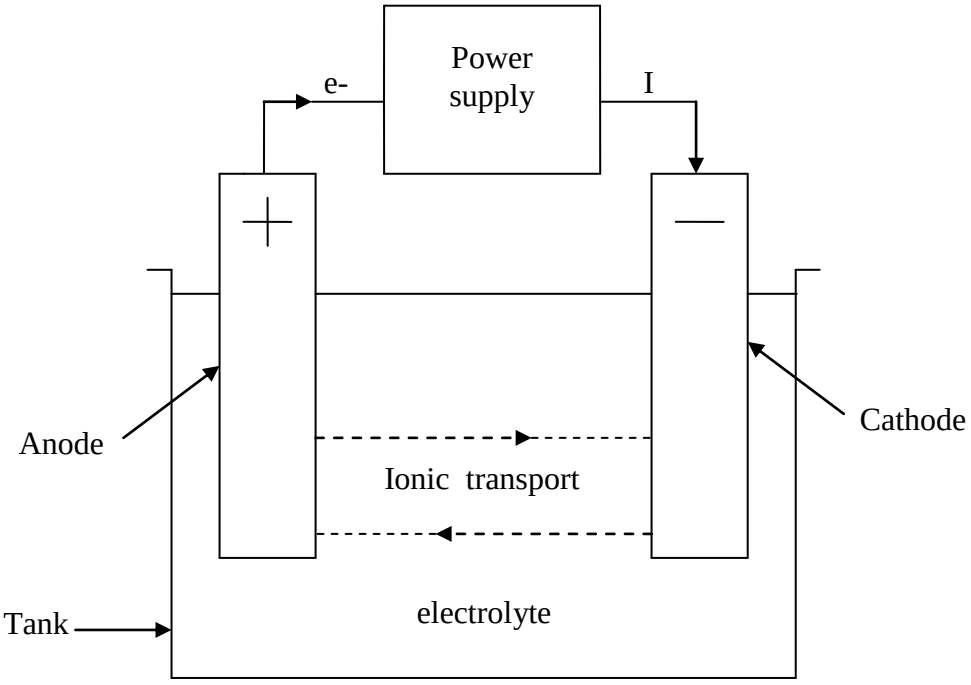

Figure (١.٩) The geometry of the cell [٣] .

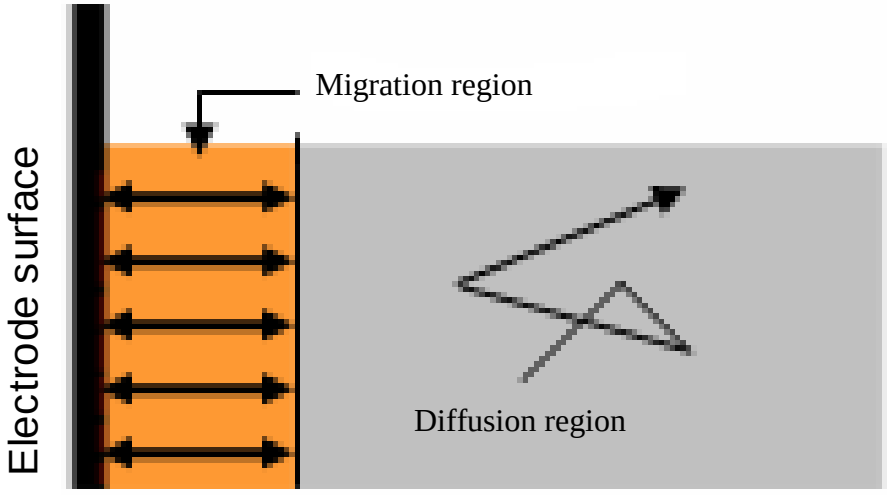

Figure (١.١٠) Diffusion and migration in an electrolytic cell [٣].

١.٤.٣ Lattice Models

Several types of models have been proposed for the kinetics of phase transformations in solids. They can be classified as macroscopic, mesoscopic, and microscopic. In the macroscopic models, also termed sharp-interface models, one considers the growth of already well-defined domains. Usually, the typical size of these domains is much larger than the intrinsic thickness of an interface. Therefore, the interfaces are described by surfaces without thickness (lines in two dimensions). Sharp interface models have been successfully used in the theory of dendritic growth and for a description of late-stage domain growth during phase separation , as well as in many other pattern-forming systems.

Mesoscopic models are based on the principles of out-of-equilibrium thermodynamics. One assumes that, even if the system as a whole is in a state far from thermodynamic equilibrium on a small scale of the order of the interface thickness, the system is in local equilibrium and the intensive thermodynamic quantities vary only very slightly on this scale. Under this condition, one may write down a free energy functional, which depends on the local fields, and postulate an equation of motion.

Microscopic models are usually based on lattice models of the Ising type, also called lattice gases or more precisely stochastic lattice gases to distinguish them from Boltzmann lattice gases used to model hydrodynamic flows [١٢].

In this study a lattice gas model will be used that includes charged particles and that uses simple microscopic characteristics to simulate the salient features of electrochemical process,including both the diffusion kinetics of the charged and neutral species, and the oxido-reduction phenomena on the electrode interfaces.

١.٤.٤ Mean-Field Kinetic Equations(MFKE)

Mean-field kinetic equations are a valuable tool to study the atomic dynamics and spin dynamics of simple lattice gas and Ising models. They can be derived from the microscopic master equation of the system and contain analytical expressions for kinetic coefficients and thermodynamic quantities which are usually introduced phenomenologically. MFKE will be used to study diffusion and ordering kinetics, spinodal decomposition and dendritic growth.Presence of charged particles implies that, in addition to the kinetic equation driving the particle motion , the Poisson equation is to be solved for the electrical potential .The chemical potentials present in the MFKE are then replaced by electrochemical potentials . MFKE establishes a link between a microscopic lattice model and macroscopic phenomenological equations [١٣].

١.٥ Objective and Scope

The main objective of this investigation is to study the kinetic of chemical and electrochemical reactions and the effect of different conditions by modeling the assential electrochemical and chemical reactions accompanied during electroplating processes basing on the mean-filed kinetic equations a long together with a Poission equation for the electrical potential.

A computer program in visual basic language is specially designed for this purpose for all these configurations.

CHAPTER TWO

LITERATURE SURVEY

٢.١ Introduction

The interest in this work is directed towards simulation of electrochemical cells . Hence the literature survey is directed toward dendritic growth , mean-field kinetic equation and mass transport in electrochemical cells.

٢.٢ Dendritic Growth

Barton and Bockris,[١٤],١٩٦٢,showed the Barton and Bockris model of propagation ,this model described growth in well- supported electrolytes , calling into question its applicability to polymer electrolyte systems . In addition ,the model assumed that propagation dendrite tips were relatively isolated and hemispherical in shape . Diggle et. al , [١٥] , ١٩٦٩, improved the Barton and Bockris model of propagation .

Mullins and Sekerka ,[١٦],١٩٦٣, developed linear stability analyses and stability criteria in one-dimensional thermal systems where surface tension forces slow the rate of solid deposition from melts. The Mullins-Sekerka method was extended to unsteady galvanostatic deposition from a two-dimensional semi-infinite region by Aogaki and Makino,[١٧],١٩٨١.

Chen and Jorne , [١٨], ١٩٩٠ , developed the most applicable fractal propagation model . Chazalviel , [١٣] , ١٩٩٠ , described migration-limited mechanisms in his work . Both approaches rely on the assumption that high voltages(١٠v) are applied to the electrochemical cell.

Harris et. al , [١٩] , ١٩٩٢ , studied the dynamics of interfaces in two dimensions by using Monte Carlo simulations. They observed the roughening dynamics and the Mullins–Sekerka instability.

Dobretsov et. al , [٢٠],١٩٩٦, studied spinodal decomposition in alloys where ordering and phase separation occur simultaneously. Chen,[٢١],١٩٩٤, studied spinodal decomposition in a ternary system.

Losert et. al ,[٢٢],١٩٩٦,showed the spatial period-doubling instability of dendritic arrays in directional solidification as suggested theoretically by Warren and Langer,[٢٣],١٩٩٠.

Jean-Franqois Gouyet and Mathis Plapp,[٢٤],١٩٩٦, used Cahn-Hilliard equations to perform numerical simulations in two dimensions of the growth of regular "snowflakes." It naturally showed curvature and kinetic effects at the interface as assumed by the classic phenomenological equations of dendritic growth. In addition, they found solute trapping. The dendrite tips were stabilized by the Gibbs- Thomson boundary condition. They compare their models and the phase-field models and discuss the influence of noise.

Bernard et. al , [٢٥],٢٠٠١, studied analytically the kinetics of growth of parallel needles. They established a discrete Fokker-Planck equation for the probability of finding at time (t) a given distribution of needle lengths. In the linear regime, it shows a short-wavelength Laplacian instability which they investigated in detail. From the crossover of the solutions to the nonlinear regime, they deduced analytically the general scale invariance of the two-dimensional models.

Charles Monroe and John Newman , [٢٦] , ٢٠٠٤, used two methods,Mullins-Sekerka linear stability analysis and the Barton and Bockris dendrite-propagation model . Both described cathodic roughening and dendritic growth and contain the effects of surface tension and local concentration deviations induced by surface roughening. Here, a kinetic model is developed which additionally includes mechanical forces such as elasticity, viscous drag, and pressure, showing their effect on exchange current densities and potentials at roughening interfaces.

٢.٣ Mean- Field Kinetic Equations(MFKE)

Suzuki and Kubo,[٢٧],١٩٦٨, derived the first general of mean-field kinetic equations for the spin-flip Ising model . Binder,[٢٨],١٩٧٤,derived mean-field kinetic equations for the spin-exchange model of binary alloys. Binder and Frisch,[٢٩],١٩٩١, connected between these discrete mean-field kinetic equations and continuum equations.

Mathis Plapp and Jean-Franqois Gouyet,[٣٠],١٩٩٩, developed the mean-field kinetic equations for a lattice gas model of a binary alloy with vacancies (ABv model) in which diffusion takes place by a vacancy mechanism. These equations are applied to the study of phase separation of finite portions of an unstable mixture immersed in a stable vapor. Due to a larger mobility of surface atoms, the most unstable modes of spinodal decomposition are localized at the vapor-mixture interface. Simulations show checkerboard-like structures at the surface or surface-directed spinodal waves. They determined the growth rates of bulk and surface modes by a linear stability analysis and deduce the relation between the parameters of the model and the structure and length scale of the surface patterns. The thickness of the surface patterns is related to the concentration fluctuations in the initial state.

Bernard et. al , [٧],٢٠٠١, have built electrochemical mean-field kinetic equations modelling electrochemical cells and growth structures that form during electrodeposition. They confirmed the viability of this approach by simulating the ion kinetics in front of planar electrodes during growth on the cathode and dissolution of the anode(double layer,space charge,due to an anion depletion ahead of the growing front,…).Two dimensional simulations of growing dendrites are also presented.

In ٢٠٠٢ the same researchers published this paper with another arrangement including some extensions [٣١]. In ٢٠٠٣ they published the research with new arrangement and new aspects as following[٣٢]:

- equation of jumping rate from site to another i.e. from site k to k+a

- calculation of diffusion current by a method independent of gradient of the electrochemical potential and depending on procces of replacement different species in vacancies.
- add electron relaxation to the evolution equation for the electron.

Gouyet et. al ,[٣٣],٢٠٠٣, reviewed several methods to obtain mean-field kientic equations, and discuss applications to the dynamics of order–disorder transitions, spinodal decomposition, and dendritic growth in the isothermal or chemical model. In the case of dendritic growth they showed that the mean field kinetic equations are equivalent to standard continuum equations and derive expressions for macroscopic quantities. In spinodal decomposition, they focused their attention on the vacancy, which is a more faithful picture of diffusion in solids than the more widely examined exchange mechanism. They have studied the interfaces between an unstable mixture and a stable 'vapour' phase, and analyze surface modes that lead to specific surface patterns. For order–disorder transitions, studied in the frame work of a repulsive two-sublattice model, they have derived sets of coupled equations for the mean concentration and for the occupational difference between the two sublattices emerging from the symmetry breaking due to ordering . These equations are applied to transport in the presence of ordered domains. Finally, they discussed the possibilities of improving the simple mean-field approximation by density functional theories and various forms of the dynamic pair approximation, including the path-probability method.

٢.٤ Mass Transport in Electrochemical Cells

Spalart,[٣٤],١٩٨٨, and Watmuff ,[٣٥],١٩٩٣, studied mass transfer in electrochemical systems and reported global information on the process such as total cell potential drop,the electrical current and the global density variation of ionic species. As result, other tools must be used in order to provide detailed data on the structure of the flow.

Franqois Gurniki,[٣٦],٢٠٠٠, studied of mass transport in turbulent flow of electrochemical cells. The investigation is performed through numerical simulations. The mathematical models account both for turbulence and the properties of electrochemical mass transfer. Different models were tested for the electrochemical process at the electrodes. Natural and forced convection were investigated. The electrolyte considered is binary. The transport equations for mass are consequently reduced to one equation only, and is identical to the transport equation for a passive scalar, or temperature. No volume reaction is considered. The major contribution of that work was the validation of a numerical method to compute turbulent mass transfer in near-electrode regions. A class of turbulence models with a fairly simple formulation was validated for electrochemical processes.

٢.٥ Summary

It is clear from the preceding studies that some researchers had treated the deposition process or the simulation of electrochemical deposition in one- dimension depending on concentrations differences in the reaction kinetics , while there is no other works adopting other than this concept.Most of those researchers studied the dendritic growth through the alloys solidification process and derived the pertaining relevant equations of the reactions kinetics basing on solidification equations, while this work has discussed the previons models(gradient of an electrochemical potential) mentioned earlier i.e. depending on concepts and equations of alloys solidification besides the study of other parameters effects which have not been discussed formerly , such as changing of concentration, voltage , Fermi energy and electrode spacing during deposition . A mathematical model is constructed in this study depending on other criterion which are cations and anions replacement instead of the solvent it self, then a comparison between the two methods is achieved.

CHAPTER THREE

THEORETICAL ANALYSIS OF MEAN-FIELD KINETIC AND POISSON EQUATIONS

٣.١ Introduction

In this chapter , the theoretical analysis of the mean-field kinetic and Poisson equations will be presented. The local concentration of species metal atoms and metallic cation is modified by transport(diffusion and migration in the electric field) and by the electron transfer; for other species anions and solvent .The modification is achived by only transport . The transport term is active only in the solid-electrolyte interface . In addition , Poisson equation will be used to determine the electrostatic potential for a given charge distribution.

٣.٢ Butler-Volmer Model of Electrode Kinetics

Experience demonstrates that the potential of an electrode strongly affects the kinetics of reactions occurring on its surface. Hydrogen evolves rapidly at some potentials ,but not at others. Copper dissolves from a metallic sample in a clearly defined potential range; yet the metal is stable outside that range , and so it is for all Faradaic processes. Because the interfacial potential difference can be used to control reactivity, it is required to be able to predict the precise way in which heterogeneous rate constant for reduction and heterogeneous rate constant for oxidation depend on potential. A predictive model based purely on classical concepts. Even though it has significant limitations, it is very widely used in the electrochemical literature and must be understood by any student of the field [٣٧] .

٣.٣ Microscopic Theories of Charge Transfer

There is a generalized theory of heterogeneous electron-transfer kinetics based on macroscopic concepts, in which the rate of the reaction was expressed in terms of the phenomenological parameters , standard heterogeneous rate constant and transfer coefficient. While it is useful in helping to organize the results of experimental studies and in providing information about reaction mechanisms, such an approach cannot be employed to predict how the kinetics are affected by such factors as the nature and the structure of the reacting species, the solvent , the electrode material, and adsorbed layers on the electrode. To obtain such information, one needs a microscopic theory that describes how molecular structure and environment affect the electron-transfer process [٣٧].

A great deal of work has gone into the development of microscopic theories over the past ٤٥ years. The goal is to make predictions that can be tested by experiments, so that one can understand the fundamental structural and environmental factors causing reactions to be kinetically facile or sluggish. With that understanding , there would be a firmer basis for designing superior new systems for many scientific and technological applications. Major contributions in this area have been made by Marcus, Hush, Levich, Dogonadze, and many others. Comprehensive reviews are available , as are extensive treatments of the broader related field of electron-transfer reactions in homogeneous solution and in biological systems [٣٧].

At the outset,it is useful to distinguish between inner-sphere and outer-sphere electron-transfer reactions at electrodes (figure ٣.١) . This terminology was adopted from that used to describe electron-transfer reactions of coordination compounds. The term " outer-sphere" denotes a reaction between two species in which the original coordination spheres are maintained in the activated complex["electron transfer from one primary bond system to another"].In contrast, " inner-sphere" reactions occur in an activated

complex where the ions share a ligand ["electron transfer within a primary bond system"][٣٧].

Likewise, in an outer-sphere electrode reaction, the reactant and product do not interact strongly with the electrode surface, and they are generally at a distance of at least a solvent layer from the electrode. A typical example is the heterogeneous reduction of $Ru(NH_3)_6^{3+}$, where the reactant at the electrode surface is essentially the same as in the bulk. In an inner-sphere electrode reaction , there is a strong interaction of the reactant, intermediates, or products with the electrode; that is such reactions involve specific adsorption of species involved in the electrode reaction. The reduction of oxygen in water and the oxidation of hydrogen at pt are inner-sphere reactions. Another type of inner-sphere reaction features a specifically adsorbed anion that serves as a ligand bridge to a metal ion. Obviously outer-sphere reactions are less dependent on electrode material than inner-sphere ones. Even if there is not a strong interaction with the electrode , an outer-sphere reaction can depend on the electrode material, because of (a) double-layer effects , (b) the effect of metal on the structure of the Helmholtz layer, or (c) the effect of the energy and distribution of electronic states in the electrode.

Outer-sphere electron transfers can be treated in a more general way than inner-sphere processes, where specific chemistry and interactions are important . For this reason, the theory of outer-sphere electron transfers is much more highly developed. However, in practical applications, such as in fuel cells and batteries, the more complicated inner-sphere reactions are important . A theory of these requires consideration of specific adsorption effects, as well as many of the important factors in heterogeneous catalytic reactions[٣٧].

Homogenous Electron Transfer

Outer-sphere

$$Co(NH_3)_6^{3+} + Cr(bpy)_3^{2+} \rightarrow Co(NH_3)_6^{2+} + Cr(bpy)_3^{3+}$$

Inner-sphere

$$Co(NH_3)_5Cl^{2+} + Cr(H_2O)_6^{2+} \rightarrow (NH_3)_5CoClCr(H_2O)_3^{4+}$$

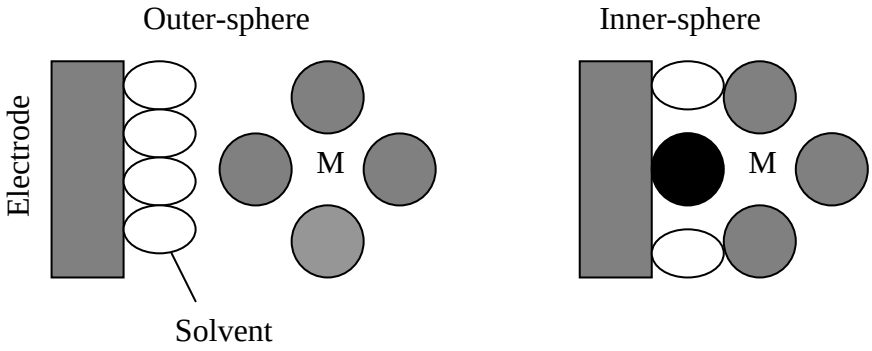

Figure (٣.١) Outer-sphere and inner-sphere reactions[٣٧].

٣.٤ lattice Gas Model

Lattice gas model is used to study and analyze the electrochemical process as a model involves various electrochemical mechanisms governing the dendritic growth and including charged particles and using simple microscopic characteristics to simulate the salient features of the electrochemical process consisting of both the diffusion kinetics of the charged and neutral species, and the oxido-reduction phenomena on the electrode interfaces. Due to non-availability of theoretical studies of the behavior of an entire electrochemical cell based on a microscopic model, lattice gas model are still used up to now to simulate the phenomena located on the electrode surfaces , such as adsorption or underpotential deposition and for studies of ionic transport at liquid-liquid interfaces[٧].

An electrochemical cell made of a dilute binary electrolyte and two metallic electrodes of the same metal is to be considered. No supporting electrolyte , generally used to suppress ion migration .The electrodes are modeled by a lattice that reflects the underlying crystalline structure, and whose sites are occupied by metallic atoms or vacancies. It is convenient to represent the electrolyte by the same lattice, occupied by a solvent, cations, anions, or vacancies[٣٢].

In a two-dimensional lattice gas on a square lattice with lattice spacing (a) in figure (٣.٢) which shows this model , a fixed potential difference is applied across the cell. The ions in the electrolyte are subjected to an electric field E_k (and hence a force $F_k = qE_k$) at their lattice site position k. The various species have short-range interactions (here, attractive interactions are considered between solvent and ions, solvent and solvent, and metal and metal). Electron transfer takes place on the electrode surfaces . Cations M^+ give metallic atoms M^o after reduction, while anions A^- are supposed to be nonelectroactive. Solvent *S* is neutral, but can interact through short-range interactions with other species and with itself. A microscopic configuration is specified by the set $\{n\}$ of the occupation numbers n_k^α on each site k: $n_k^\alpha = 1$ if k is occupied by species $\alpha = M^o$, M^+, A^-,S, or a vacancy *v*, and ٠ otherwise. It is supposed that there is a steric exclusion between the different species, that is, a given site can be occupied by only one species or it can be empty(vacancy)[٣١,٣٢]:

$$\sum_\alpha n_k^\alpha + n_k^v = 1$$

(٣.١)

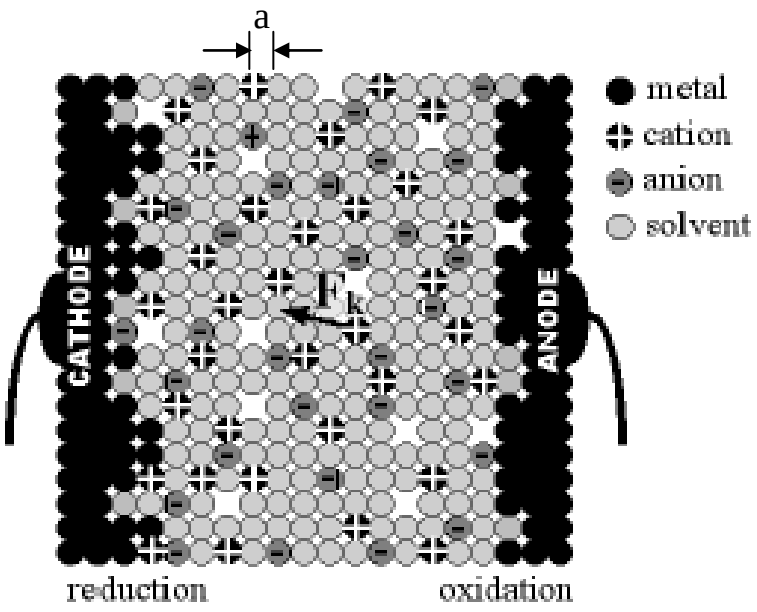

Figure (٣.٢) The lattice-gas model considered in the present study [٧].

Two very different types of interactions are existed in the electrochemical cell depending on electric field intensity between charged species and the spacing among them , namely[٧,٣١,٣٢]:-

١. Short-rang interactions: - which are taking place between the nearest - neighbors and different - in - charge species having rather weak inter-connection bonds between different species such as (Van Der Waals forces , solvation effects , and chemical interactions) are modeled here by nearest - neighbor interactions $\varepsilon^{\alpha\beta}$ between species α and β (with the convention that a positive $\varepsilon^{\alpha\beta}$ corresponds to an attractive interaction). Interaction energies with vacancies are taken to be zero.

٢. Long-range interactions:- occur between the species of higher intensities of electric fields separated by longer spaces having stronger inter - connection than the former type bonds such as (coulomb interactions between the charged species).

In short-range interactions, the particle (metal, ion, or solvent) jumps to one of its vacant nearest-neighbor sites. In principle, an exchange process between occupied nearest-neighbor sites is also included. This leads to more complicated kinetic equations and will not be considered here. To specify the jump rates, it can be assumed that the atoms perform activated jumps. The height of the activation barrier depends on the local binding energy, that is, the number and type of bonds that need to be broken as shown in figure (٣.٣)[٣٢].

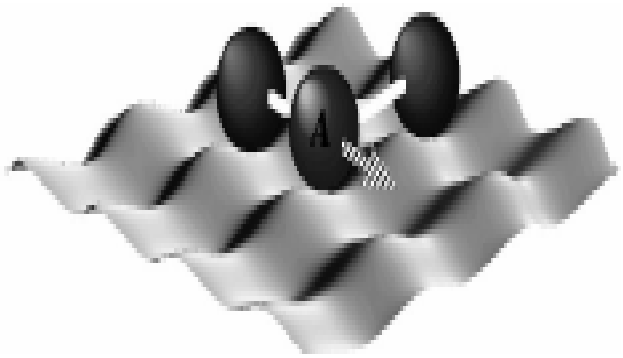

Figure (٣.٣) In the lattice-gas model, an *A* atom makes activated jumps to empty nearest-neighbor sites. The barrier has to overcome depends on its interactions (white links) with its nearestneighbor atoms.

Also for charged particles, it depends on the local electric field that shifts the barrier height as shown i.e. for a moving particle carrying a charge (q) to be shifted from site k to site k+a a long the jump path X, in the presence of electrical field , the potential energy is superimposed to the local potential of that particle as shown in figure (٣.٤) [٣٢].

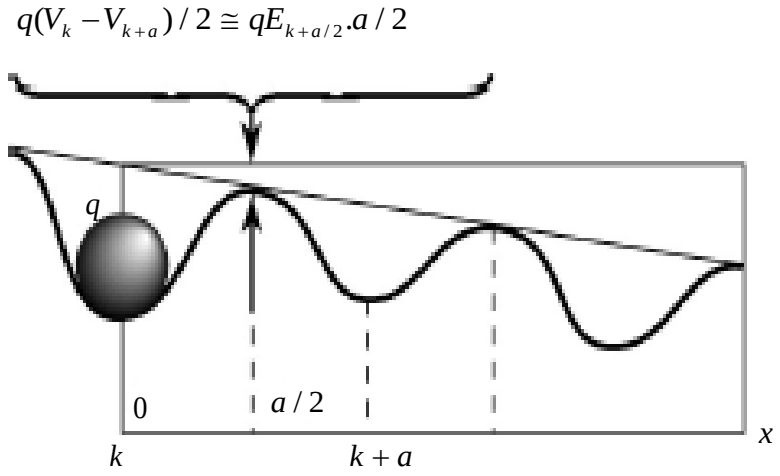

Figure (٣.٤) In the presence of electric field E, a potential energy, which varies, to first order, like $qE.X$ along the jump path X, is superimposed to the local potential seen by a moving particle (with charge q) .

where:-

E : the electrical field

q : charge of particle

X : the jump path

V_k : electrical potential defined on the lattice sites k.

The result for the jump rate from site k to site k+a is[٣٢],

$$\tilde{w}^{\alpha}_{k,k+a}(\{n\}) = w^{\alpha} \exp\left(\frac{1}{\mathrm{KT}} \sum_{\beta} \sum_{a'} \varepsilon^{\alpha\beta} n^{\beta}_{k+a'}\right) \times \exp\left(\frac{q^{\alpha}}{2\mathrm{KT}} (V_k - V_{k+a})\right) \qquad (٣.٢)$$

where:-

KT : the (fixed) thermal energy.

w^{α}: a fixed jump frequency that may be different for each species.

q^{α} : charge for each species.

٣.٥ Mean-Field Kinetic Equations

The establishment of the mean-field kinetic equations follows the same procedure as for neutral particles [٣٨,٣٩]. When the particles jump form site to site , the probability of finding a given configuration $\{n\}$ evolves with time

according to the master equation . Let $p(\{n\},t)$ denote the probability of finding the configuration $\{n\}$ at time t .The master equation reads[٣٢]:

$$\frac{\partial}{\partial t} p(\{n\},t) = \sum_{\{n'\}} [w(\{n'\} \to \{n\}) p(\{n'\},t) - w(\{n\} \to \{n'\}) p(\{n\},t)] \qquad (٣.٣)$$

where $w(\{n\} \to \{n'\})$ is the transition probability from $\{n\}$ to $\{n'\}$. In the time evolution of the average concentration of the various species $(\alpha = +,-,o,s)$,

$$p_k^{\alpha}(t) = \left\langle n_k^{\alpha} \right\rangle_t = \sum_{\{n\}} n_k^{\alpha} p(\{n\},t) \qquad (٣.٤)$$

In the absence of electrochemical processes at the electrodes, the number of each type of particles remains constant, and the kinetic equation of the average concentration has the structure of a conservation equation,

$$\frac{\partial P_k^{\alpha}}{\partial t} = - \sum_a \tilde{J}_{k,k+a}^{\alpha} \qquad (٣.٥)$$

where:-

P_k^{α} : the concentration of species α at site k.

$\tilde{J}_{k,k+a}^{\alpha}$: The diffusion current of species α on the bond linking site k to nearest neighbor site k+a.

a : spacing between neighbors species α.

٣.٥.١ Diffusion Current

The diffusion current of species α on the bond linking site k to nearest neighbor site k+a defined by two methods[٣٢]:-

١. First method:-

$$\tilde{J}_{k,k+a}^{\alpha} = \left\langle \tilde{w}_{k,k+a}^{\alpha}(\{n\}) n_k^{\alpha} n_{k+a}^{v} - \tilde{w}_{k+a,k}^{\alpha}(\{n\}) n_{k+a}^{\alpha} n_k^{v} \right\rangle \qquad (٣.٦)$$

with $\tilde{w}_{k,k+a}^{\alpha}(\{n\})$ given by equation (٣.٢). The factor $n_k^{\alpha} n_{k+a}^{v}$ (and $n_{k+a}^{\alpha} n_k^{v}$ for the reverse jump) means that for a jump of α to be possible , the start site must be occupied by species α, while the target site must be empty (occupied by a vacancy v).

The occupation numbers n_k^α in the above expressions are replaced by their average p_k^α. This replacement is not unique because of different possible choices for the factorization of the occupation number operators [٣٩]. A convenient choice [٣٩,٤٠], is the direct replacement of all occupation numbers by their averages in equation(٣.٦) and (٣.٢), which leads to:

$$\tilde{J}^\alpha_{k+k+a} = w^\alpha [P_k^\alpha P^\nu_{k+a} \exp(-\frac{1}{\mathrm{KT}} \sum_\beta \sum_{a'} \varepsilon^{\alpha\beta} P^\beta_{k+a'} + \frac{q^\alpha}{2\mathrm{KT}} (V_k - V_{k+a})$$

$$- P^\alpha_{k+a} P^\nu_k \times \exp(-\frac{1}{\mathrm{KT}} \sum_\beta \sum_{a'} \varepsilon^{\alpha\beta} P^\beta_{k+a+a'} + \frac{q^\alpha}{2\mathrm{KT}} (V_{k+a} - V_k))]$$

(٣.٧)

٢. <u>Second method:-</u>

$$\tilde{J}^\alpha_{k,k+a} = -\tilde{M}^\alpha_{k,k+a} D_a \tilde{\mu}^\alpha_k \qquad (٣.٨)$$

In this method as the product of an electrochemical bond mobility $\tilde{M}^a_{ij}$ a times the (discrete) gradient of an electrochemical potential $\tilde{\mu}^\alpha_i$.

Where D_a is a difference operator acting on the site coordinates, $D_a F_k = F_{k+a} - F_k$. The electrochemical potential:

$$\tilde{\mu}^\alpha_k = \mu^\alpha_k + q^\alpha V_k = -\sum_\beta \sum_a \varepsilon^{\alpha\beta} p^\beta_{k+a} + \mathrm{KT} \ln(\frac{p^\alpha_k}{p^\nu_k}) + q^\alpha V_k \qquad (٣.٩)$$

where:-

($-\sum_\beta \sum_a \varepsilon^{\alpha\beta} p^\beta_{k+a}$): a local energy due to the interaction of species α with its local environment

$\mathrm{KT} \ln(\frac{p^\alpha_k}{p^\nu_k})$: an entropy term.

$q^\alpha V_k$: electrostatic energy.

The mobility along a bond k,k+a is given by:

$$\tilde{M}^\alpha_{k,k+a} = \frac{w^\alpha}{\mathrm{KT}} P^\nu_k P^\nu_{k+a} \exp \frac{(\tilde{\mu}^\alpha_k + \tilde{\mu}^\alpha_{k+a})}{2\mathrm{KT}} \, shc \, \frac{D_a \tilde{\mu}^\alpha_k}{2\mathrm{KT}}$$

(٣.١٠)

where it is used the notation shc u=sinh u/u (close to equilibrium , $\tilde{\mu}^{\alpha}_{k+a} \cong \tilde{\mu}^{\alpha}_{k}$ and shc[$D_{\alpha} \tilde{\mu}^{\alpha}_{k} / 2KT] \cong 1$) .

٣.٦ The Poisson Equation

Consider an infinitesimally small volume element dv ion, upon which attention is to be fixed during the discussion (figure ٣.٥),and let the net charge density inside the volume element be q_r . Further , let the average electrostatic potential in the volume element be V_r [٤١].

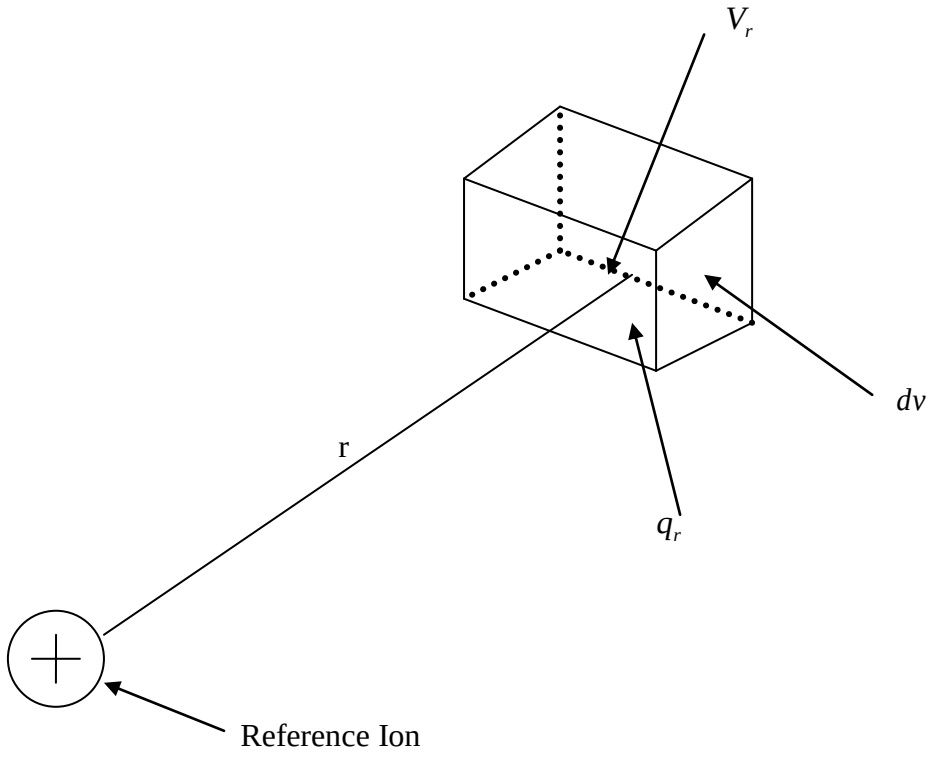

Figure(٣.٥) At a distance r from the reference ion, the excess charge density and electrostatic potential , in an infinitesimal volume element q_r , V_r , and dv respectively.

One relation between q_r and V_r is given by Poisson's equation . There is no reason to doubt that there is spherically symmetrical distribution of positive and negative charge and , therefore , excess charge density around a given central ion . Hence , Poisson's equation can be written as[٤١],

$$\frac{1}{r^2}\frac{d}{dr}(r^2\frac{dV_r}{dr}) = -\frac{4\pi}{\varepsilon} q_r \qquad (٣.١١)$$

where:-

ε the dielectric constant (permittivity).

$$q_r = -\sum_i \frac{n_i^o z_i^2 e_o^2 V_r}{\mathrm{KT}} \qquad (٣.١٢)$$

where:-

z_i : the valency of the ion .

e_o : the electronic charge .

n_i^o : the concentration of the ionic species i .

Equation (٣.١٢) is termed as linearized Boltzmann equation . Substitution of equation (٣.١٢) in equation (٣.١١) results the linearized Poisson-Boltzmann equation [٤١].

$$\frac{1}{r^2}\frac{d}{dr}(r^2\frac{dV_r}{dr}) = (\frac{4\pi}{\varepsilon \mathrm{KT}}\sum_i n_i^o z_i^2 e_o^2)V_r \qquad (٣.١٣)$$

Using the formulation and discussion above to determine the electrostatic potential for a given charge distribution, a discrete version of the Poisson equation is solved using the lowest order discretization for the Laplacian that involves only nearest neighbor sites[٧,٣١,٣٢],

$$\sum V_{k+a} - 4V_k = -\frac{a^{2-d}}{\varepsilon}\sum_{\alpha=+,-,e} q^\alpha p_k^\alpha \qquad (٣.١٤)$$

where:-

q^α : the charge of species α ($q^e = -e$, for the electron).

a : the lattice spacing.

d : the spatial dimension.

The boundary conditions at the metal-electrolyte interface have to be considered with special care. In a “macroscopic” picture where this interface is of arbitrary form but sharp (i.e. represented by a mathematical line), the electric field is zero in the metal, and the potential is constant and equal to the imposed boundary condition up to the sharp interface. If there is an electric field in the electrolyte, surface charges are created. In the mean-field representation outlined above, the interface is diffuse, i.e. “smeared out” over

several lattice sites, and both the definition of the boundary condition and the creation of surface charges have to be consistently implemented.

These problems are solved by the introduction of very mobile electrons diffusing from site to site in the metal, and solve the Poisson equation for all the charges, including electrons. More precisely, it is denoted by P_k^e the deviation from the neutral state expressed in electrons per site. Hence, $P_k^e > ٠$ corresponds to an excess of electrons, $P_k^e < ٠$ to an electron deficit.The time evolution of the excess electron concentration is[٣٢] ,

$$\frac{\partial P_k^e}{\partial t} = -\sum_a \tilde{J}^e_{k,k+a} \qquad (٣.١٥)$$

where:-

$\tilde{J}^e_{k,k+a}$: electronic current

The electronic current is then written as an electronic mobility times the discrete gradient of the chemical potential [٣١],

$$\tilde{J}^e_{k,k+a} = -\tilde{M}^e_{k,k+a} D_a \tilde{\mu}^e_k \qquad (٣.١٦)$$

where:-

$\tilde{M}^e_{k,k+a}$: electronic mobility from k to k+a

$\tilde{\mu}^e_k$: the local chemical potential of the electron

The electronic mobility can be determined as[٣٢],

$$\tilde{M}^e_{k,k+a} = \frac{w^e}{\mathrm{KT}} f(P_k^o) f(P_{k+a}^o)$$

(٣.١٧)

where w^e is a constant frequency prefactor and f is an interpolation function that is equal to ١ for large metal concentrations and falls to zero for low metal concentrations. With this choice, the electronic jump probability is important

only if nearest-neighbor sites k and k+a have a large enough probability to be occupied by metallic atoms. It is used for f [٣١].

$$f(P) = \frac{\tanh[(P - P_c)/\xi] + \tanh[P_c/\xi]}{\tanh[(1 - P_c)/\xi] + \tanh[P_c/\xi]} \qquad (٣.١٨)$$

a monotonic function that varies from 0 when $p = 0$ to 1 for $p = 1$, with a rapid increase through an interval in p of order ξ centered around some concentration P_c that is reminiscent of a percolation threshold. This interpolation is motivated by the fact that the metallic region must be dense enough to be connected in order to allow the electrons to propagate.

The local chemical potential of the electron is defined by[٣١,٣٢],

$$\tilde{\mu}_k^e = E_f + q^e V_k + \frac{P_k^e}{D(E_f)} \qquad (٣.١٩)$$

where:-

E_f : is the Fermi level of the metal.

$D(E_f)$: is the density of electronic state at the Fermi level.

This method provides a fast way to calculate the surface charges on the electrodes. As will be shown below, it works perfectly well at equilibrium. However, in out-of-equilibrium simulations, a problem appears on the side of the anode where the metal is dissolved. Since the mobility rapidly decreases with the metal concentration, electrons present on the metallic site before dissolution may be trapped in the electrolyte, leading to spurious electronic charges in the bulk. This problem has been solved in a phenomenological way by adding a term, which relaxes the electronic charge to zero in the electrolyte, to the evolution equation for the electrons[٣٢],

$$\frac{\partial P_k^e}{\partial t} = -\sum_a \tilde{J}_{k,k+a}^e - w^e[1 - f_r(P_k^o)]P_k^e \qquad (٣.٢٠)$$

where $f_r(p^o)$ is the same interpolation function as f , but with different parameters ξ_r and P_{cr} . With a convenient choice of these parameters, ‘‘electron relaxation’’ occurs only in the liquid.

Chapter three

٣.٧ Electron transfer

Two types of processes occur at electrodes . One kind comprises like those just discussed , in which charges (example , electron) are transferred across the metal-solution interface . Electron transfer causes oxidation or reduction to occur. Since such reactions are governed by Faraday's law (i.e., the amount of chemical reaction caused by the flow of current is proportional to the amount of electricity passed), they are called Faradaic processes. Electrodes at which Faradaic processes occur are sometimes called charge transfer electrodes . Under some conditions, a given electrode-solution interface will show a range of potentials where no charge-transfer reactions occur because such reactions are thermodynamically or kinetically unfavourable. However, processes such as adsorption and desorption can occur, and the structure of the electrode-solution interface can change with changing potential or solution composition. These processes are called nonFaradaic processes[٣٧].

When electron transfer takes places on the electrode surfaces. Metallic cations M^+ located in the electrolyte may receive an electron from a neighboring metallic site and be reduced; in turn, metal atoms in contact with the electrolyte may reject an electron to a neighboring metallic site and become an ion,

$$M_k^+ + e_{k+a}^- \Leftrightarrow M_k^o \qquad (٣.٢١)$$

The direction of the transfer depends on the relative magnitude of the electrochemical potentials of the involved species. Reduction of cations on a site k of the cathode appears when:

$$\tilde{\mu}_k^+ + \tilde{\mu}_{k+a}^e > \tilde{\mu}_k^o \qquad (٣.٢٢)$$

otherwise, the metal is oxidized. Consequently, $\sigma_{k,k+a}$ is defined as the current of electronic charges from k+a to k **(**current of positive charges from k

to k+a) reducing the cations on site k(electronic current issued from the oxidation of the metal) via a corresponding elimination (creation) of the electrons on site k+a , it is possible to write the reaction rate [٧ , ٣١ , ٣٢ ,٤٢],

$$\sigma_{k,k+a} = \omega^*_{k,k+a}(\exp\frac{\tilde{\mu}^+_k + \tilde{\mu}^e_{k+a}}{KT} - \exp\frac{\tilde{\mu}^o_k}{KT}) \qquad (٣.٢٣)$$

where:-

$\omega^*_{k,k+a}$: prefactor of the reaction rate .

This corresponds to an activated electronic charge transfer between the metal surface and the nearest-neighboring cation. The total reduction rate on site k is the sum of all the reaction paths $\sum_a \sigma_{k,k+a}$.

The coefficient $\omega^*_{k,k+a}$ determined from[٣١,٣٢],

$$\omega^*_{k,k+a} = \omega^*[1 - f(p^o_k)]f(p^o_{k+a}) \qquad (٣.٢٤)$$

where ω^* is a constant frequency factor .In this way , the transfer is localized around the metal-electrolyte interface.

The same interpolation $f(p)$ is used for the electron mobility.

Chapter three

٣.٨ **Summary of Equations used**

The different combined pieces can be divided into two groups[٧,٣١,٣٢,٣٤]:-

١. Without potential applied on the electrochemical cells:

$$\frac{\partial P_k^{\alpha}}{\partial t} = -\sum_a \tilde{J}^{\alpha}_{k,k+a} \qquad (٣.٢٥)$$

$$\alpha = +,-,o,s$$

٢. With potential applied on the electrochemical cells:

$$\frac{\partial P_k^{+}}{\partial t} = -\sum_a \tilde{J}^{+}_{k,k+a} - \sum_a \sigma_{k,k+a} \qquad (٣.٢٦)$$

$$\frac{\partial P_k^{o}}{\partial t} = -\sum_a \tilde{J}^{o}_{k,k+a} + \sum_a \sigma_{k,k+a} \qquad (٣.٢٧)$$

$$\frac{\partial P_k^{-}}{\partial t} = -\sum_a \tilde{J}^{-}_{k,k+a} \qquad (٣.٢٨)$$

$$\frac{\partial P_k^{s}}{\partial t} = -\sum_a \tilde{J}^{s}_{k,k+a} \qquad (٣.٢٩)$$

$$\frac{\partial P_k^{e}}{\partial t} = -\sum_a \tilde{J}^{e}_{k,k+a} - w^e[1 - f_r(P_k^o)]P_k^e - \sum_a \sigma_{k+a,k} \qquad (٣.٣٠)$$

$$\sum V_{k+a} - 4V_k = -\frac{a^{2-d}}{\varepsilon} \sum_{\alpha=+,-,e} q^{\alpha} p_k^{\alpha} \qquad (٣.٣١)$$

Equations (٣.٢٥) through (٣.٣١) are integrated in time by a simple Euler Scheme (with a constant or variable time step) .

CHAPTER FOUR

COMPUTER PROGRAM

٤.١ Introduction

A program is constructed in visual basic language for one-dimensional system .Through which the determination of concentration at each time and ploting the relationship between concentration (metal, cation, anion, solvent, vacancy) and position are performed which represent growth (in cathode electrode) and dissolution (in anode electrode).

٤.٢ Program for One - Dimension Cells (Method ١)

The program of one dimension cells includes two main programs:-

١. Half and Full cell without potential.

٢. Half and Full cell with potential.

٤.٢.١ Input Data for Half and Full Cells without Potential

The input data required to run the program are as follows:-

- Cell size:-
  - number of divisions of the cell.
  - electrode size in terms of divisions.
- Concentration:-
  - electrode concentrations(metal,cation,anion,solvent).
  - electrolyte concentrations(metal,cation,anion,solvent).
- Another parameters:-
  - interaction energy.
  - frequency prefactors.
  - time step.
  - number of iteration(times).

٤.٢.١.a Program Output

The outputs of the program include:-

- New concentration at any times:-
  - electrode concentrations(metal,cation,anion,solvent,vacancy).
  - electrolyte concentrations(metal,cation,anion,solvent,vacancy).
- Concentration profiles across the cell.

٤.٢.١.b Program Layout

The main program consists of six subroutine (Run new half (RN) , Run old half (RO) , Run new full (RN١) , Run old full (RN٢) , drawx and quit) .

Figure (٤.١) shows the flow chart of the main program of half and full cell without potential.

٤.٢.٢ Input Data for Half and Full Cells with Potential

The input data required to run the program are as follows:-

- Cell size :-
  - number of divisions of the cell.
  - electrode size in terms of divisions.
- Concentration:-
  - electrode concentrations(metal,cation,anion,solvent).
  - electrolyte concentrations(metal,cation,anion,solvent).
- Another parameters:-
  - interaction energy.
  - Fermi energy , density of states , permittivity.
  - frequency prefactors.
  - time step.
  - number of iteration(times).
  - pc,e,pcr,e١ for interpolations.
  - potential difference.

٤.٢.٢.a Program Output

The outputs of the program include :-

- New concentration at any times:-
  - electrode concentrations (metal , cation , anion , solvent , vacancy , electron) .
  - electrolyte concentrations (metal , cation , anion , solvent , vacancy , electron) .
- Potential and electric charge.
- Concentration profiles across a position cell.

٤.٢.٢.b Program Layout

The main program consists of six subroutine(Run new half (RN٢) , Run old half (RO٢) , Run new full (RN٣) , Run old full (RN٣) , drawx and quit) .

Figure (٤.٢) shows a flow chart of the main program of half and full cell with potential.

The subroutines (RN , RN١ , RN٢ and RN٣) determine concentrations for the first time at certain times while the subroutines (RO , RO١ , RO٢ and RO٣) determine new concentrations based on previous ones at certain times.The subroutines (RN , RO , RN١ and RO١) deal with equation (٣.٢٥) while the subroutines RN٢ , RO٢ , RN٣ and RO٣ deal with equations (٣.٢٦) , (٣.٢٧) , (٣.٢٨) , (٣.٢٩) , (٣.٣٠) and (٣.٣١) . The subroutines (drawx) plots the relation ship between concentrations and the positions of half and full cell . The subroutine (quit) is used to exit from the program .

٤.٣ Program for One - Dimension Cells (Method ٢)

The program of this method is as that of the preceding one but they are different in the following points:-

١. Using diffusion current equation (٣.٨) instead of equation (٣.٧) .
٢. Calculate of electrochemical potential in the first method (metal and cation) while the second method (metal,cation,anion and solvent).

CHAPTER FIVE

RESULTS AND DISCUSSION

٥.١ Introduction

A representation of the results obtained from running computer programs including boundary conditions stated in Tables (٥.١) and (٥.٢) to simulate growth, dissolution,ions kinetics, charges distribution and electric potential in one-dimensional cells with input of the data mentioned in articles (٤.٢) and (٤.٣) with dimensionless values given in Tables (٥.٣) and (٥.٤) . Also studying the concentrations effects , Fermi energy , potential and spacing between two electrodes on the deposition process and the comparison between the two diffusion current equations (٣.٧) and (٣.٨) from the view point of deposition ,ionic evolution,charge distribution are achieved .

CHAPTER SIX

CONCLUSIONS AND RECOMMENDATIONS

٦.١ Conclusions :-

Based on the results of this investigation, the following conclusions can be drawn :-

١. The mean-field kinetic equations (MFKE) that are able to reproduce qualitatively the behavier of electrochemical cells with planar electrodes.

٢. The growth starts in the one - dimensional electrochemical cells and continues up it maximum value and then gradually stops at time 10^6 for the cell of size (١٠٠ ×١٠) , while in the cells subjected to potential difference of ٢KT/e , the deposition process continues for a longer time up to anode collapsing .

٣. The evolution of the ion concentration is seen to be constant and unchanged in the absence of the potential difference and gradually drops until it stops at time 10^6 , while it has certain gradients under potential difference between the cathode and anode electrodes , furthermore the cation has a peak at the cathode is higher than that of anion concentration and the revers occurs at the anode electrode .

٤. Appearing of Helmholtze double layer in the absence of the potential difference while in the cell subjected to a potential difference leads naturally to the formation of the extended space charge and the Helmholtze double layer .

٥. The extended space charge to play a crucial role in the selection of the growth velocity and the dense branching structure of the deposit and that what is confirmed by Fleury and others[٤٣].

٦. Increasing of the electric potential across the sites results in deposition increasing , as well as increase of each of the initial ion concentration , Fermi energy and potential difference results in increasing of deposition

while spacing increasing between the electrodes results in decreasing of the deposition process .

٧. In the half cell , the first method of the diffusion has a higher deposition and electric potential and a wider spaced area of the charge distribution at time $t = 5\times10^{5}$ and the reverse holds for the full cell .

٨. Ionic concentration growth for the half cell is less for the first method than that of the second one while the second method ionic concentration growth at the cathode is higher than that of the first method and the reverse holds at the anode for the full cell .

٩. The (MFKE) contains all the ingredients necessary to simulate dendritic growth by electrodposition in two and three dimensions .

٦.٢ Recommendations for Future Work

The following recommendations are suggested for future work :-

١. Investigating two and three – dimensional simulations in electroplating cells .

٢. Study the effect of mass transfer / mixing on the rate of electrochemical reaction .

٣. Study the effect of heat transfer on electrochemical dynamics .

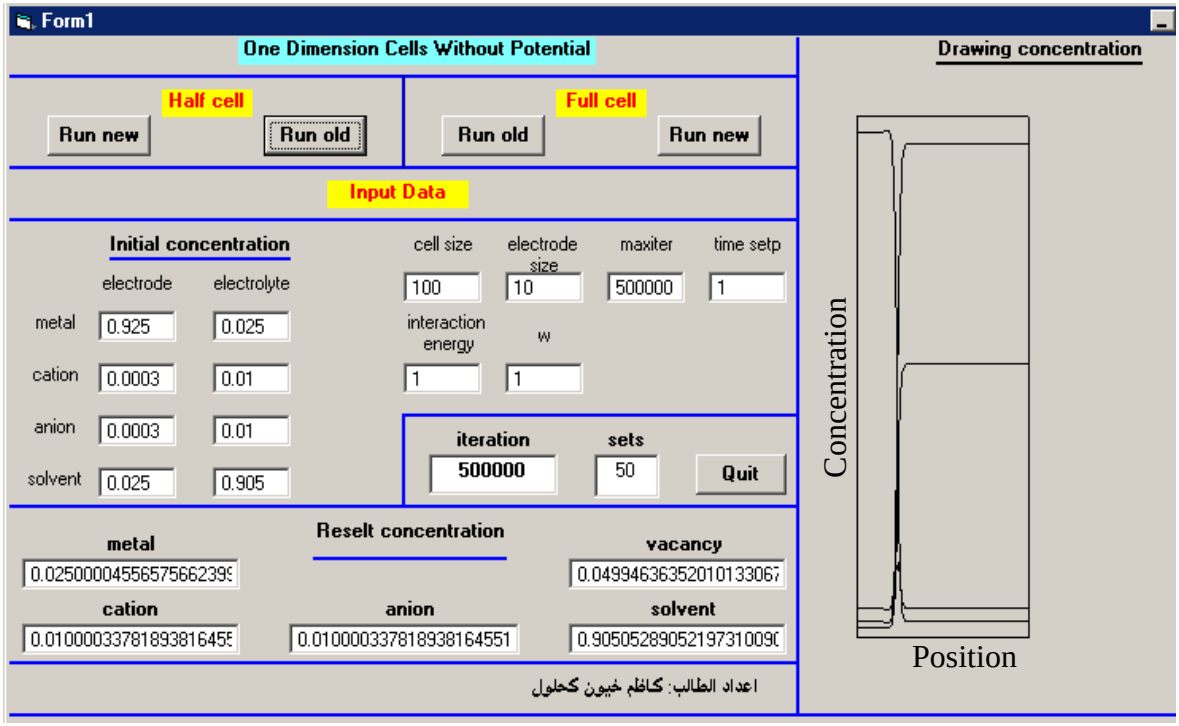

Figure (٤.١) Shows the flow chart of the main program of half and full cell without potential

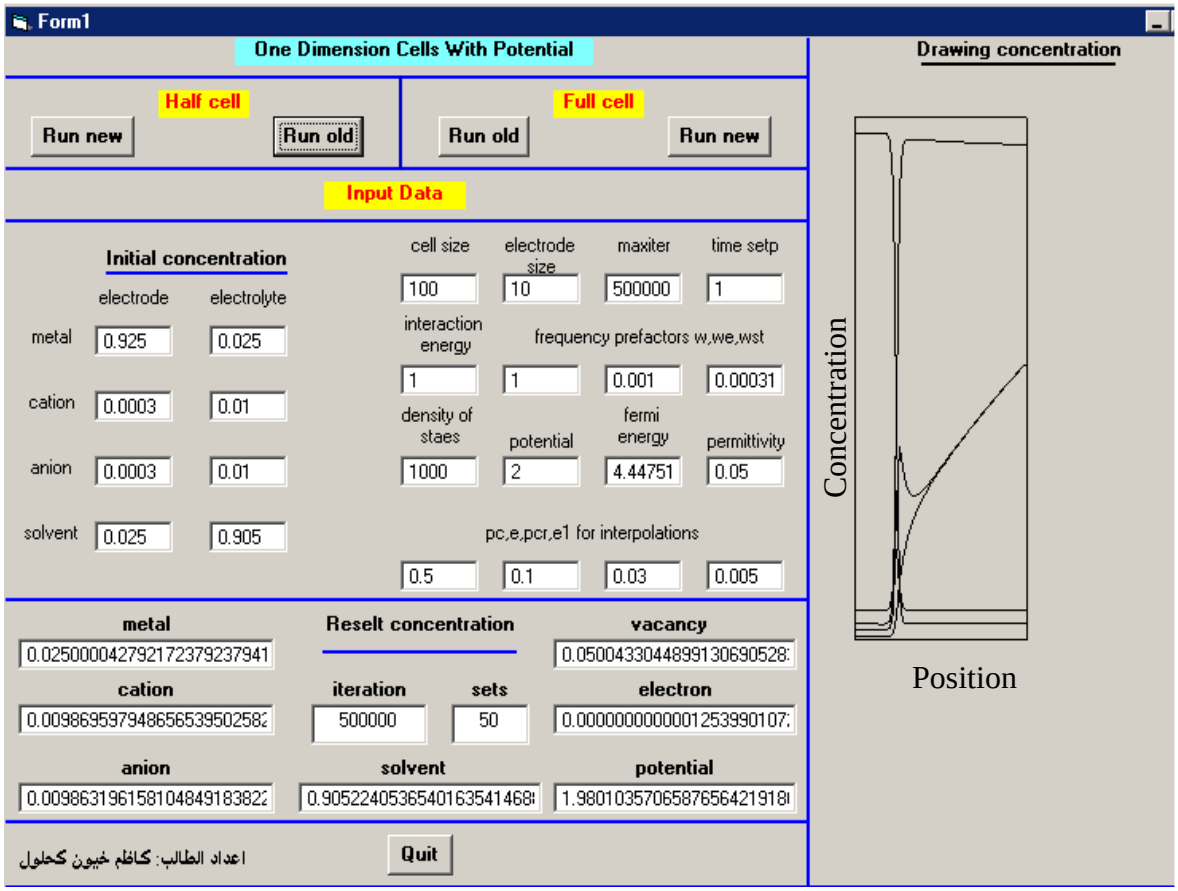

Figure (٤.٢) Shows the flow chart of the main program of half and full cell with potential

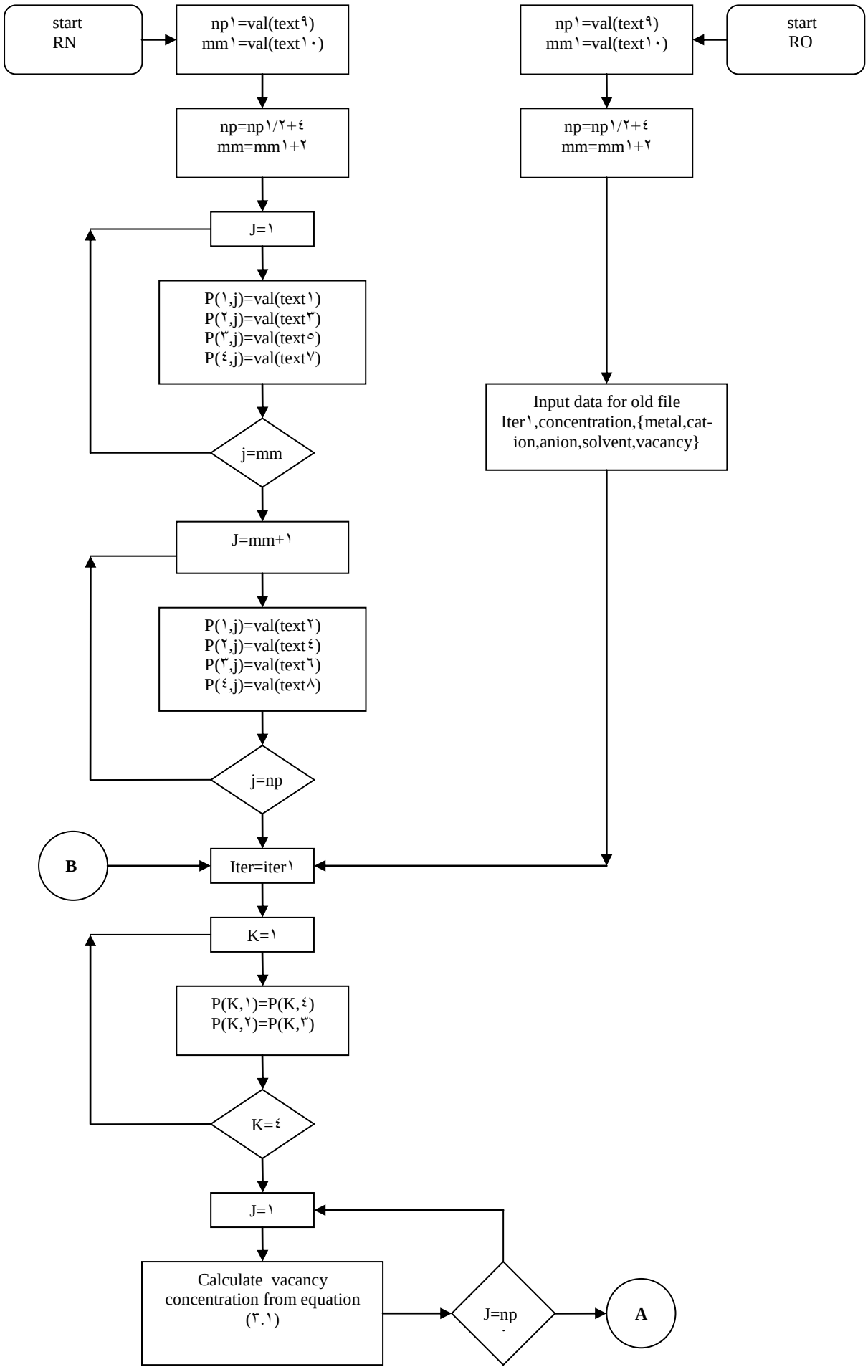
start
RN
np١=val(text٩)
mm١=val(text١٠)
np=np١/٢+٤
mm=mm١+٢
J=١
P(١,j)=val(text١)
P(٢,j)=val(text٣)
P(٣,j)=val(text٥)
P(٤,j)=val(text٧)
j=mm
J=mm+١
P(١,j)=val(text٢)
P(٢,j)=val(text٤)
P(٣,j)=val(text٦)
P(٤,j)=val(text٨)
j=np
B
Iter=iter١
K=١
P(K,١)=P(K,٤)
P(K,٢)=P(K,٣)
K=٤
J=١
Calculate vacancy concentration from equation (٣.١)
J=np
A
np١=val(text٩)
mm١=val(text١٠)
start
RO
np=np١/٢+٤
mm=mm١+٢
Input data for old file
Iter١,concentration,{metal,cat-ion,anion,solvent,vacancy}

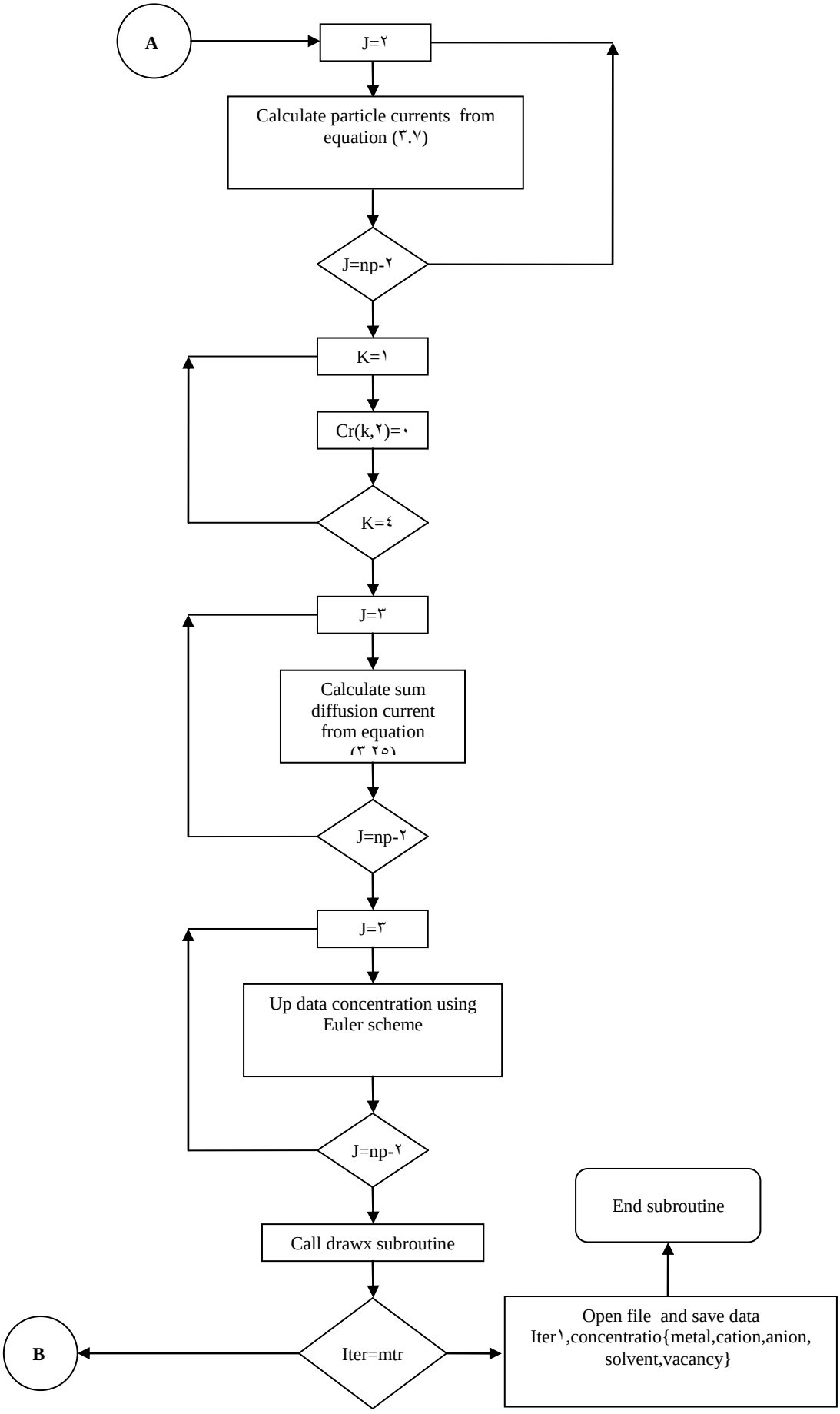

Figure (٤.٣) The logic flow chart of two subroutines RN and RO

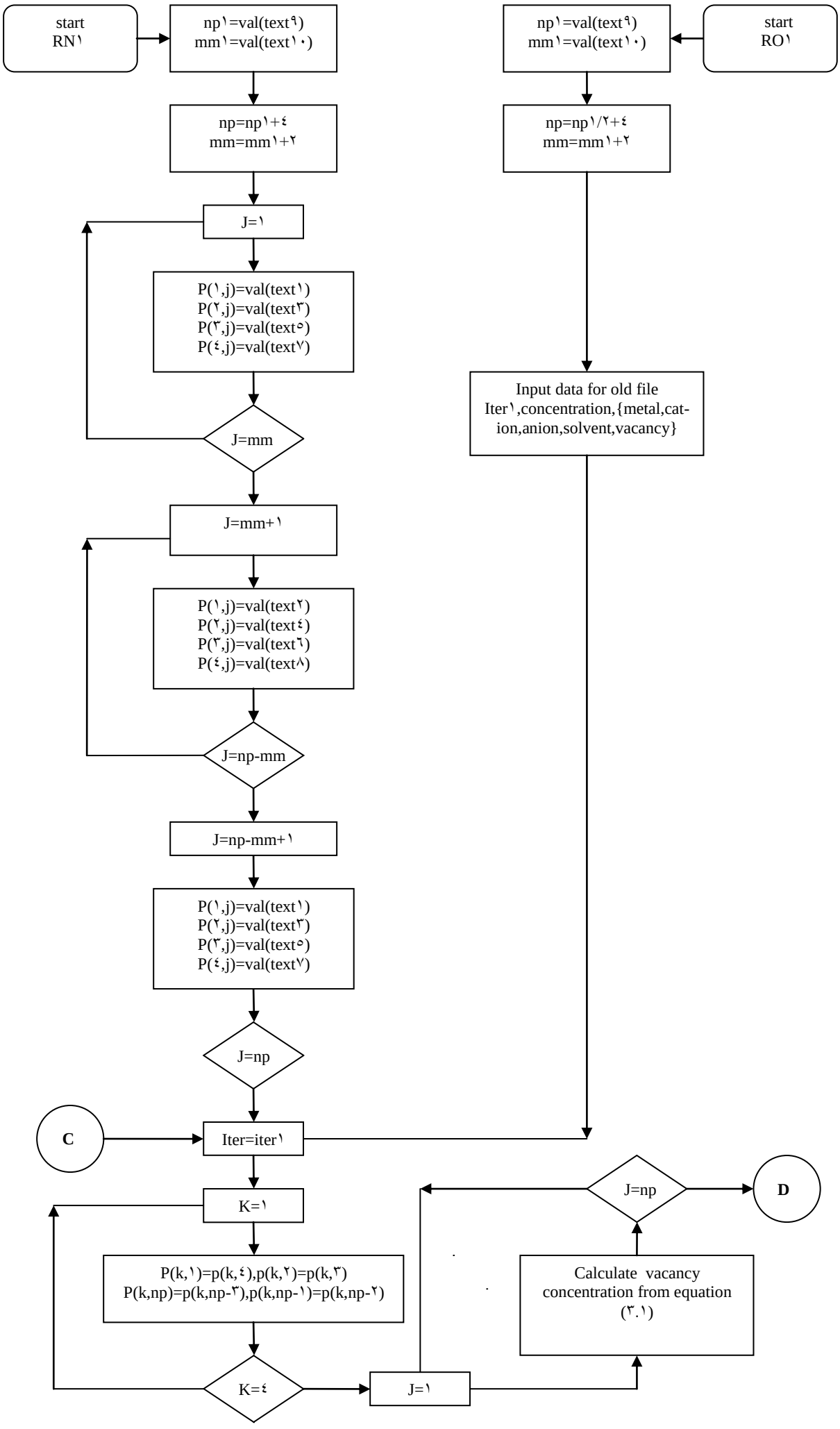
start
RN١
np١=val(text٩)
mm١=val(text١٠)
np=np١+٤
mm=mm١+٢
J=١
P(١,j)=val(text١)
P(٢,j)=val(text٣)
P(٣,j)=val(text٥)
P(٤,j)=val(text٧)
J=mm
J=mm+١
P(١,j)=val(text٢)
P(٢,j)=val(text٤)
P(٣,j)=val(text٦)
P(٤,j)=val(text٨)
J=np-mm
J=np-mm+١
P(١,j)=val(text١)
P(٢,j)=val(text٣)
P(٣,j)=val(text٥)
P(٤,j)=val(text٧)
J=np
C
Iter=iter١
K=١
P(k,١)=p(k,٤),p(k,٢)=p(k,٣)
P(k,np)=p(k,np-٣),p(k,np-١)=p(k,np-٢)
K=٤
J=١
Calculate vacancy concentration from equation (٣.١)
J=np
D
np١=val(text٩)
mm١=val(text١٠)
start
RO١
np=np١/٢+٤
mm=mm١+٢
Input data for old file
Iter١,concentration,{metal,cat-ion,anion,solvent,vacancy}

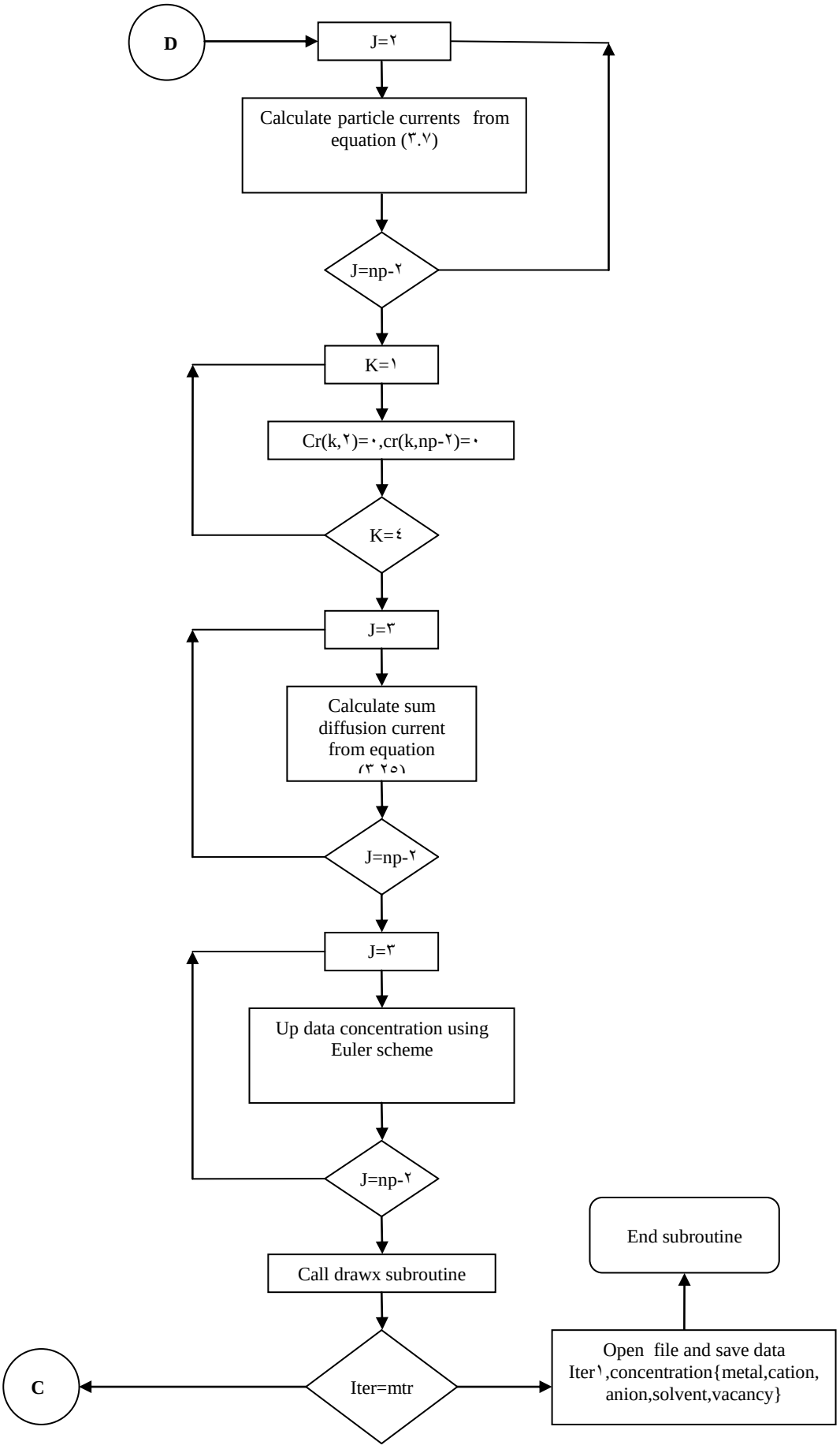

Figure (٤.٤) The logic flow chart of two subroutines RN١ and RO١

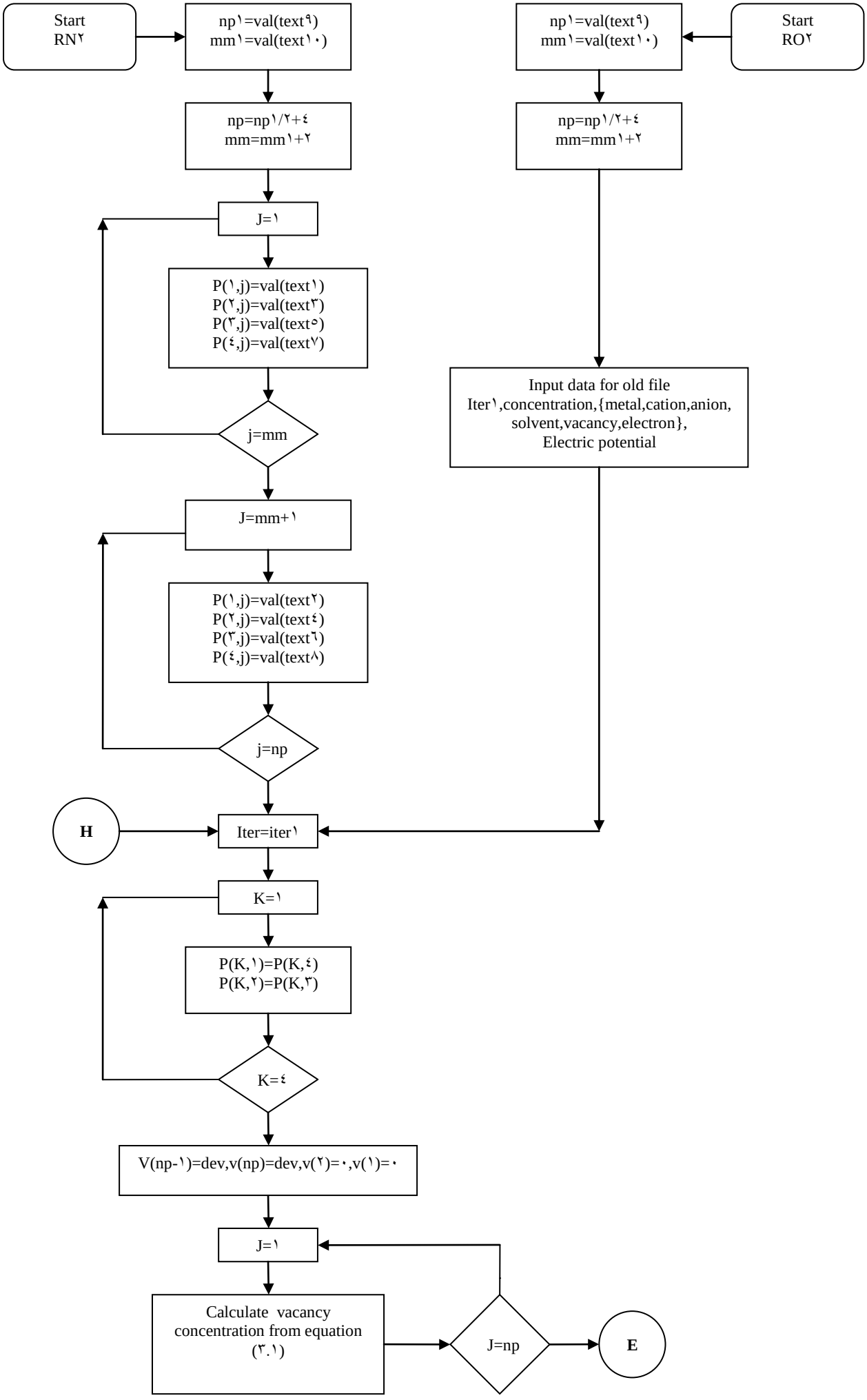
Start
RN٢
np١=val(text٩)
mm١=val(text١٠)
np=np١/٢+٤
mm=mm١+٢
J=١
P(١,j)=val(text١)
P(٢,j)=val(text٣)
P(٣,j)=val(text٥)
P(٤,j)=val(text٧)
j=mm
J=mm+١
P(١,j)=val(text٢)
P(٢,j)=val(text٤)
P(٣,j)=val(text٦)
P(٤,j)=val(text٨)
j=np
H
Iter=iter١
K=١
P(K,١)=P(K,٤)
P(K,٢)=P(K,٣)
K=٤
V(np-١)=dev,v(np)=dev,v(٢)=٠,v(١)=٠
J=١
Calculate vacancy concentration from equation (٣.١)
J=np
E
np١=val(text٩)
mm١=val(text١٠)
Start
RO٢
np=np١/٢+٤
mm=mm١+٢
Input data for old file
Iter١,concentration,{metal,cation,anion,
solvent,vacancy,electron},
Electric potential

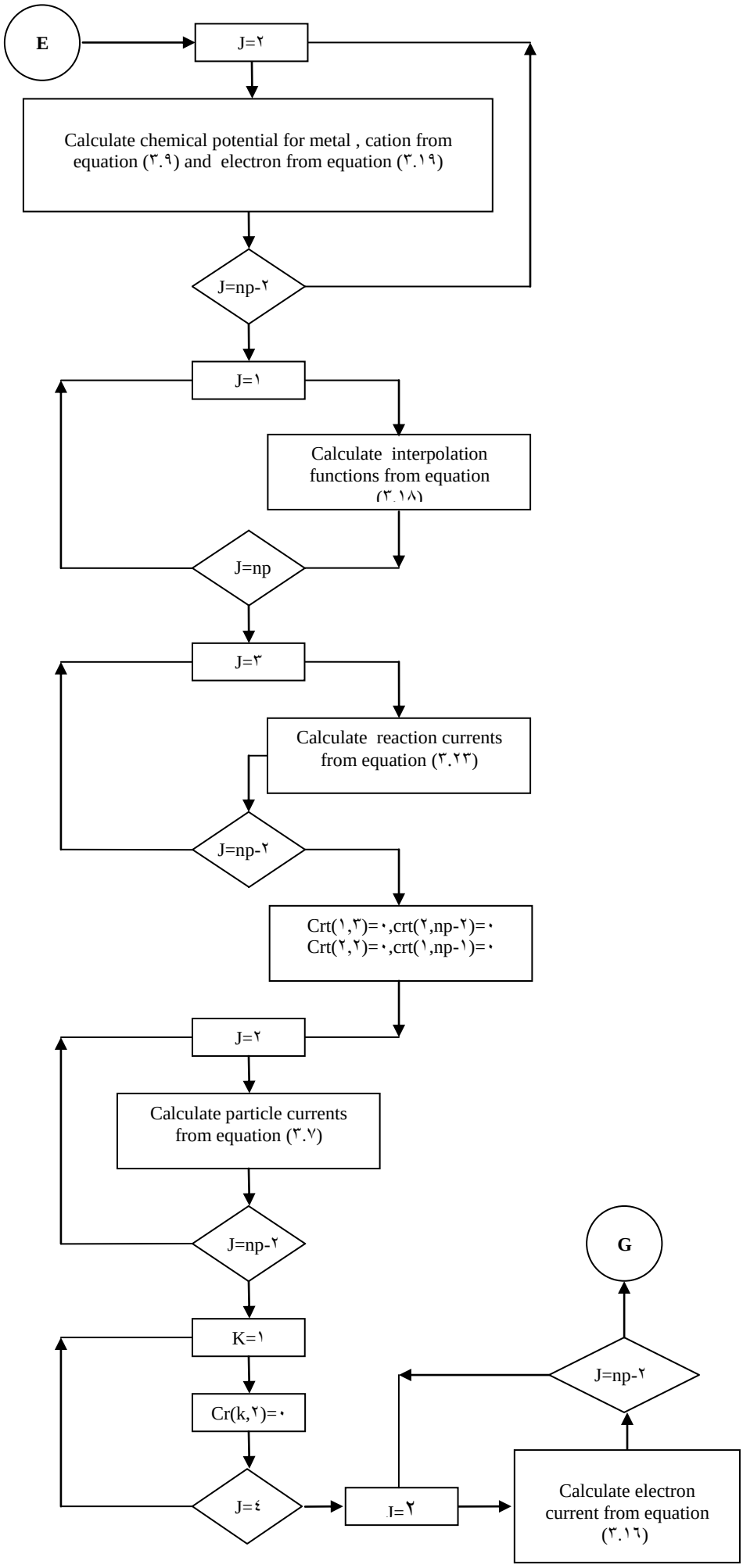
E
J=٢
Calculate chemical potential for metal , cation from equation (٣.٩) and electron from equation (٣.١٩)
J=np-٢
J=١
Calculate interpolation functions from equation (٣.١٨)
J=np
J=٣
Calculate reaction currents from equation (٣.٢٣)
J=np-٢
Crt(١,٣)=٠,crt(٢,np-٢)=٠
Crt(٢,٢)=٠,crt(١,np-١)=٠
J=٢
Calculate particle currents from equation (٣.٧)
J=np-٢
K=١
Cr(k,٢)=٠
J=٤
I=٢
Calculate electron current from equation (٣.١٦)
J=np-٢
G

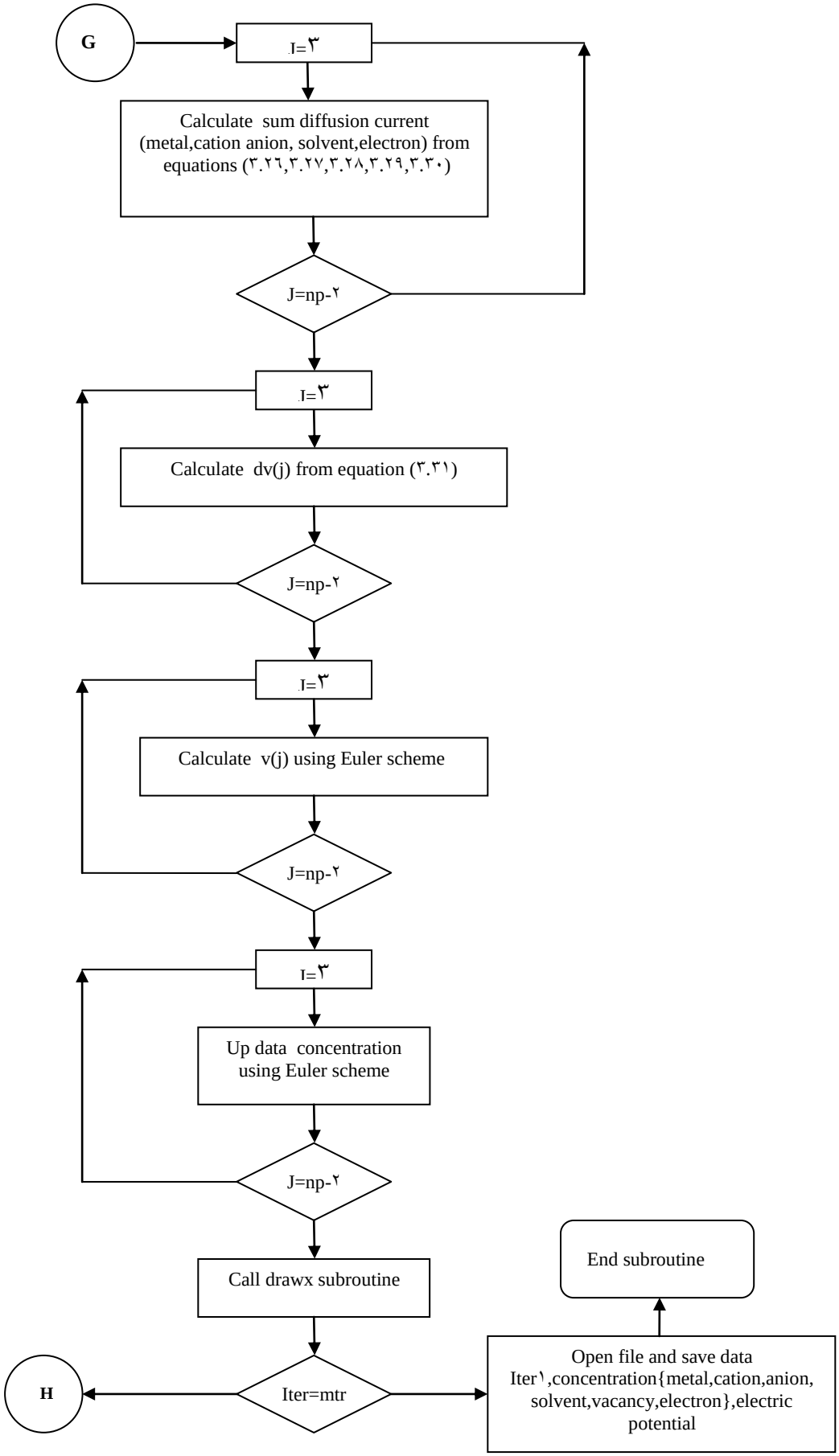

Figure (٤.٥) The logic flow chart of two subroutines RN٢ and RO٢

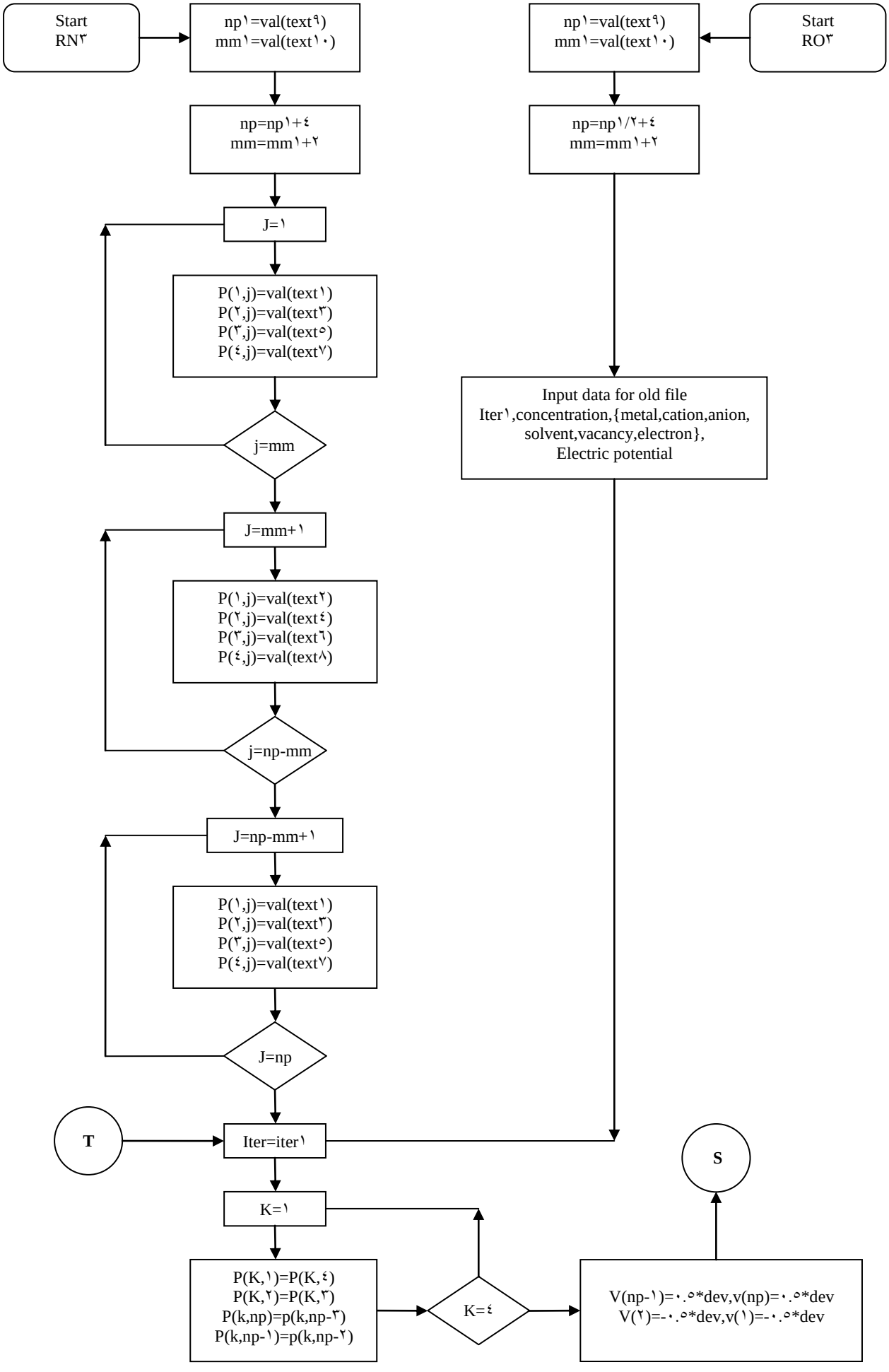
Start
RN٣
np١=val(text٩)
mm١=val(text١٠)
np=np١+٤
mm=mm١+٢
J=١
P(١,j)=val(text١)
P(٢,j)=val(text٣)
P(٣,j)=val(text٥)
P(٤,j)=val(text٧)
j=mm
J=mm+١
P(١,j)=val(text٢)
P(٢,j)=val(text٤)
P(٣,j)=val(text٦)
P(٤,j)=val(text٨)
j=np-mm
J=np-mm+١
P(١,j)=val(text١)
P(٢,j)=val(text٣)
P(٣,j)=val(text٥)
P(٤,j)=val(text٧)
J=np
T
Iter=iter١
K=١
P(K,١)=P(K,٤)
P(K,٢)=P(K,٣)
P(k,np)=p(k,np-٣)
P(k,np-١)=p(k,np-٢)
K=٤
V(np-١)=٠.٥*dev,v(np)=٠.٥*dev
V(٢)=-٠.٥*dev,v(١)=-٠.٥*dev
S
np١=val(text٩)
mm١=val(text١٠)
Start
RO٣
np=np١/٢+٤
mm=mm١+٢
Input data for old file
Iter١,concentration,{metal,cation,anion,
solvent,vacancy,electron},
Electric potential

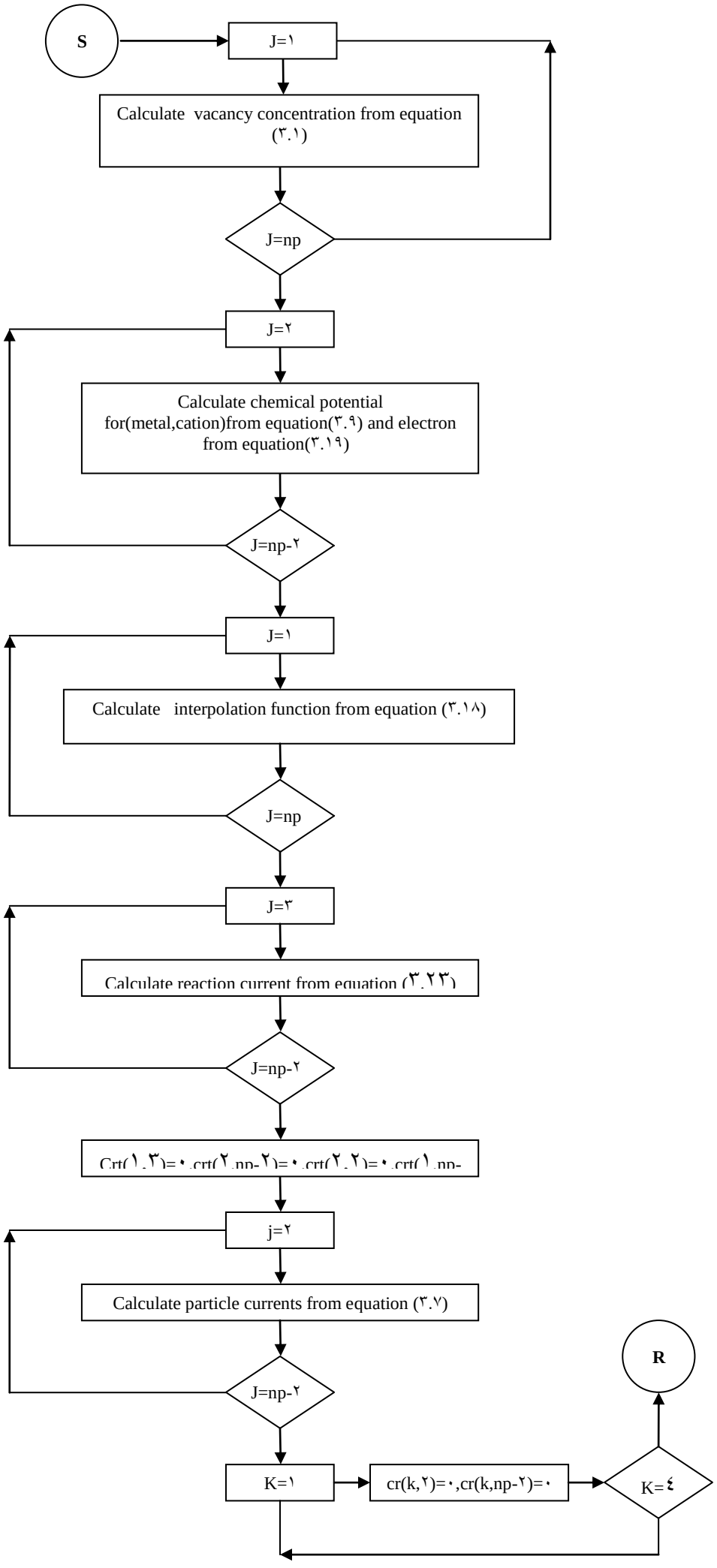
S
J=١
Calculate vacancy concentration from equation (٣.١)
J=np
J=٢
Calculate chemical potential for(metal,cation)from equation(٣.٩) and electron from equation(٣.١٩)
J=np-٢
J=١
Calculate interpolation function from equation (٣.١٨)
J=np
J=٣
Calculate reaction current from equation (٣.٢٣)
J=np-٢
Crt(١,٣)=٠,crt(٢,np-٢)=٠,crt(٢,٢)=٠,crt(١,np-
j=٢
Calculate particle currents from equation (٣.٧)
J=np-٢
K=١
cr(k,٢)=٠,cr(k,np-٢)=٠
K=٤
R

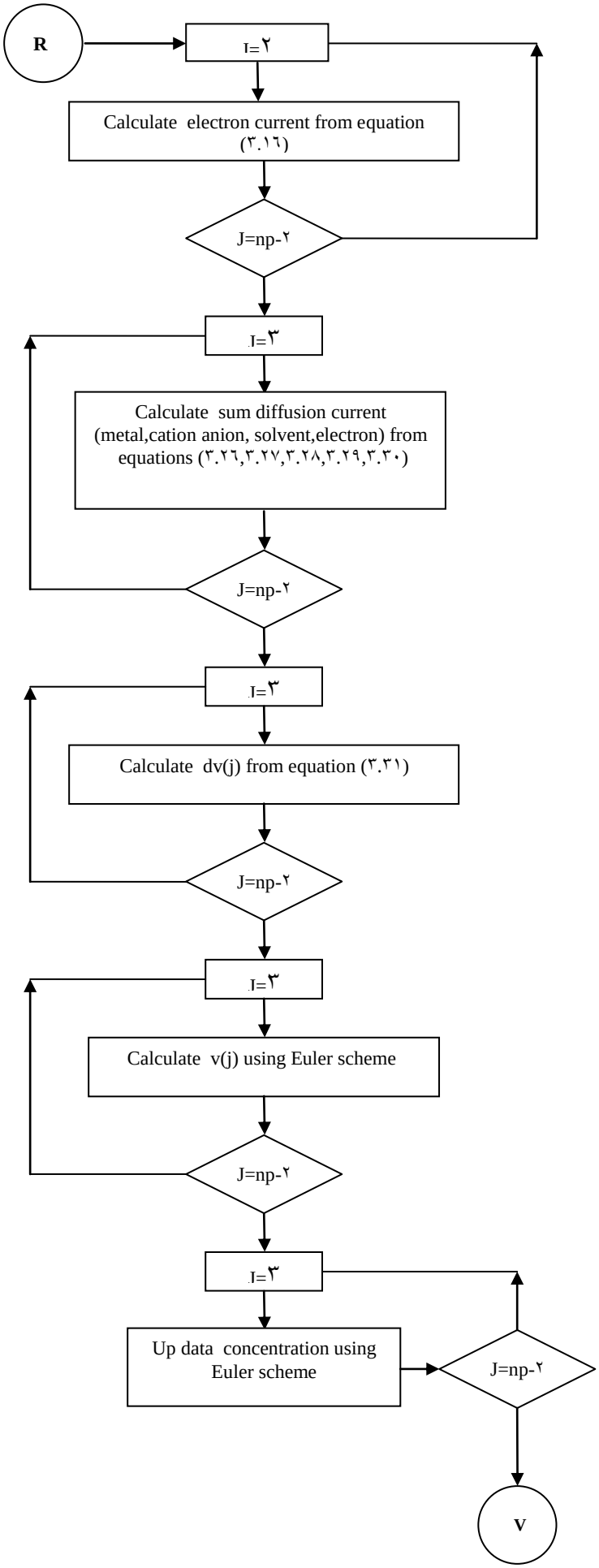
R
I=٢
Calculate electron current from equation (٣.١٦)
J=np-٢
I=٣
Calculate sum diffusion current (metal,cation anion, solvent,electron) from equations (٣.٢٦,٣.٢٧,٣.٢٨,٣.٢٩,٣.٣٠)
J=np-٢
I=٣
Calculate dv(j) from equation (٣.٣١)
J=np-٢
I=٣
Calculate v(j) using Euler scheme
J=np-٢
I=٣
Up data concentration using Euler scheme
J=np-٢
V

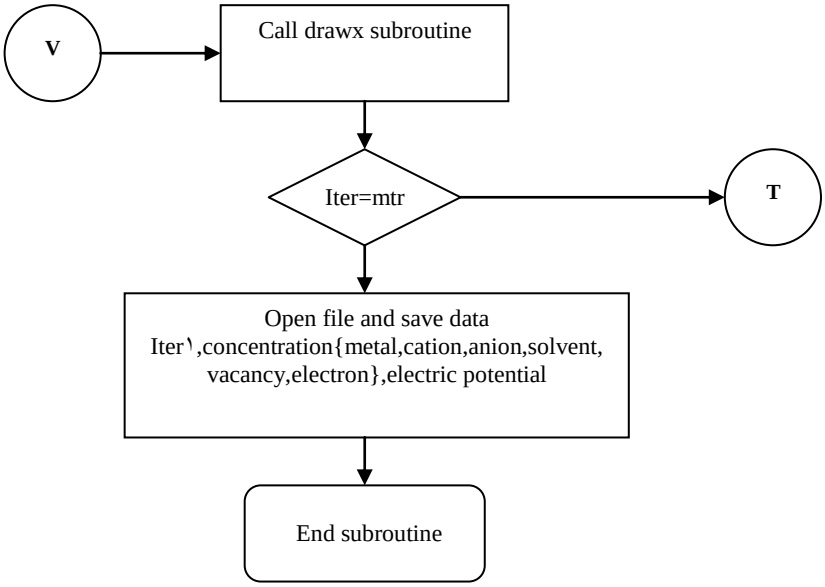

Figure (٤.٦) The logic flow chart of two subroutines RN٣ and RO٣

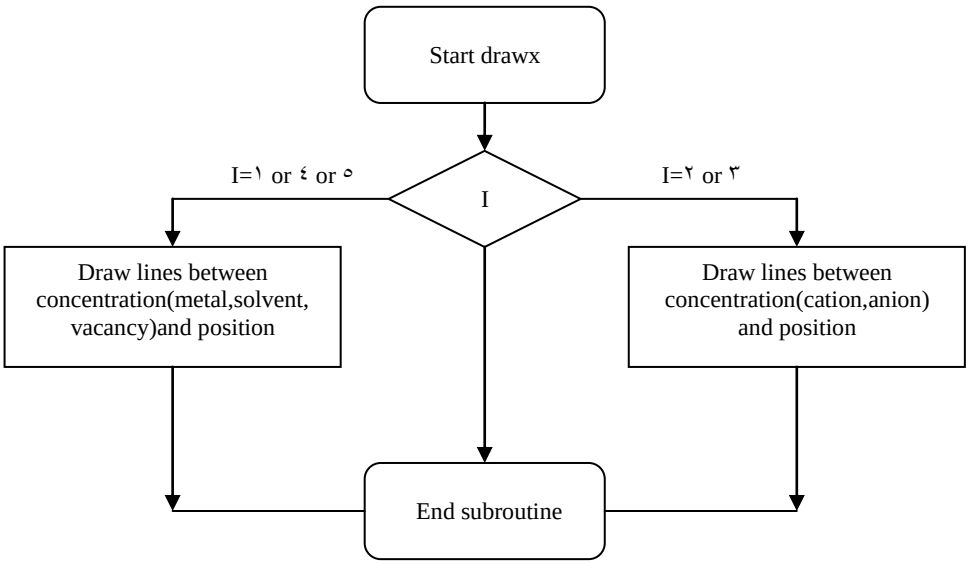

Figure (٤.٧) The logic flow chart of the subroutine drawx

Table (٥.١) Boundary conditions for one-dimensional cells without potential

Half cell	Full cell
١. no - flux boundary conditions in the solid ٢. fixed concentration in the liquid ٣. no - flux boundary conditions for particles at solid side	١. no - flux boundary conditions in the solid and liquid ٢. no - flux boundary conditions for particles at both sides

Table (٥.٢) Boundary conditions for one-dimensional cells with potential

Half Cell	Full Cell
١. no -flux boundary conditions in the solid ٢. fixed concentration in the liquid ٣. potential zero at solid side. Potential at liquid side. ٤. no - flux boundary conditions for the reaction current ٥. no - flux boundary conditions for particles at solid side	١. no - flux boundary conditions in the solid and liquid ٢. +/- potential /٢ at both side ٣. no - flux boundary conditions for the reaction current ٤. no - flux boundary conditions for particles at both side

Table (٥.٣) Program input data without potential

Type of cell	Number of divisions of the cell	Electrode size		Initial concentration of electrode	Initial concentration of electrolyte	$\varepsilon^{\alpha\beta}$	w^{α}	Δt	Times (t)	
		cathode	anode							
Half cell	٥٠	١٠	-	$P^{O}s = 0.925$ $P^{\pm}s = 0.0003$ $P^{S}s = 0.025$	$P^{O}l = 0.025$ $P^{\pm}l = 0.01$ $P^{S}l = 0.905$	١	١	١	٥٠٠٠٠	١٠٠٠٠٠٠
Full cell	١٠٠	١٠	١٠	=	=	١	١	١	=	=

Calculate initial concentration:

, KT=١ , Q=٠.٩ , pl =٠.٠١, z=٤ $\varepsilon^{oo} = 1, \varepsilon^{ss} = 1, \varepsilon^{\pm s} = 1, \varepsilon^{os} = 0$

$\varepsilon^{-} = (\varepsilon^{oo} + \varepsilon^{ss} - 2\varepsilon^{os})/2 = 1$

$p = Q/\tanh(\frac{z\varepsilon^{-}Q}{2KT}) = 0.95056$, $p^{\pm}l = pl = 0.01$, $p^{o}s = 0.5(p+Q) = 0.925$

, $P^{S}s = 0.5(P-Q) = 0.025$, $p^{\pm}s = p^{\pm}l \times \exp(\frac{-2\varepsilon^{\pm}Q}{KT}) = 0.0003$ $p^{o}l = 0.5(p-Q) = 0.025$, $p^{s}l = 0.5(p+Q) - 2\times pl = 0.905$

Z : the coordination number(z=٤ for a square lattice in two dimensions)

pl : the ion concentration in liquid

: the reduced interaction energy ε^{-}

p: total concentration in liquid and solid

Table (٥.٤) Program input data with potential

Type of cell	Number of divisions of the cell	Electrode size		Initial concentration of electrode	Initial concentration of electrolyte	$\varepsilon^{\alpha\beta}$	E_f	$D(E_f)$	ε	w^{α}	w^{e}	w^{*}	parameters of interpolation	dV	Δt	Times (t)
		Cathode	Anode													
Half cell	٥٠	١٠	-	$p^{o}s = 0.925$ $p^{\pm}s = 0.0003$ $p^{s}s = 0.025$	$p^{o}l = 0.025$ $p^{\pm}l = 0.01$ $p^{s}l = 0.905$	١	٤.٤٤٧٥١٤	١٠٠٠/KT	٠.٠٥	١	٠.٠٠١	٠.٠٠٠٣١٦	$p_c = 0.5$ $e = 0.1$ $p_{cr} = 0.03$ $e_1 = 0.001$	٢KT/e	١	١٠٠٠٠٠ ٣٠٠٠٠٠ ٥٠٠٠٠٠
Full cell	١٠٠	١٠	١٠	=	=	=	=	=	=	=	=	=	=	=	=	=
$q^{o} = ٠$		$q^{-} = -e = -١$		$q^{e} = -e = -١$	$q^{+} = e = ١$	e = ١		KT = ١	Number of substeps=١		Freqnency wpoiss=٠.١		dimenionless			

٥.٢ Simulation of One-Dimensional Cells without Potential

When there is no applied potential across a cell of size ١٠٠ sites contains two identical electrodes with thickness of ١٠ layers , the ionic species start to diffuse and migration , a double layer appear on the interface , reduction process on the cathode and oxidation process on the anode take place .

Figures (٥.١ - ٥.٤) represents simulation of the different species , namely : (metal,cation,anion,solvent and vacancy) across the sites ٥٠ for the half cell and ١٠٠ sites for the full cell with initial ion concentration of ٠.٠١ during time intervals of $t = (0.5,10)\times10^{5}$.

Figures (٥.٥ – ٥.٧) show the growth (deposition) occurred at the cathode and dissolution at the anode . It is noted from these figures that the doposition starts to be minimized (dropped) until it reachs a time of 10^{6} at which it is stopped , because of dropping the chemical potential differences across the cell below 10^{-9}, due to the fact that there is no deposition at lower chemical potentials.

Figures (٥.٨ - ٥.١٣) show the gradient of evolution of the ionic concentrations , while there is no such a gradient between the cathode and the anode electrodes but it is approximately constant. These ionic concentration slowly drop with time till it stopped, and hence , the deposition also stop, this is matched with (Bernard , Plapp and Gouyet),[٣٢] .

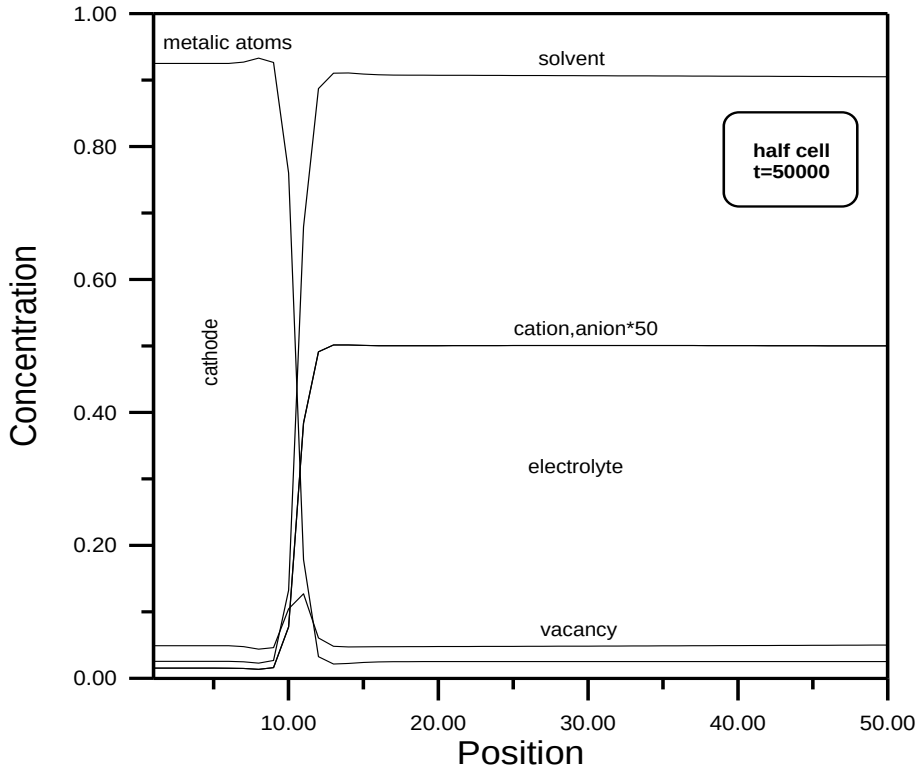

Figure(٥.١) Concentration profiles across a ٥٠-site cell.

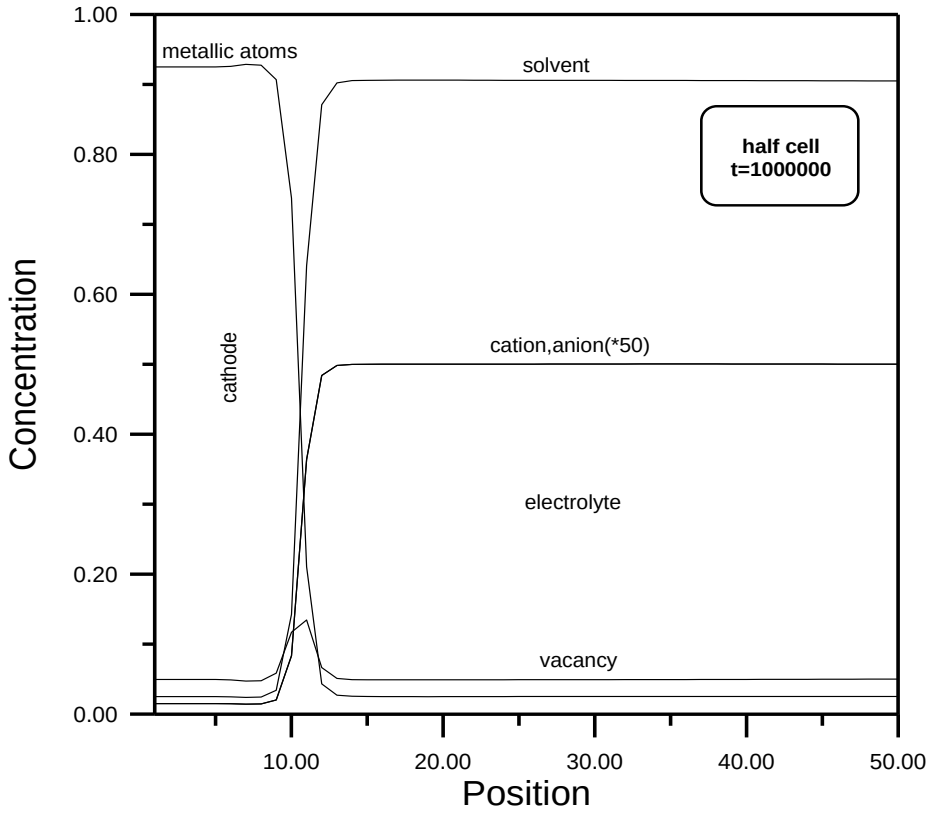

Figure(٥.٢) Concentration profiles across a ٥٠-site cell.

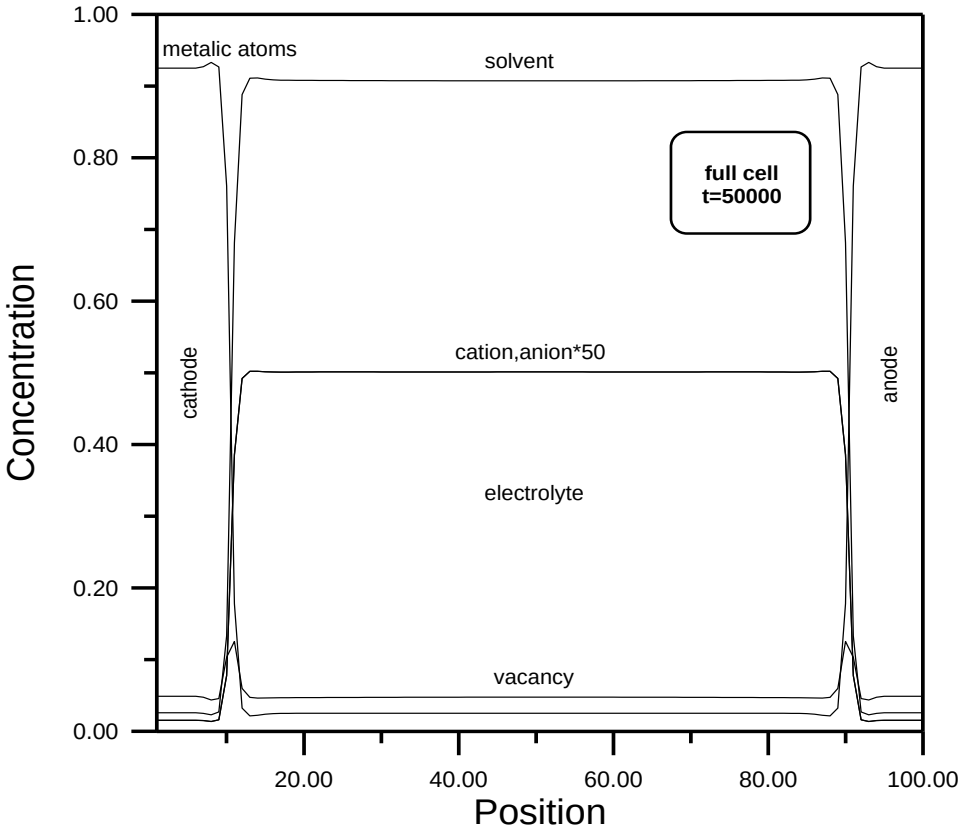

Figure(٥.٣) Concentration profiles across a ١٠٠-site cell.

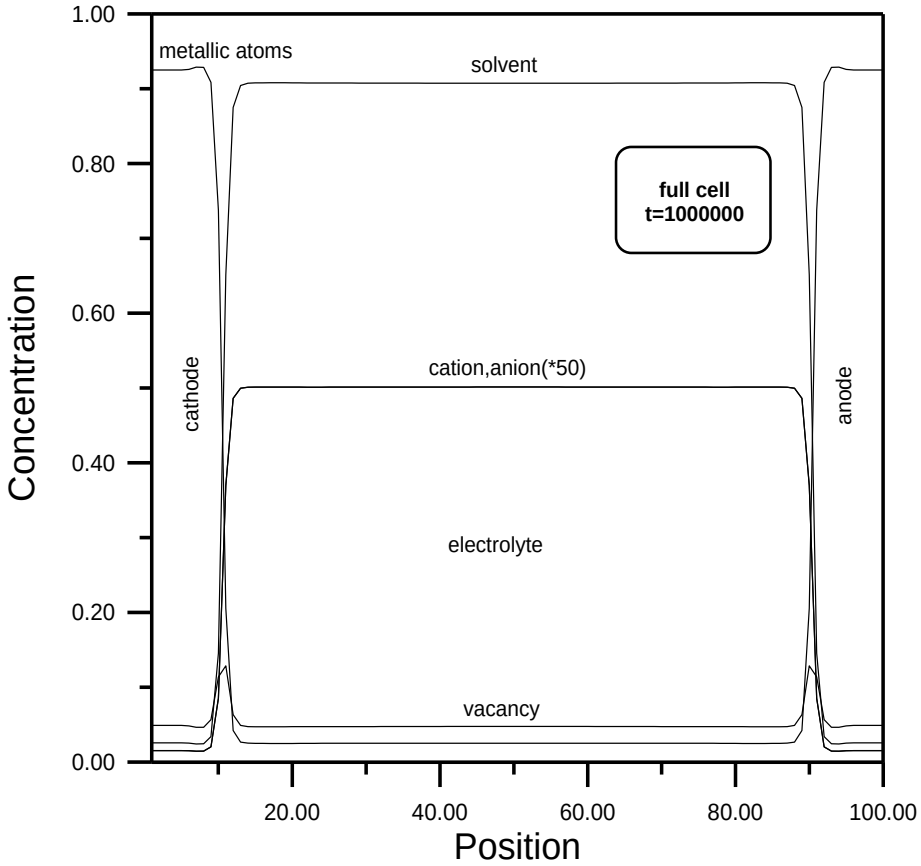

Figure(٥.٤) Concentration profiles across a ١٠٠-site cell .

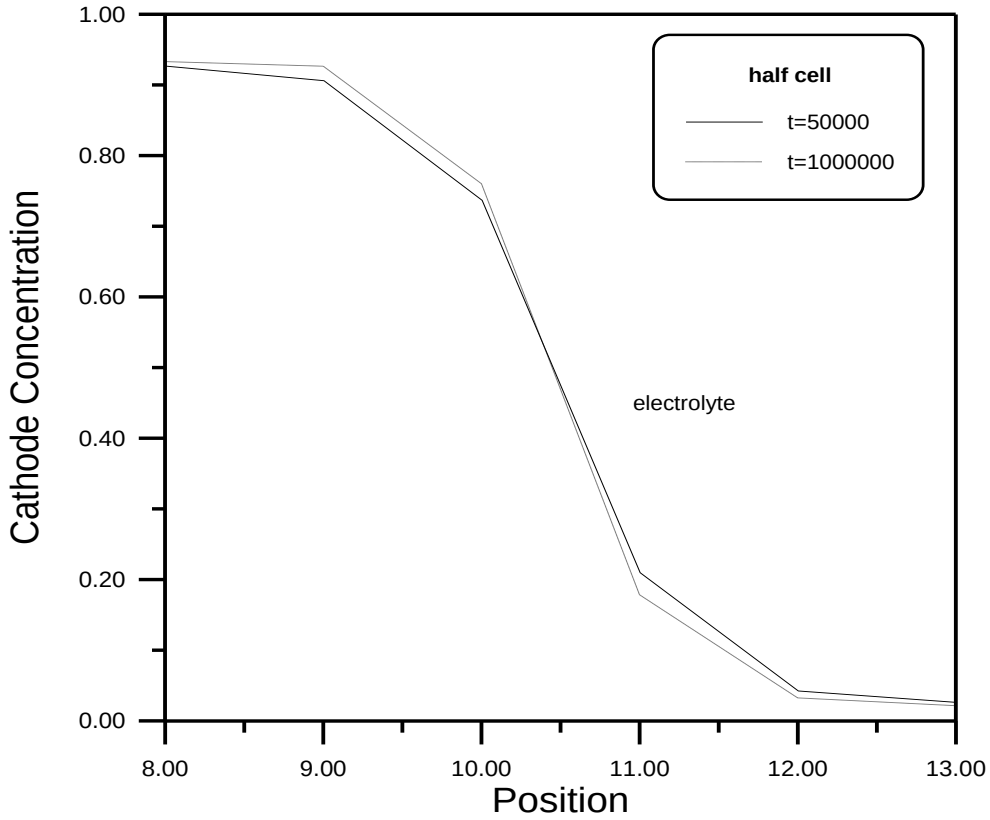

Figure(٥.٥) Showing the electrode position (reduction) at the cathode.

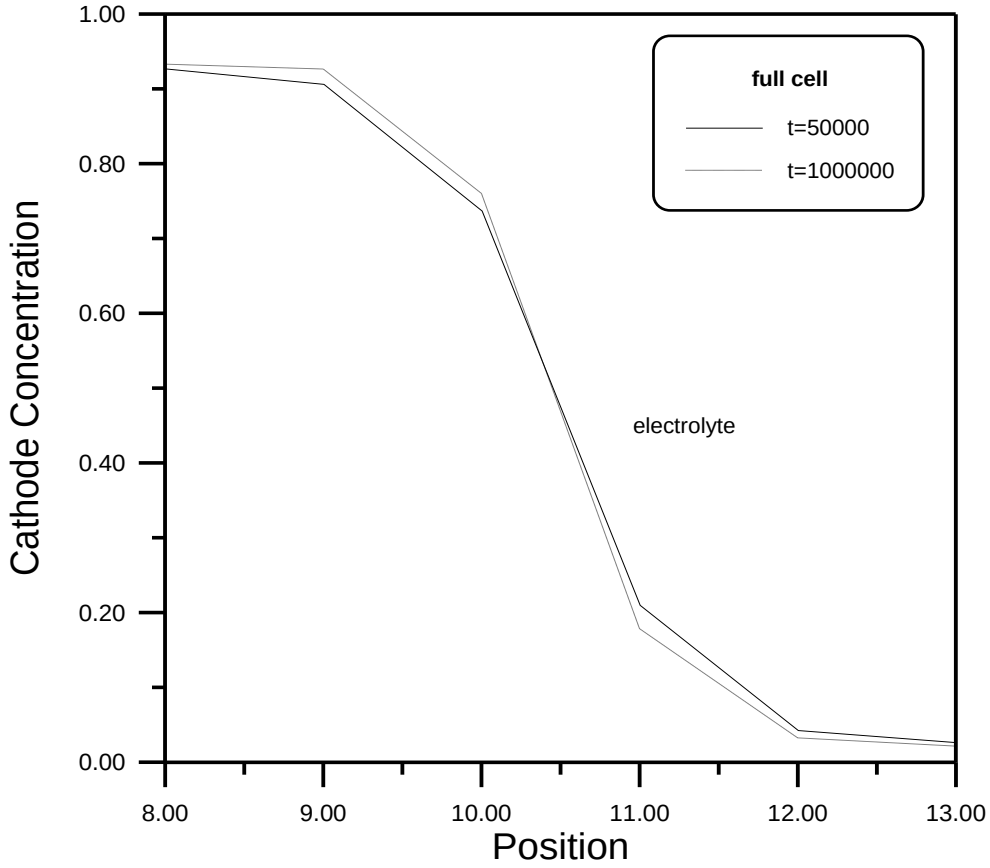

Figure(٥.٦) Showing the electrode position (reduction) at the cathode.

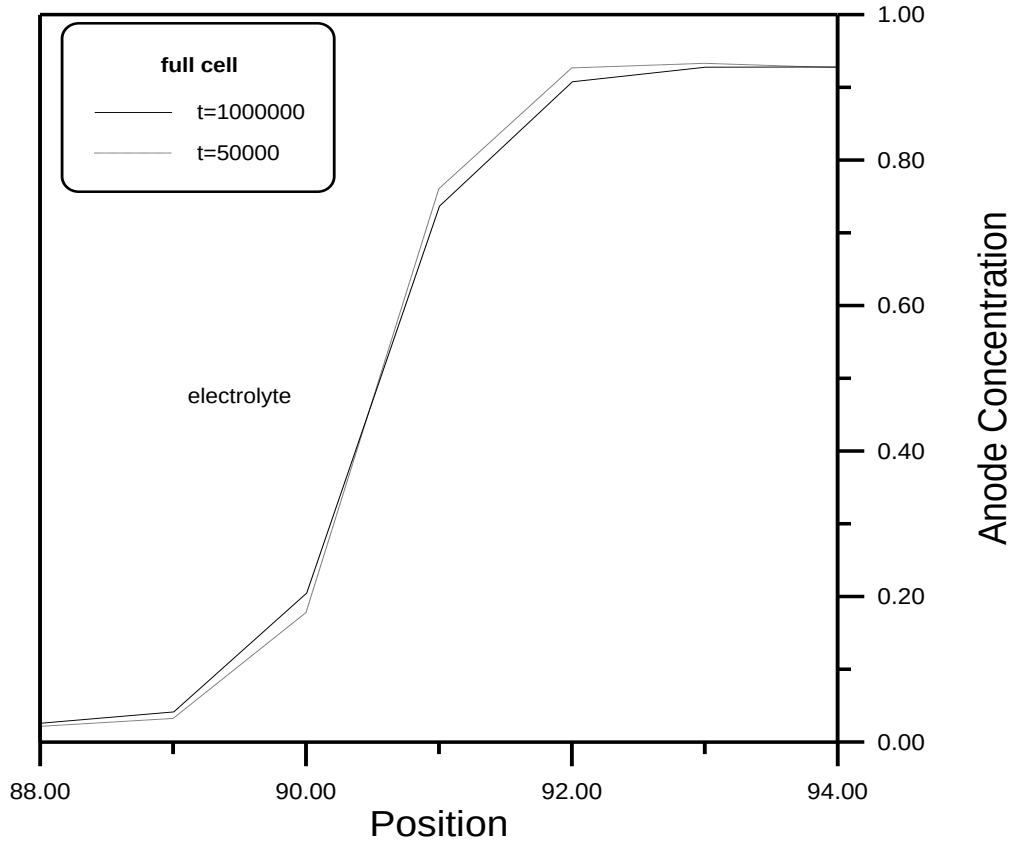

Figure(٥.٧) Showing the dissolution of metal at the anode.

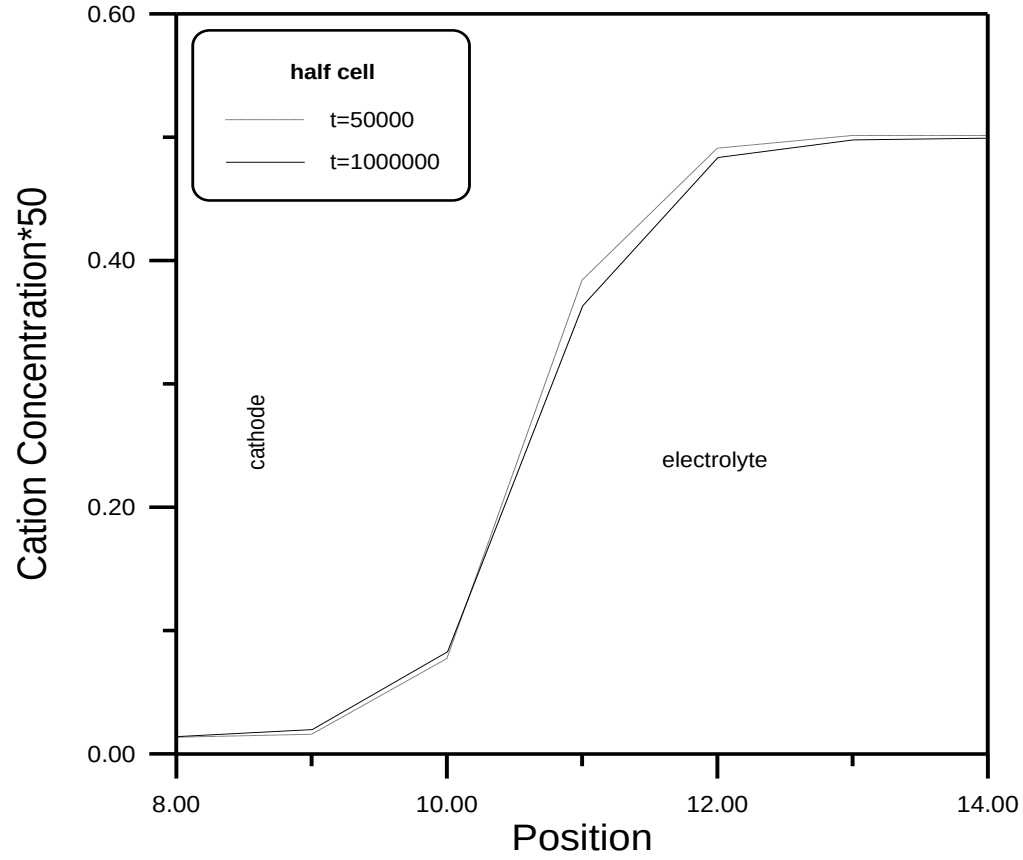

Figure(٥.٨) Cation concentration profiles .

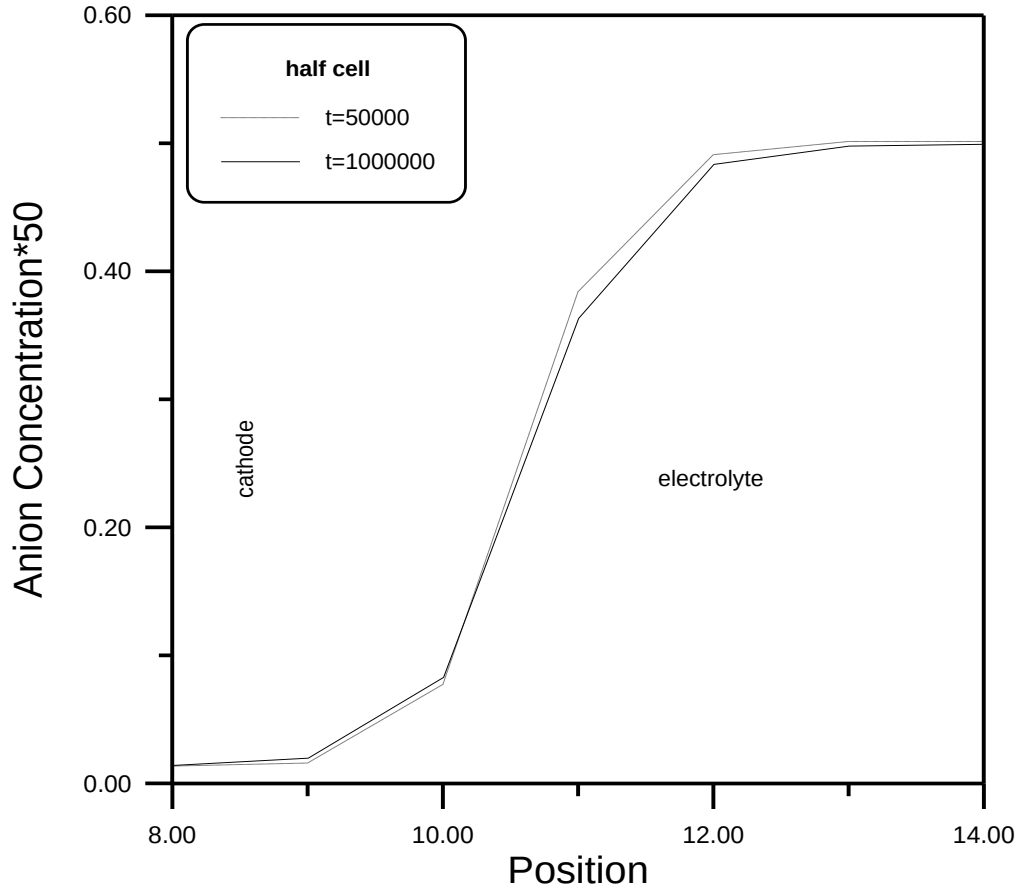

Figure(٥.٩) Anion concentration profiles .

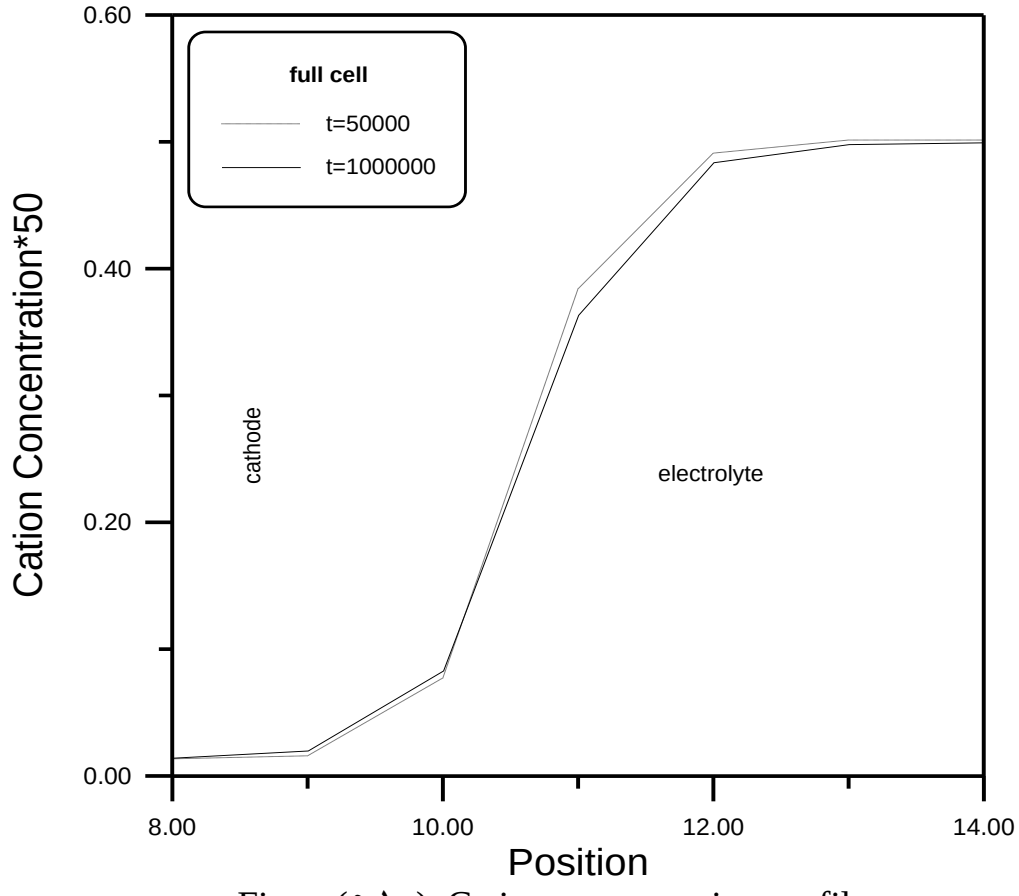

Figure(٥.١٠) Cation concentration profiles.

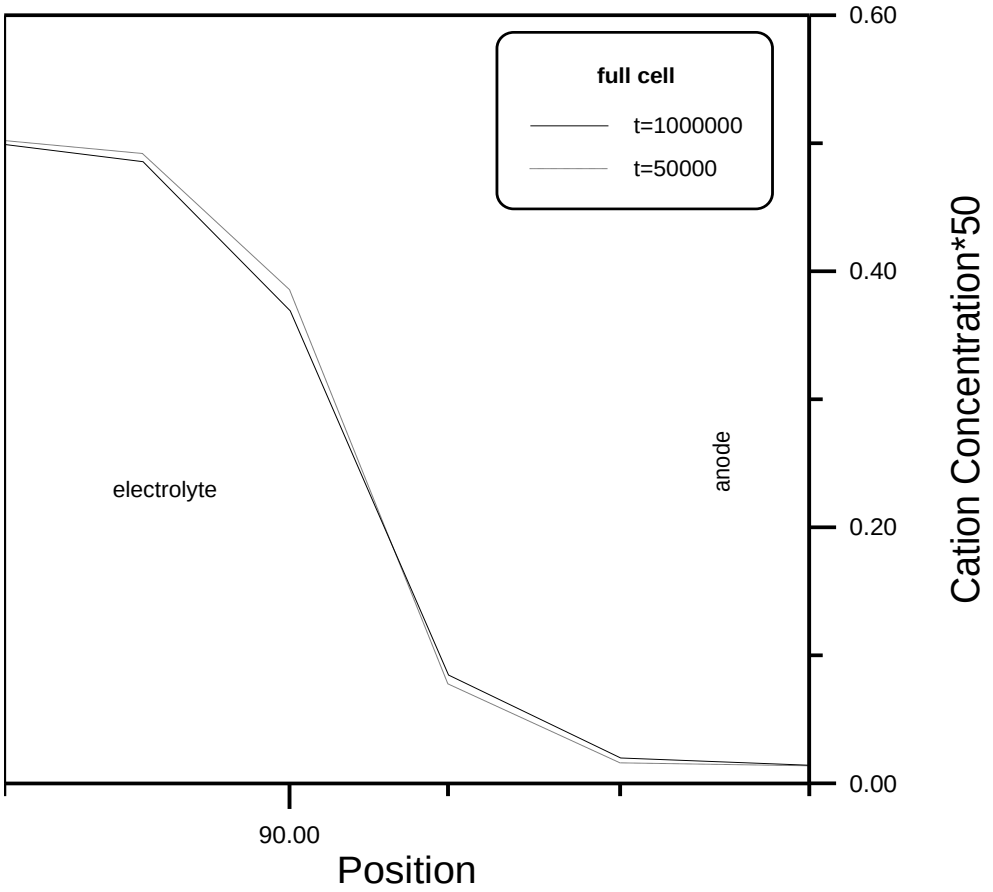

Figure(٥.١١) Cation concentration profiles.

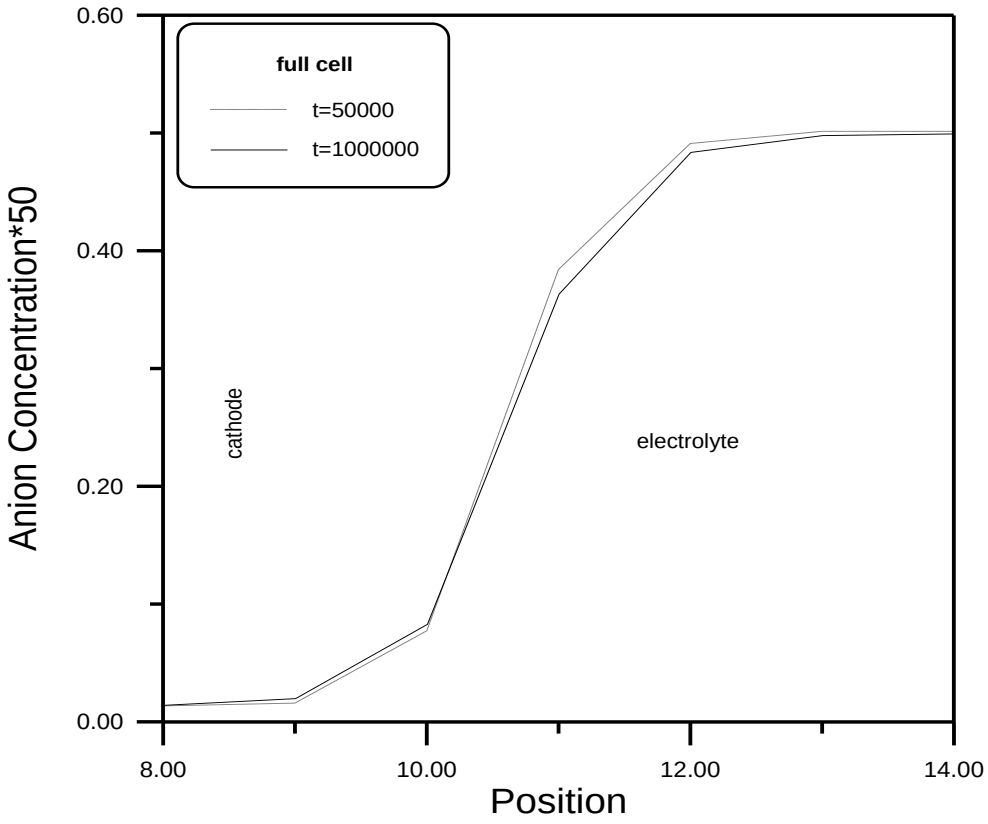

Figure(٥.١٢) Anion concentration profiles.

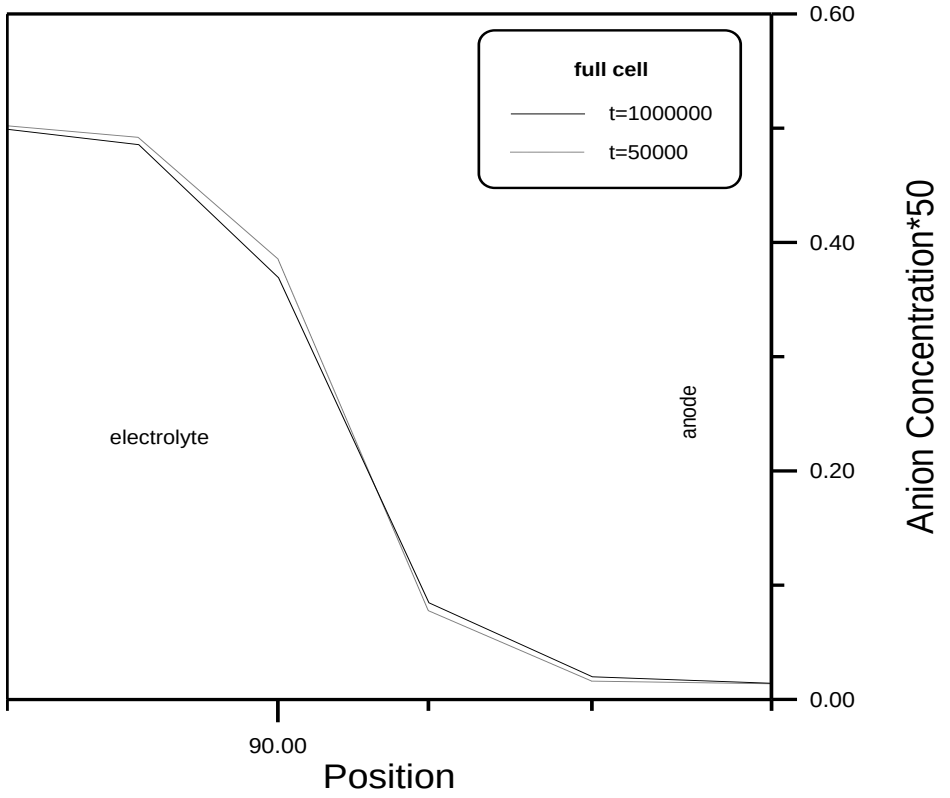

Figure(٥.١٣) Anion concentration profiles .

٥.٣ Simulation of One-Dimensional Cells with Potential

When a potential difference(dv) of ٢KT/e is applied across the cell of size ١٠٠ sites contains two identical electrodes of the same thickness of ١٠ layers . The ionic species start to migrate , a double layer appears on the interface , a reduction process take place at the cathode and the oxidation process take place on the anode . These processes are accelerated by the electric field that can achieved the ions kinetics .

Figures (٥.١٤ – ٥.١٩) represents simulation of the different species , namely : (metal,cation,anion,solvent and vacancy) across the sites ٥٠ for the half cell and ١٠٠ sites for the full cell with initial ion concentration of ٠.٠١ during the three times intervals $t = (1,3,5)\times 10^{5}$.

Figures (٥.٢٠ – ٥.٢٢) show the growth of the cathode and the dissolution of the anode . It is noted that the shape of the metal concentration profile across the interface is essentially preserved from the overall configuration view point but with different values .

The interesting results concern the kinetics of the ions . Figures (٥.٢٣ – ٥.٢٦)show the evolution of the ion concentration, it is observed that the progressive formation of a concentration gradient between the anode and the cathode with , for cations , a concentration peak on the cathode (accompanied by an electronic layer on the metal surface) . The anion concentration profile presents on the contrary an increase close to the anode . Figures (٥.٢٧) and (٥.٢٨) show the total charge distribution at three successive times t= $(1,3,5)\times 10^{5}$, in addition to the double-layers located around the interfaces, an excess of cations over the anions, on a range of about ٣٠ lattice distances. This extended space charge leads to an important potential drop on the cathode side, as can be seen in figures (٥.٢٩) and (٥.٣٠) that show the electric potential , this is matched with (Bernard , Plapp and Gouyet),[٧,٣١,٣٢] .

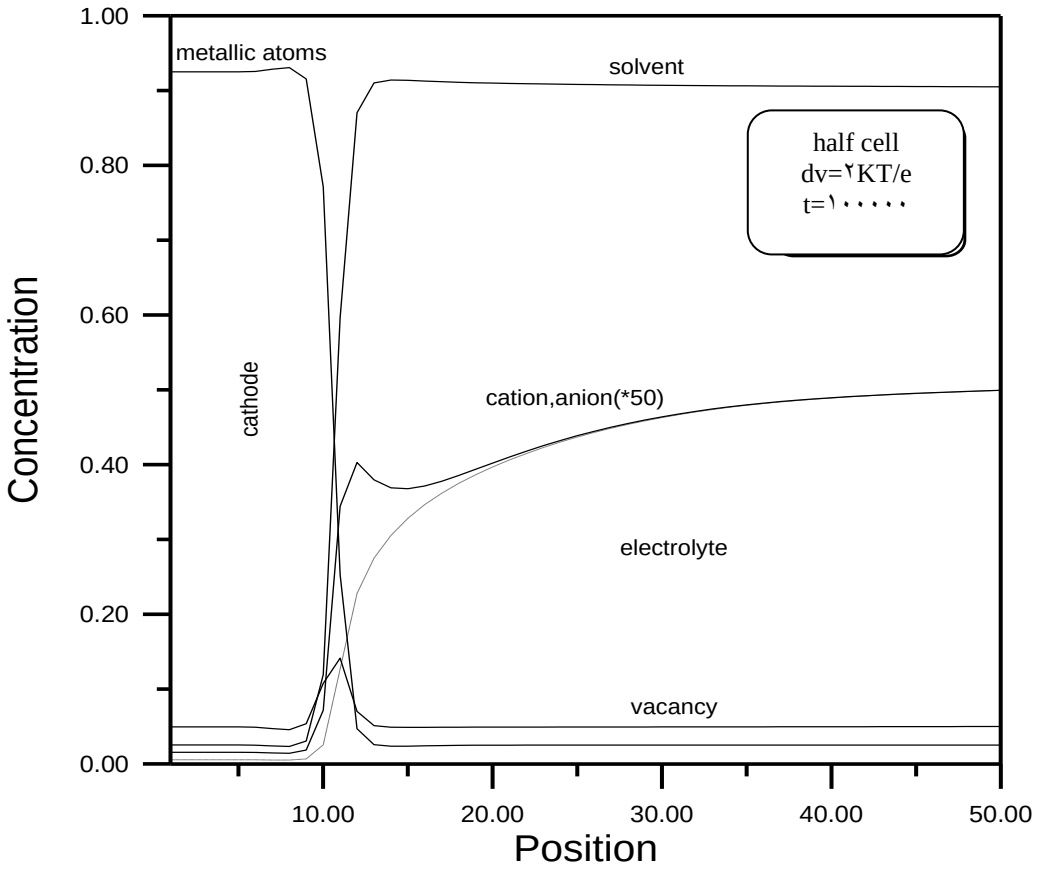

Figure(٥.١٤) Concentration profiles across a ٥٠-site cell.

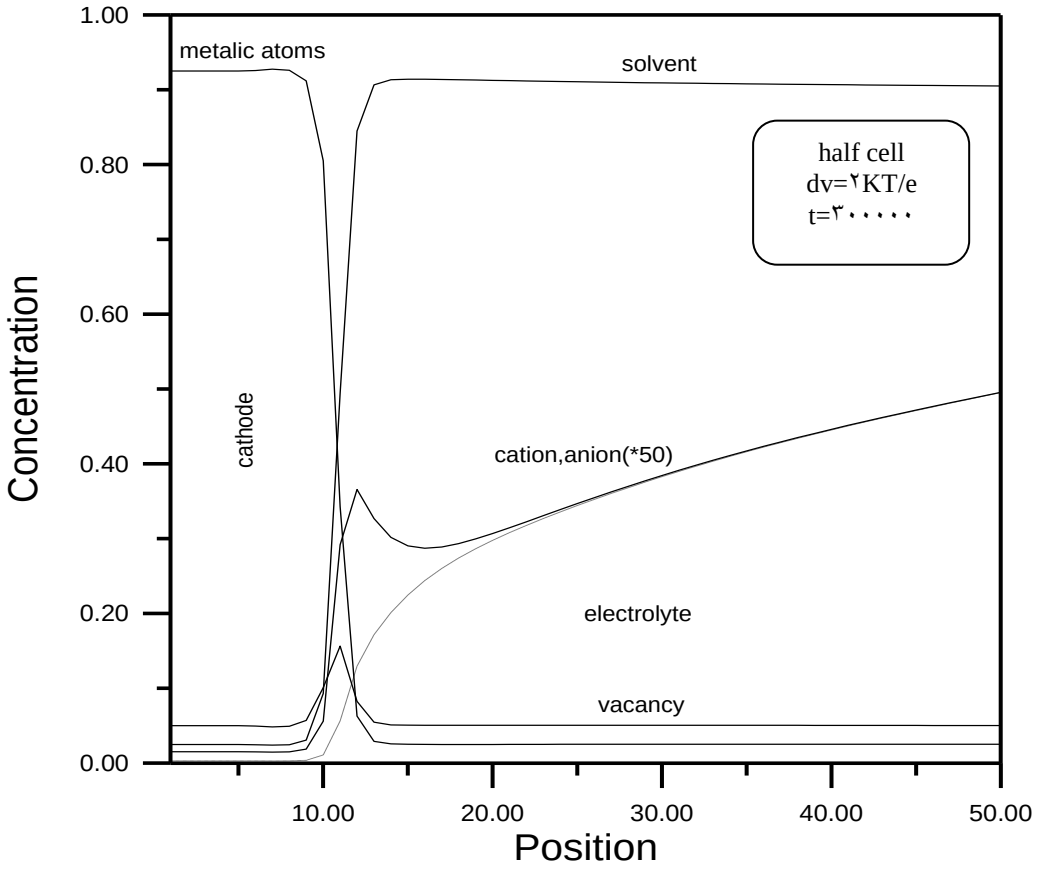

Figure(٥.١٥) Concentration profiles across a ٥٠-site cell.

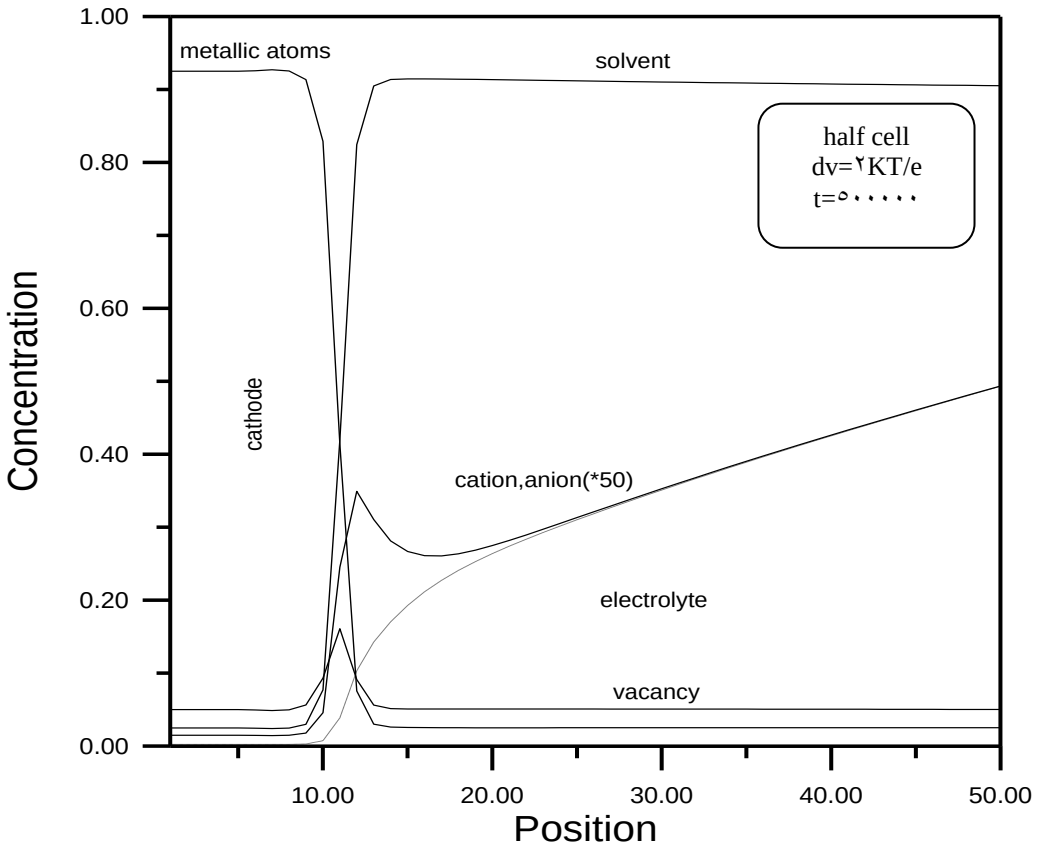

Figure(٥.١٦) Concentration profiles across a ٥٠-site cell.

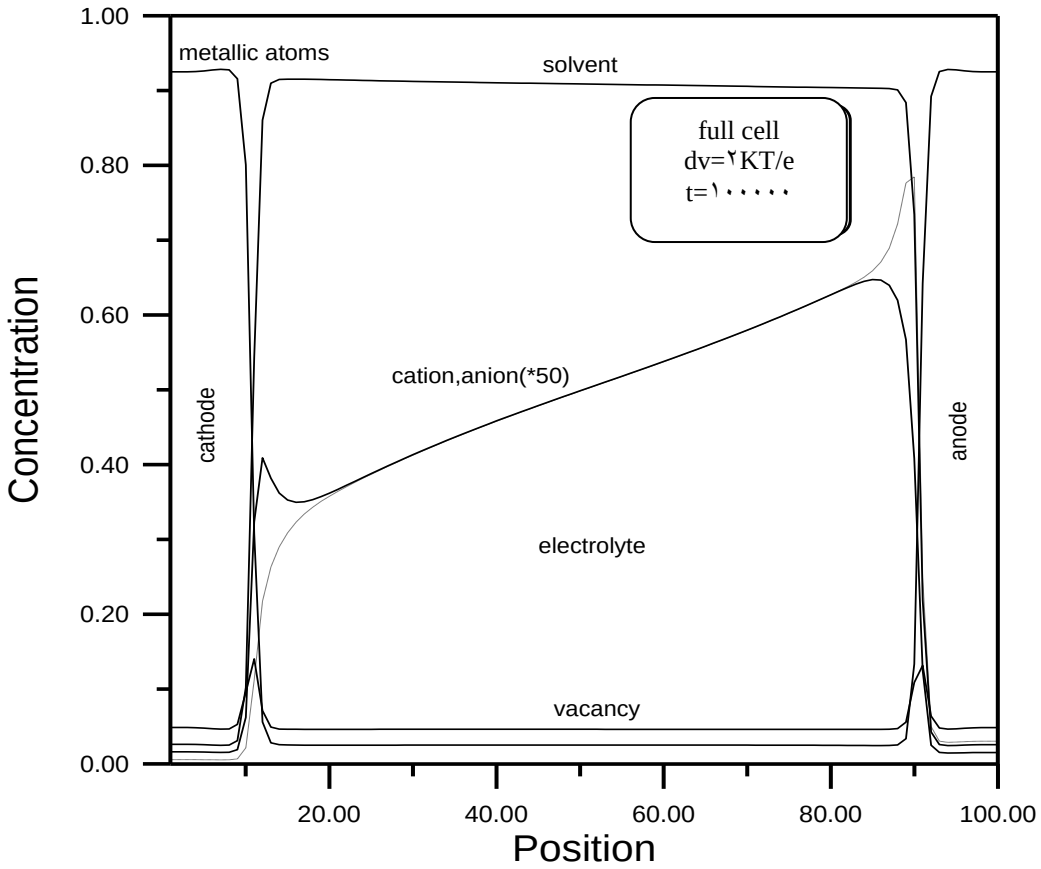

Figure(٥.١٧) Concentration profiles across a ١٠٠-site cell.

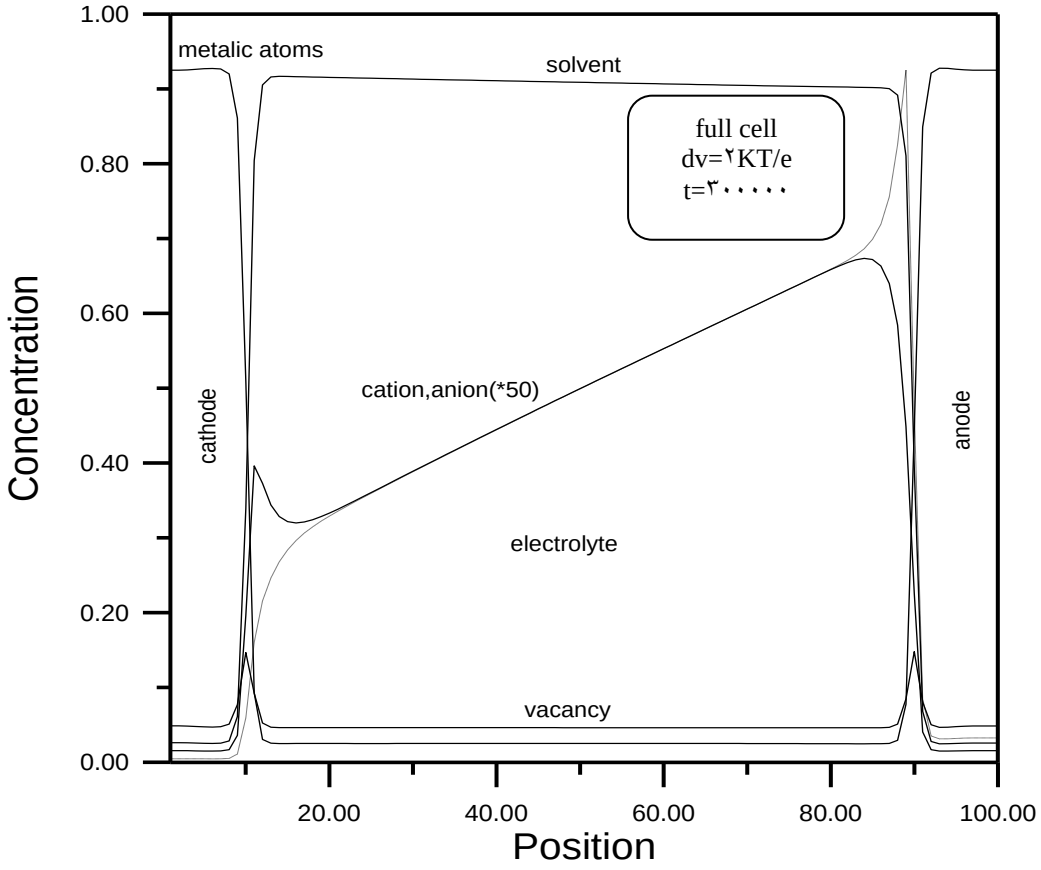

Figure(٥.١٨) Concentration profiles across a ١٠٠-site cell.

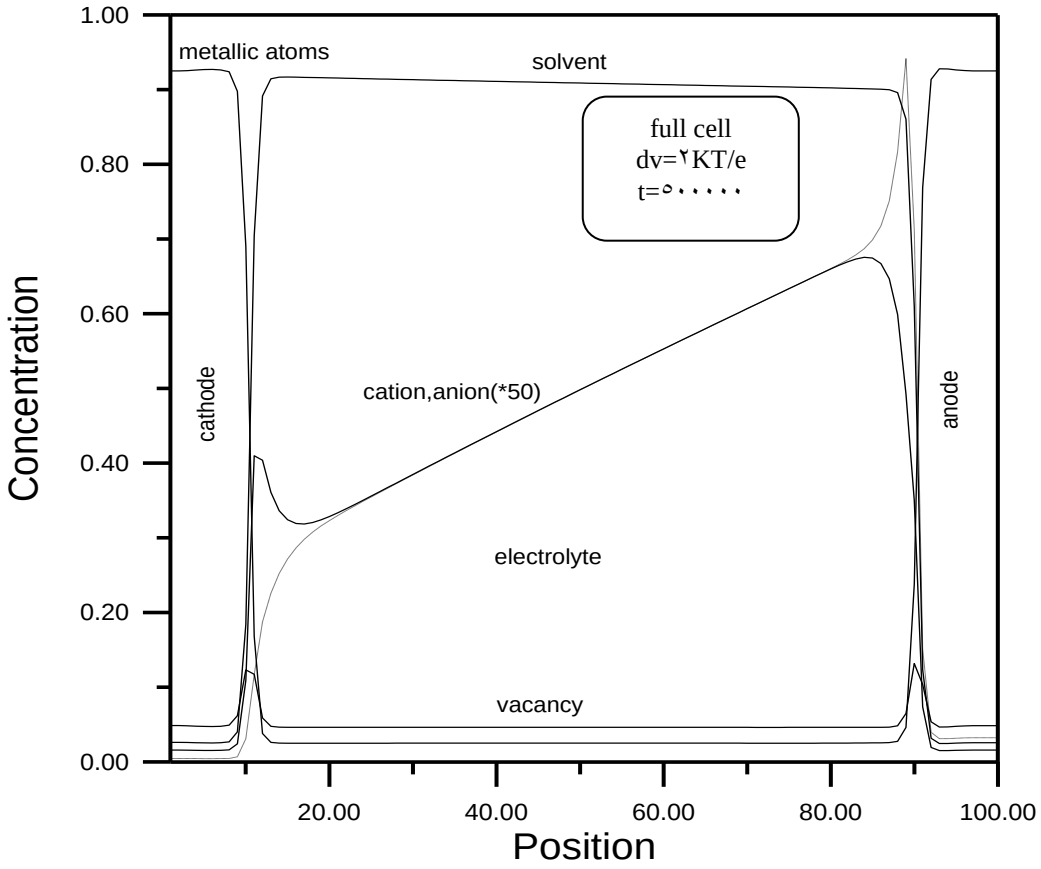

Figure(٥.١٩) Concentration profiles across a ١٠٠-site cell.

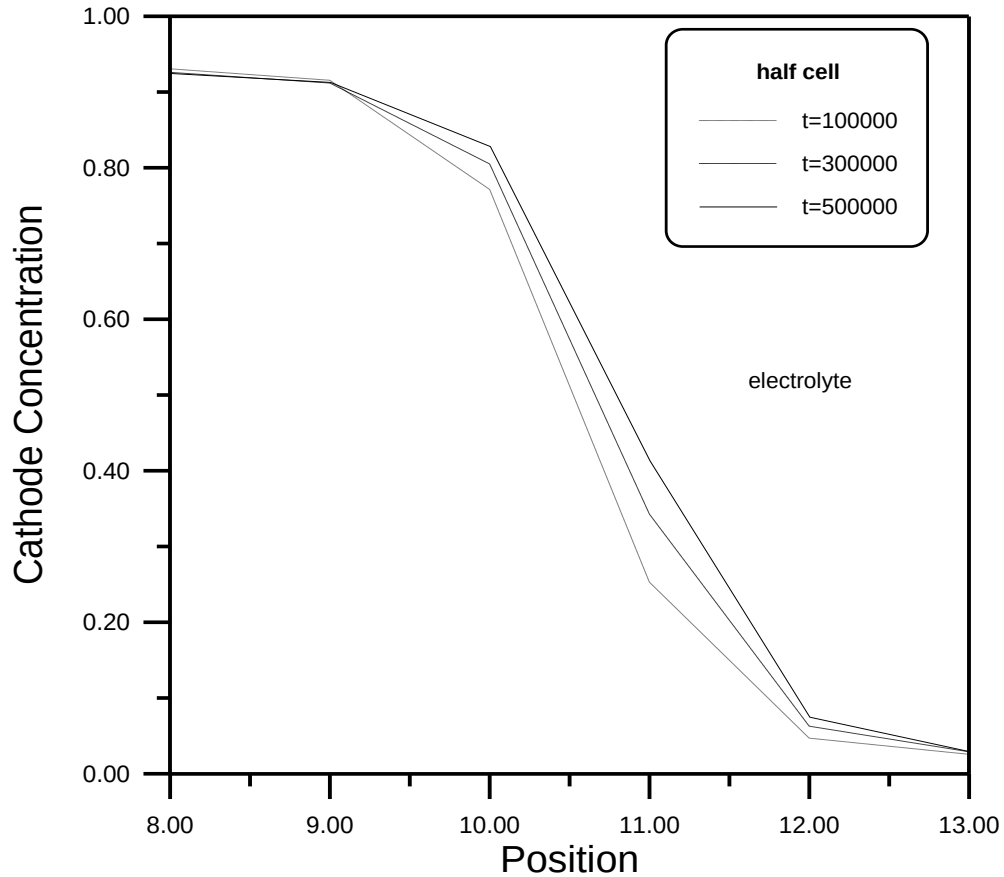

Figure(٥.٢٠) Showing the electrode position (reduction) at the cathode.

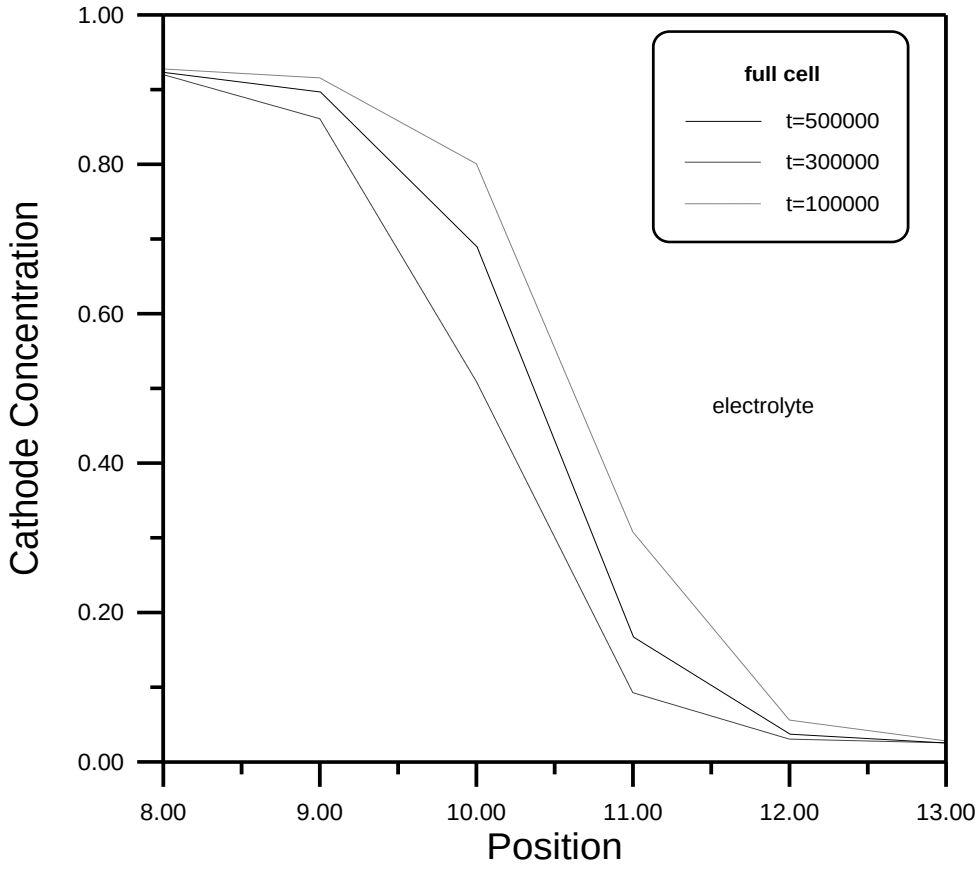

Figure(٥.٢١) Showing the electrode position (reduction) at the cathode.

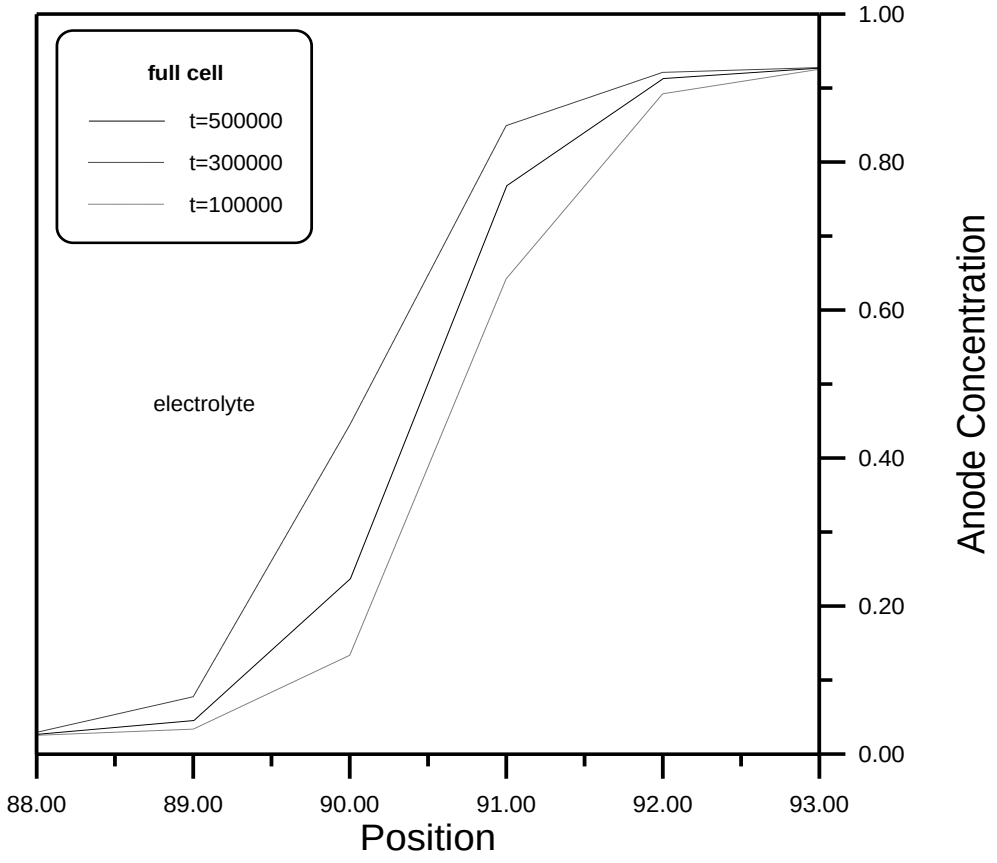

Figure(٥.٢٢) Showing the dissolution of metal at the anode .

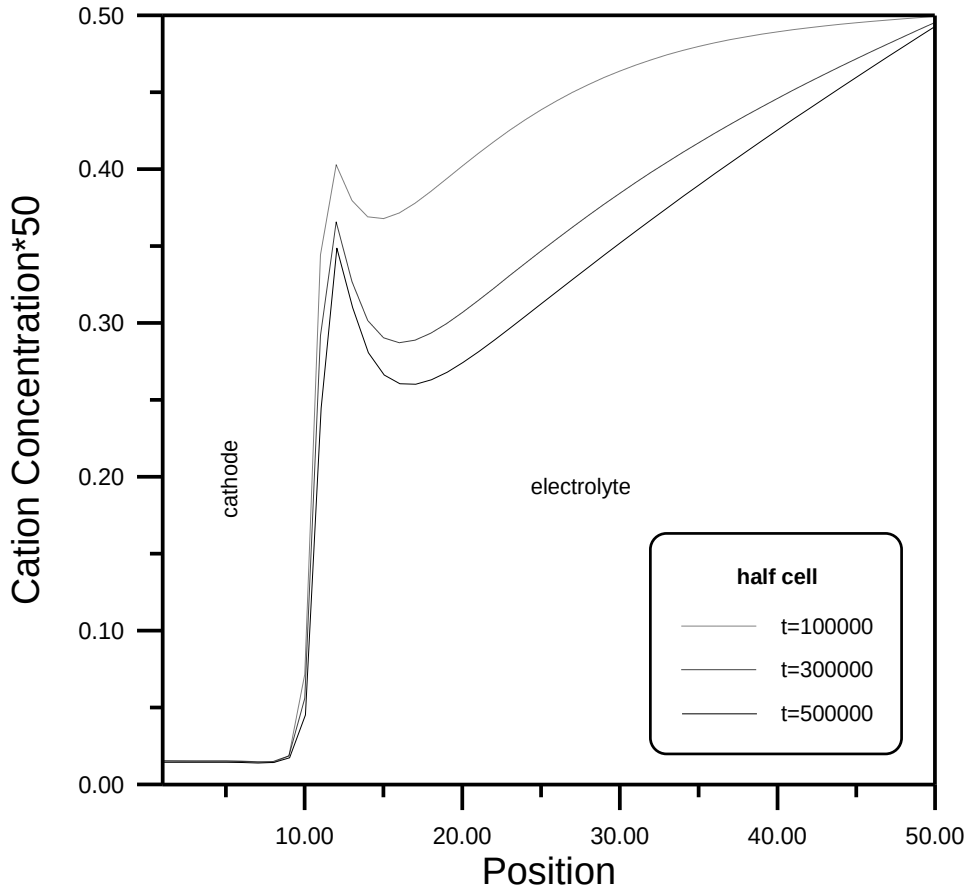

Figure(٥.٢٣) Cation concentration profiles.

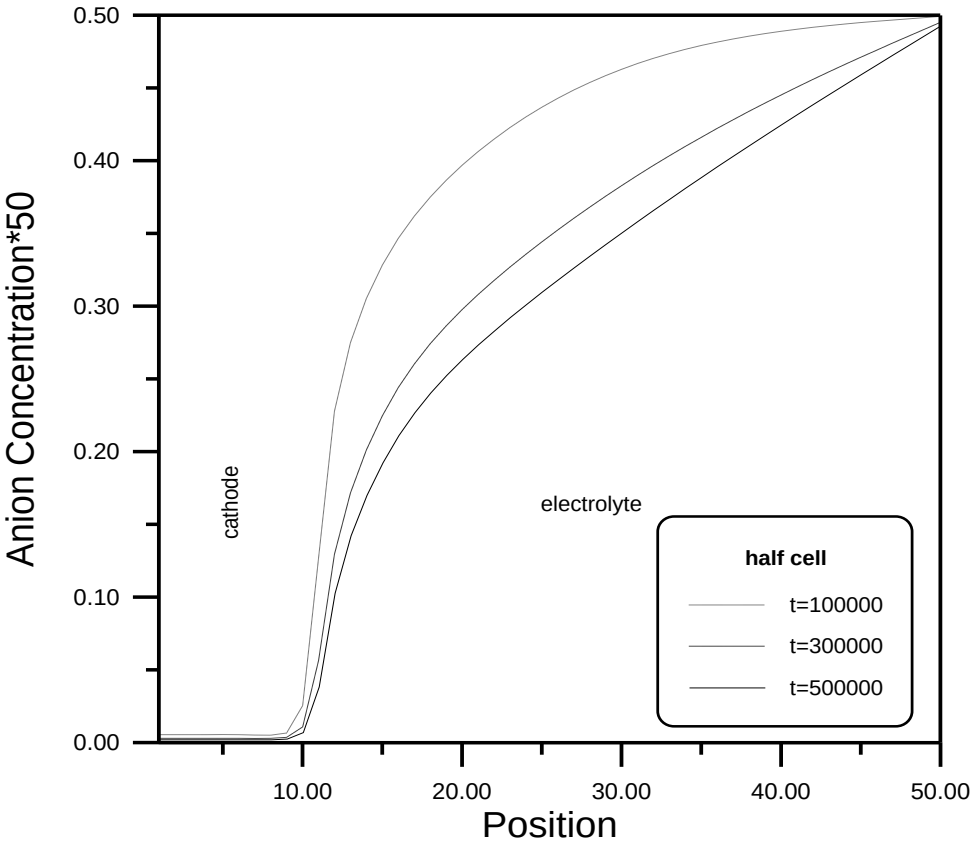

Figure(٥.٢٤) Anion concentration profiles.

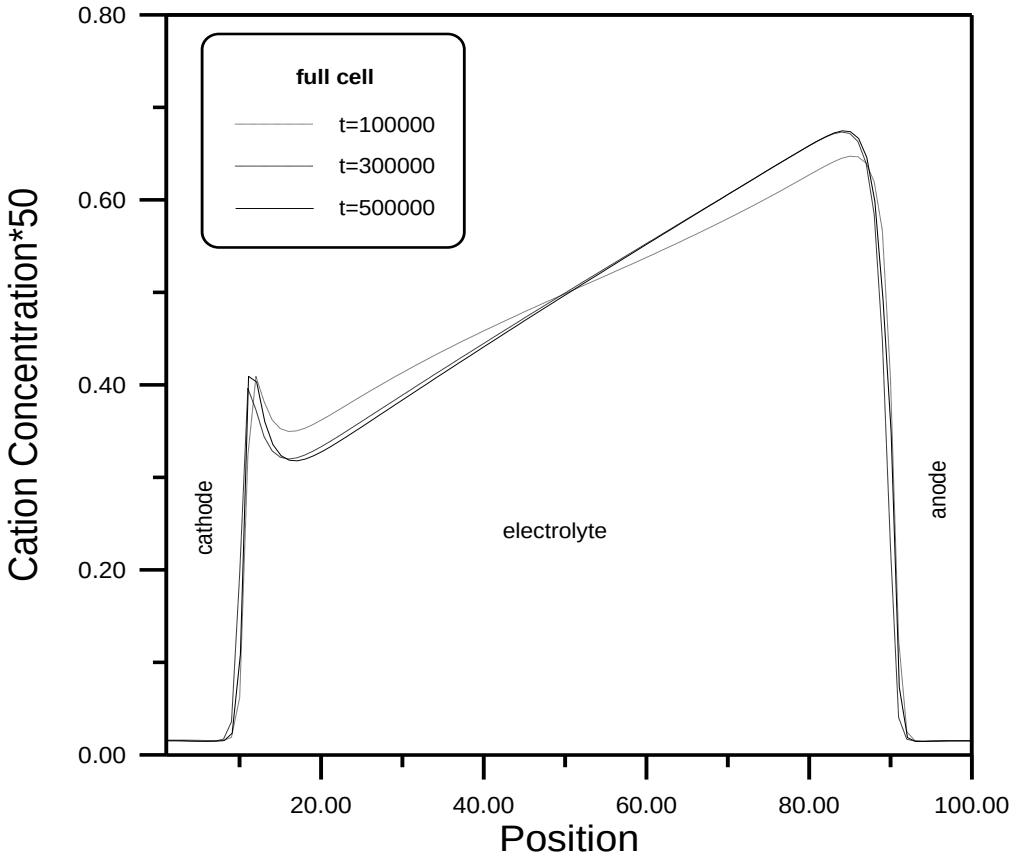

Figure(٥.٢٥) Cation concentration profiles .

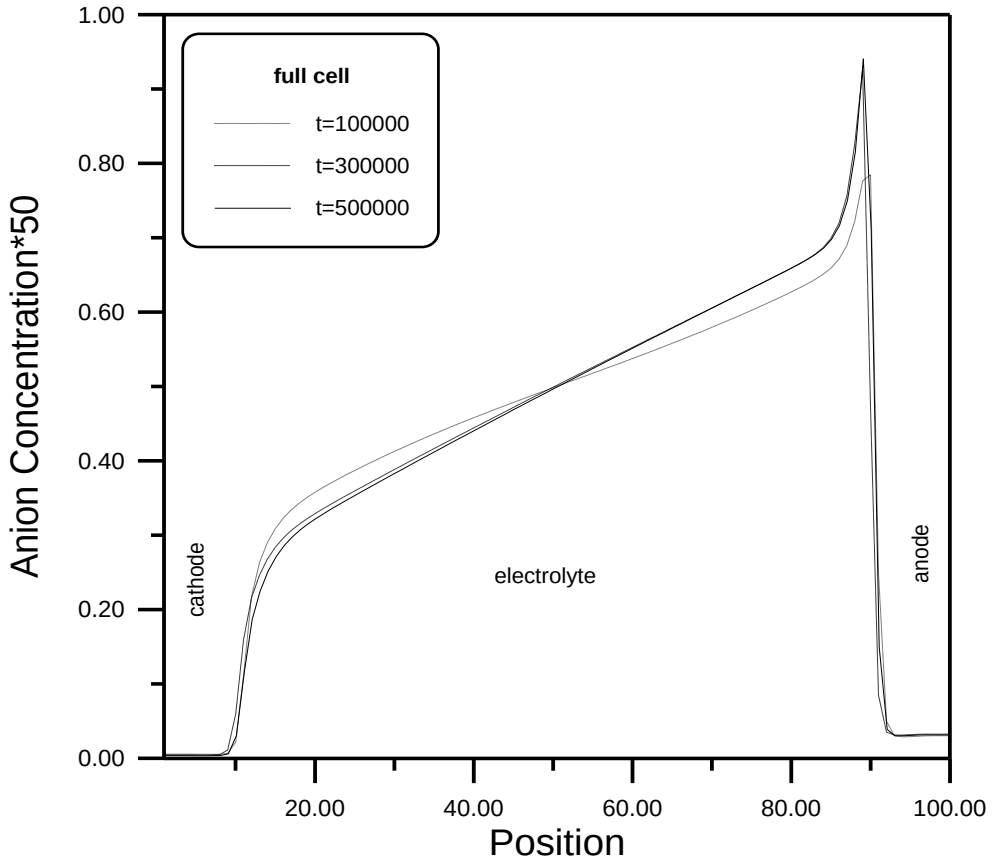

Figure(٥.٢٦) Anion concentration profiles.

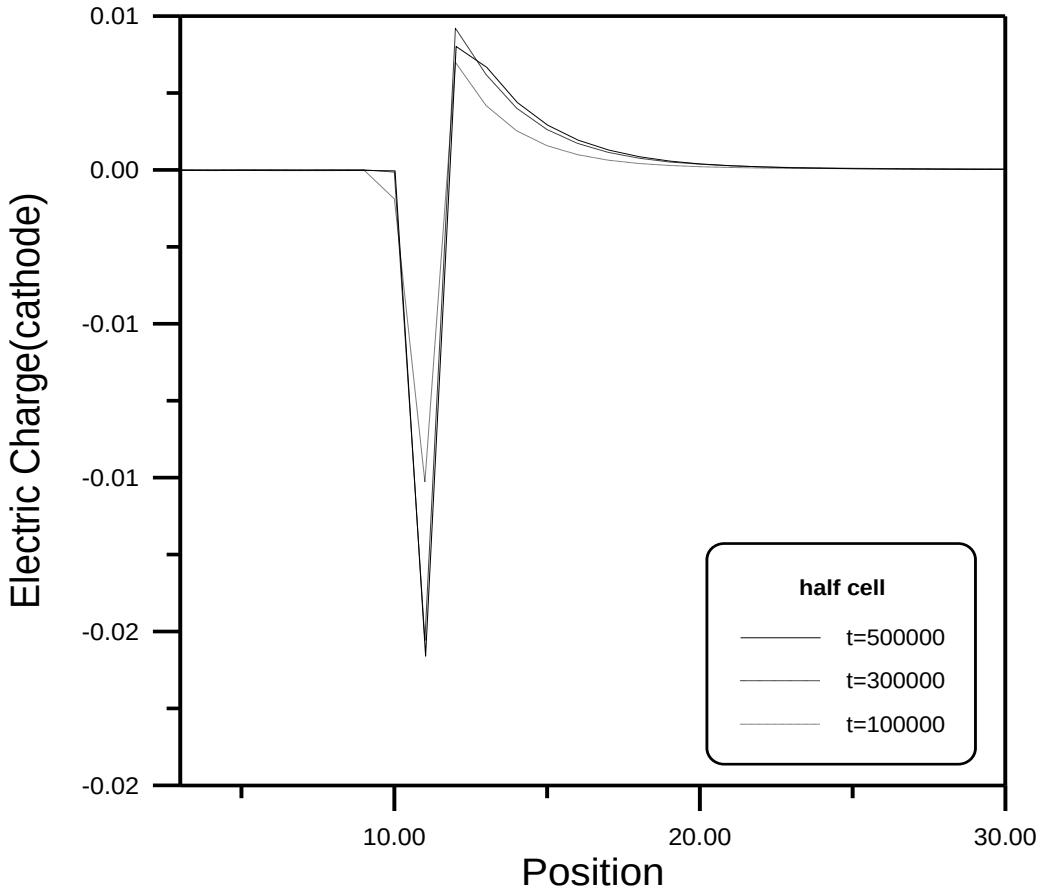

Figure(٥.٢٧) Charge distribution.

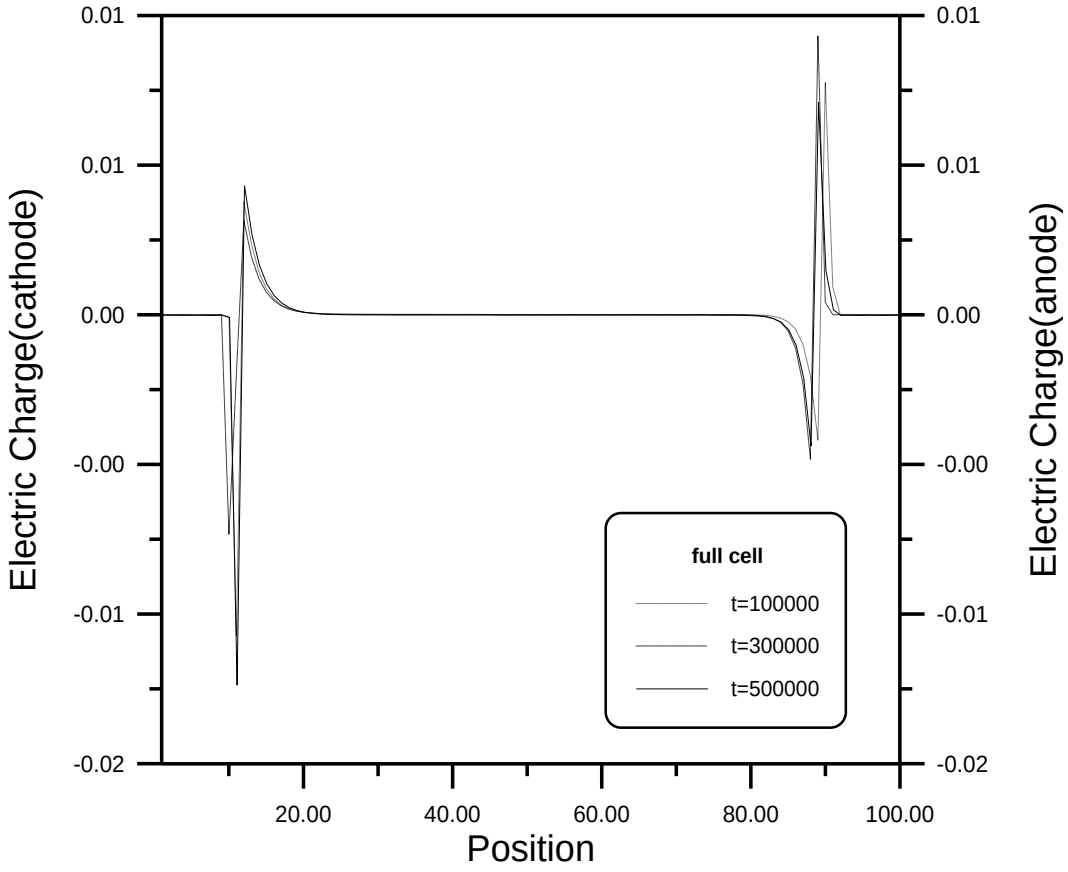

Figure(٥.٢٨) Charge distribution.

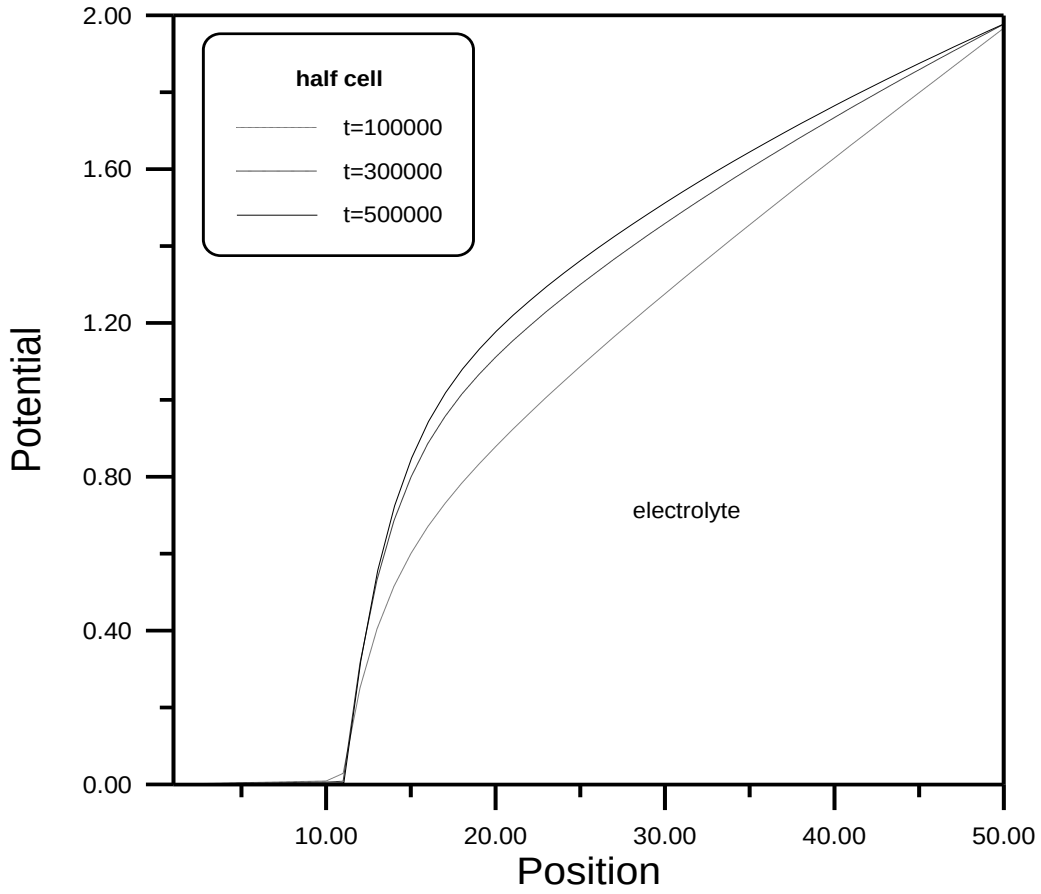

Figure (٥.٢٩) Potential profiles.

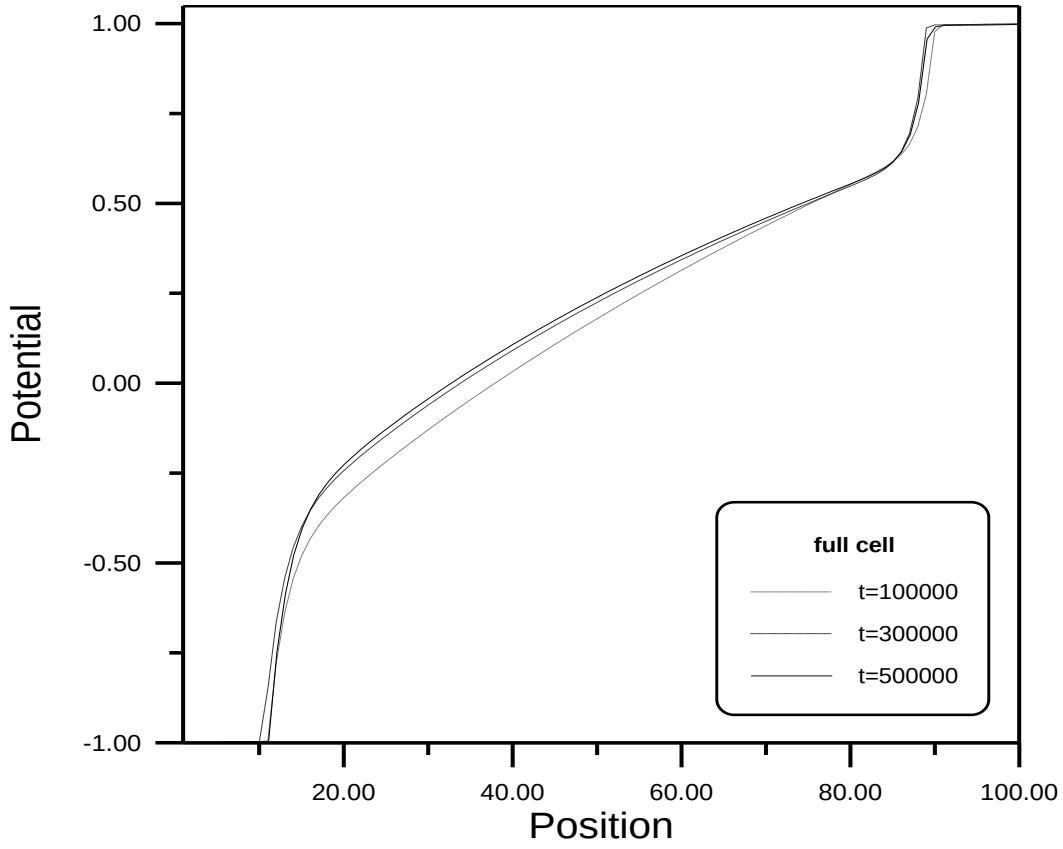

Figure (٥.٣٠) Potential profiles .

٥.٤ Factors Effecting the Deposition Process

١. Concentration :-

It is seen from figure (٥.٣١) that the deposition occurred at the cathode at time t = 0.5×10^5 for different ionic concentrations is increased with increasing of the ionic concentration in electrolyte due to increasing of the reduction processes at the cathode and oxidation processes at the anode . In figures (٥.٣٢ – ٥.٣٥) it is clearly seen the evolution of the ion concentration , charges distribution at the cathode electrode and electric potential distribution across the sites ٥٠ for the half cell at time t= 0.5×10^5 for these different concentrations (٠.٠١,٠.٠٢ and ٠.٠٣) .

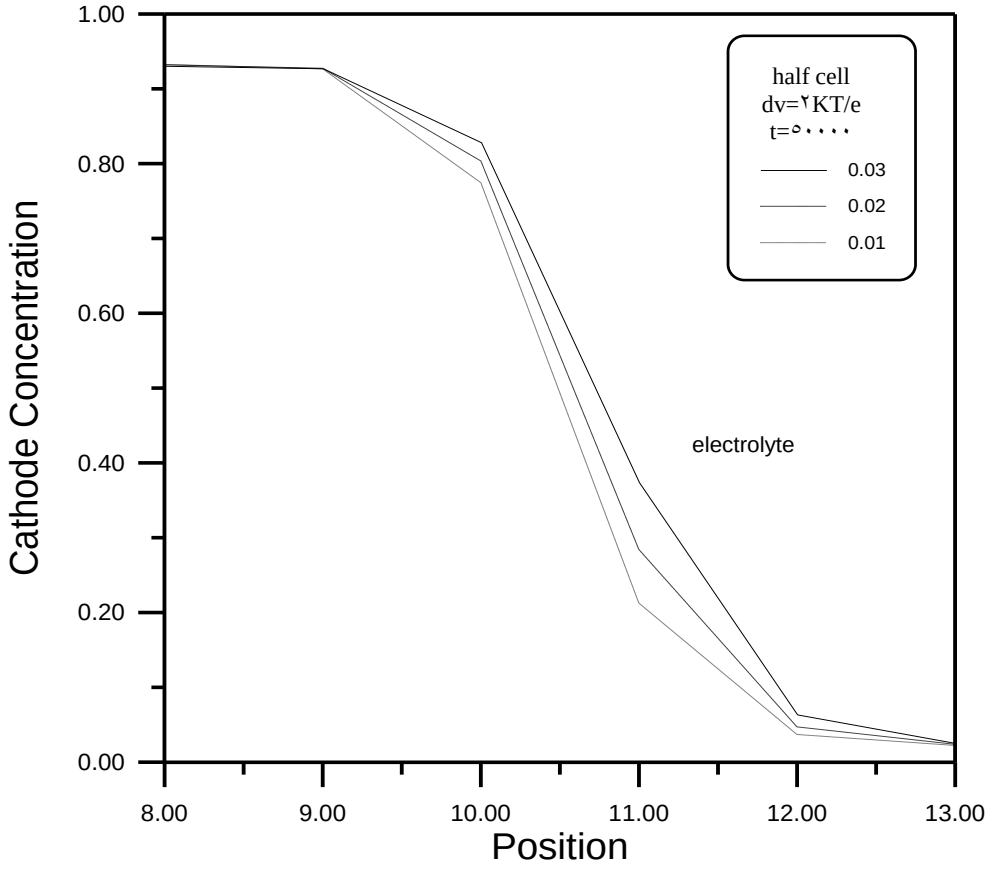

Figure(٥.٣١) Cathode concentration profiles across a ٥٠-site cell.

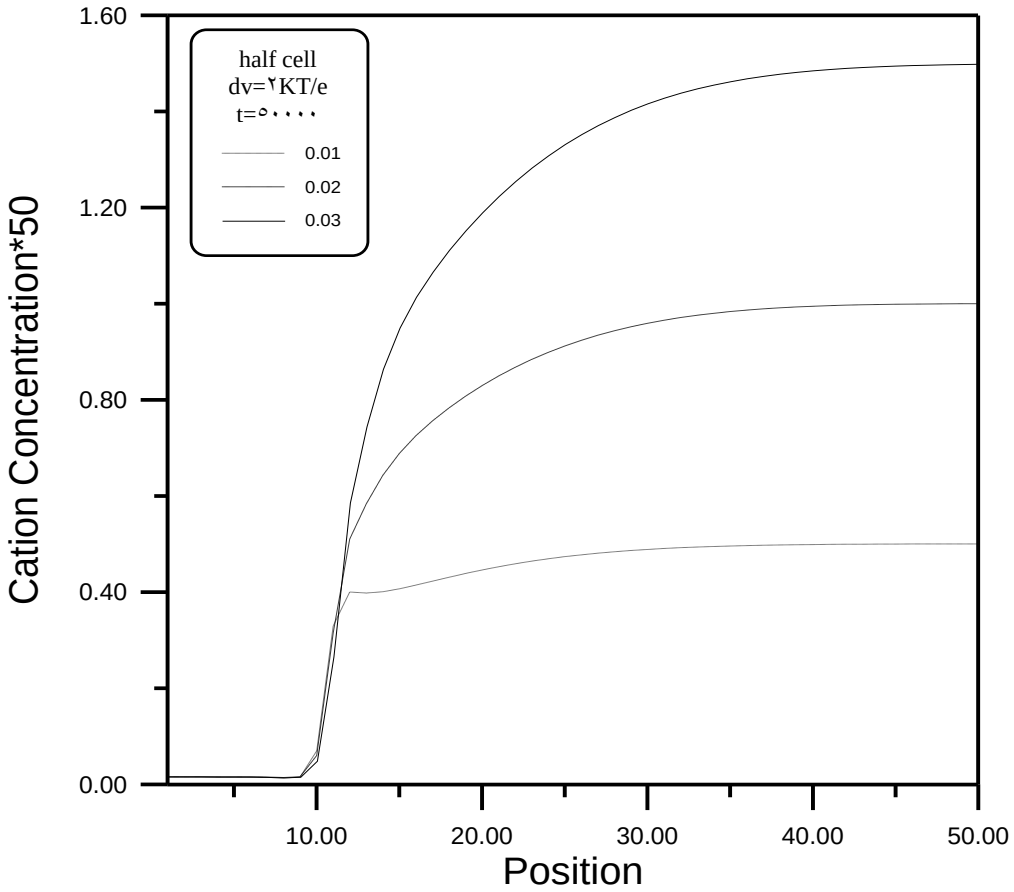

Figure(٥.٣٢) Cation concentration profiles across a ٥٠-site cell.

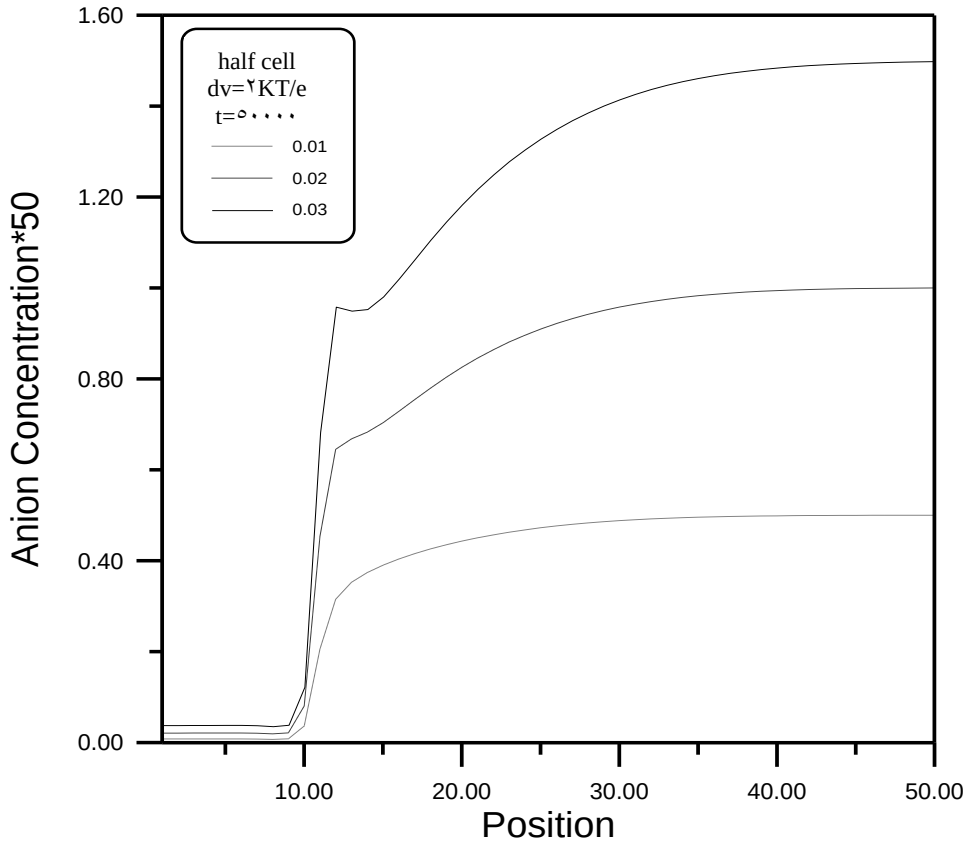

Figure(٥.٣٣) Anion concentration profiles across a ٥٠-site cell .

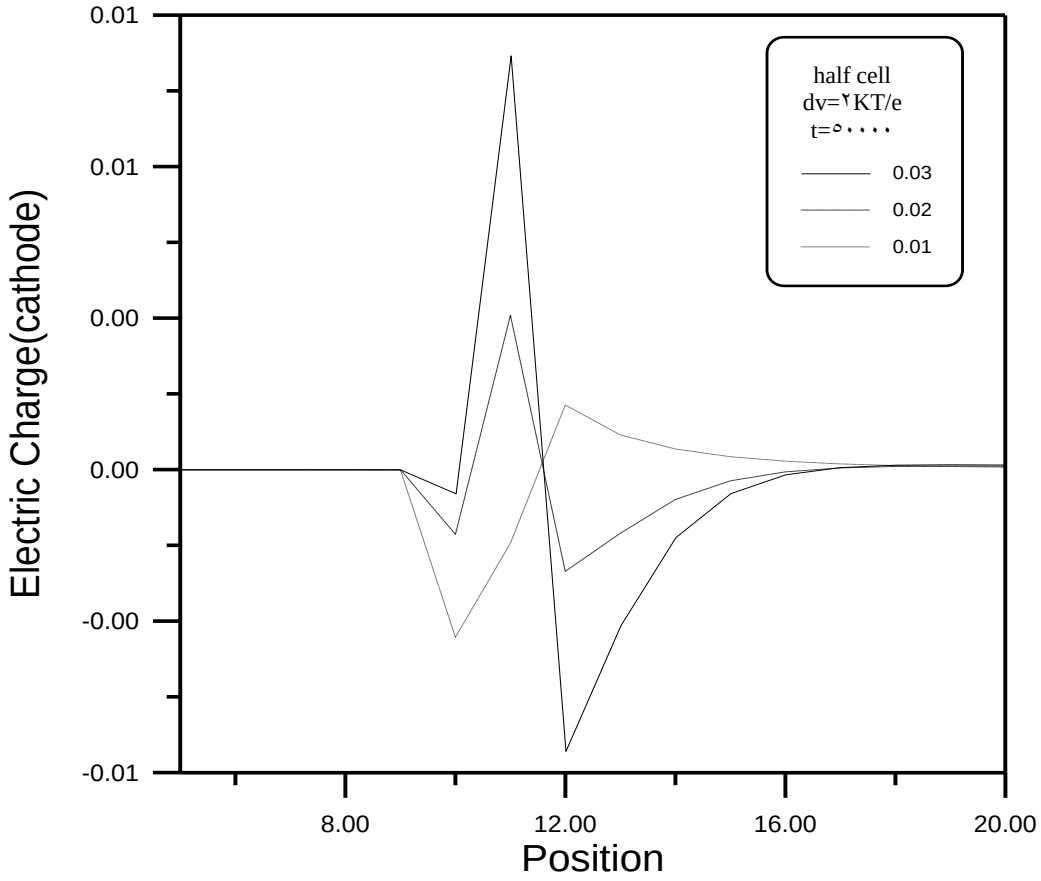

Figure(٥.٣٤) Electric charge(cathode) profiles across a ٥٠-site cell.

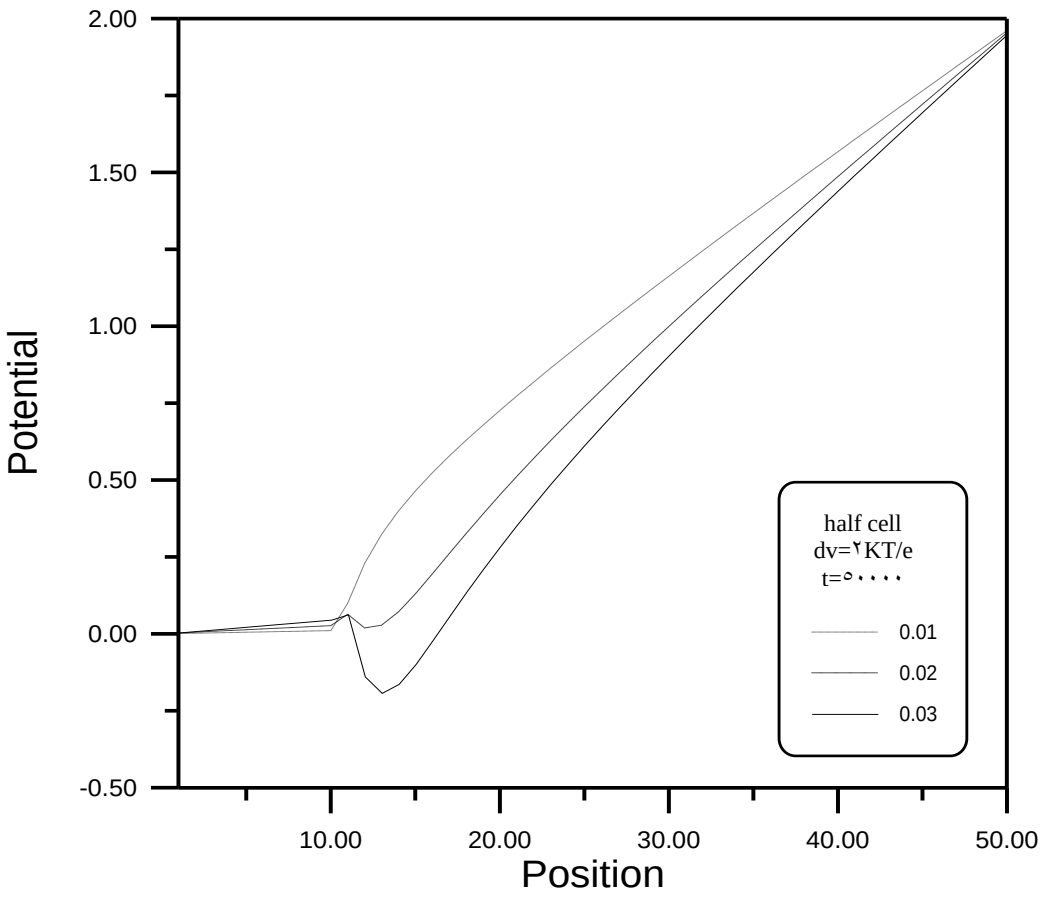

Figure(٥.٣٥) Potential profiles across a ٥٠-site cell .

٢. Fermi energy :-

Figure (٥.٣٦) shows the deposition taken place at the cathode at time $t = 0.5\times10^5$ for different values at Fermi energy and it is observed that there is a direct proportional relation between deposition and Fermi energy due to the increasing of the electron chemical potential , and hence the electrochemical reactions are accelerated resulting in increasing the reduction and oxidation processes. It is observed from figures (٥.٣٧ – ٥.٤٠) the evolution of the ion concentration , electric charges distributions and electric potential distributions across the sites ٥٠ for half cell at time $t = 0.5\times10^5$ for Fermi energy of (٣.٤٤٧٥١٤ , ٤.٤٤٧٥١٤ and ٥.٤٤٧٥١٤) . These values are arbitrary chosen to check the proportionally of deposition with Fermi energy.

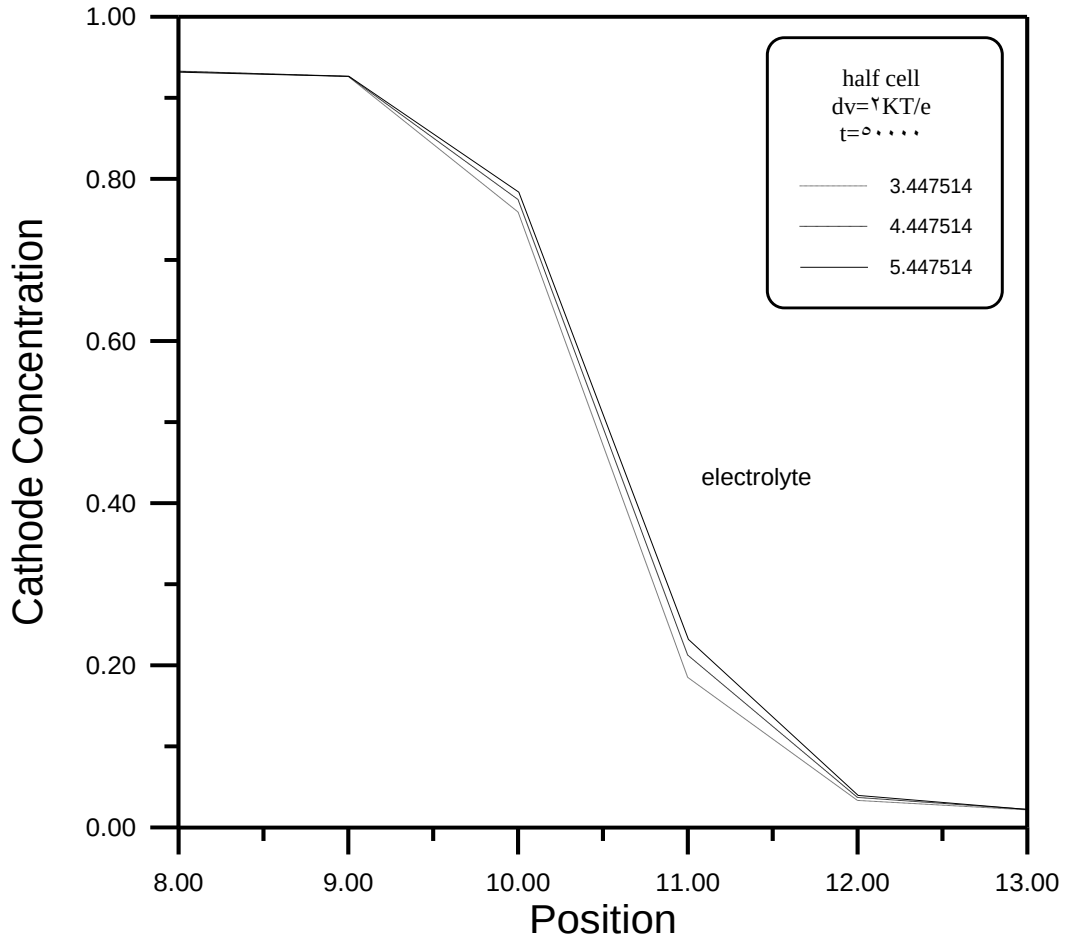

Figure(٥.٣٦) Cathode concentration profiles across a ٥٠-site cell.

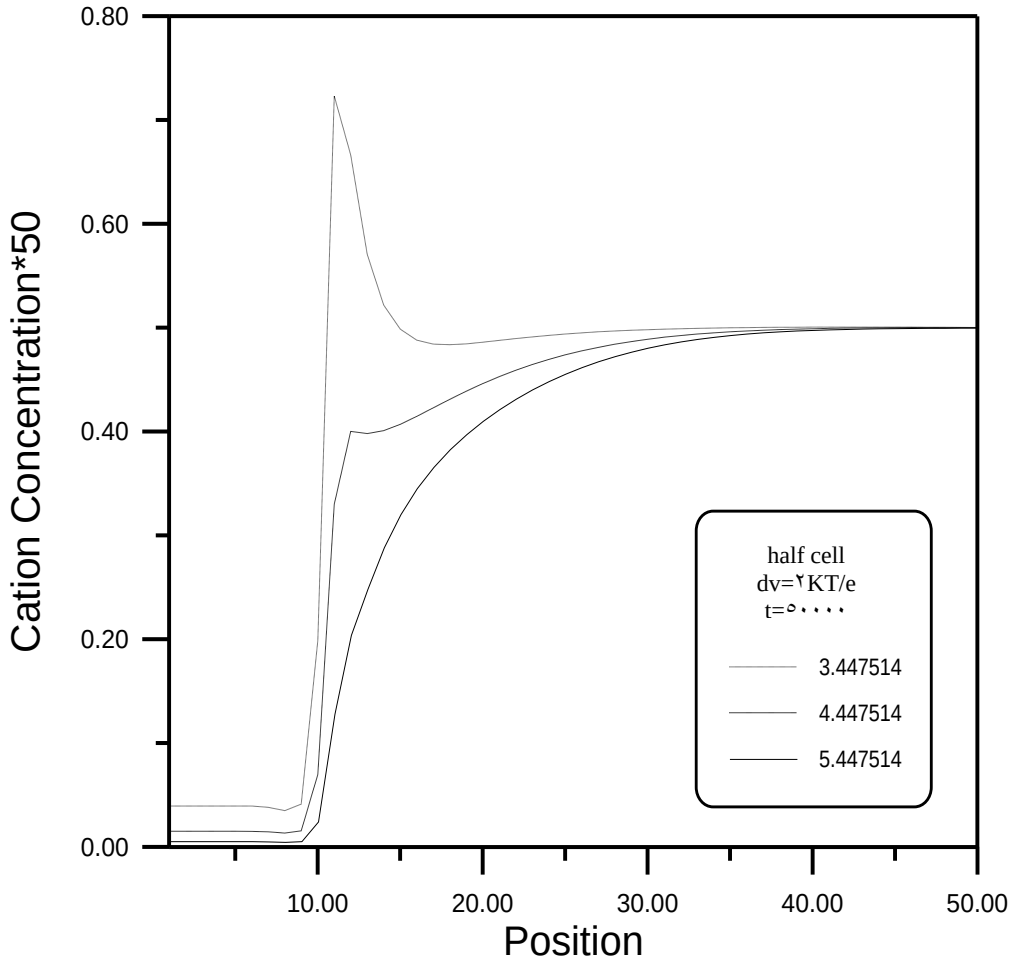

Figure (٥.٣٧) Cation concentration profiles across a ٥٠-site cell.

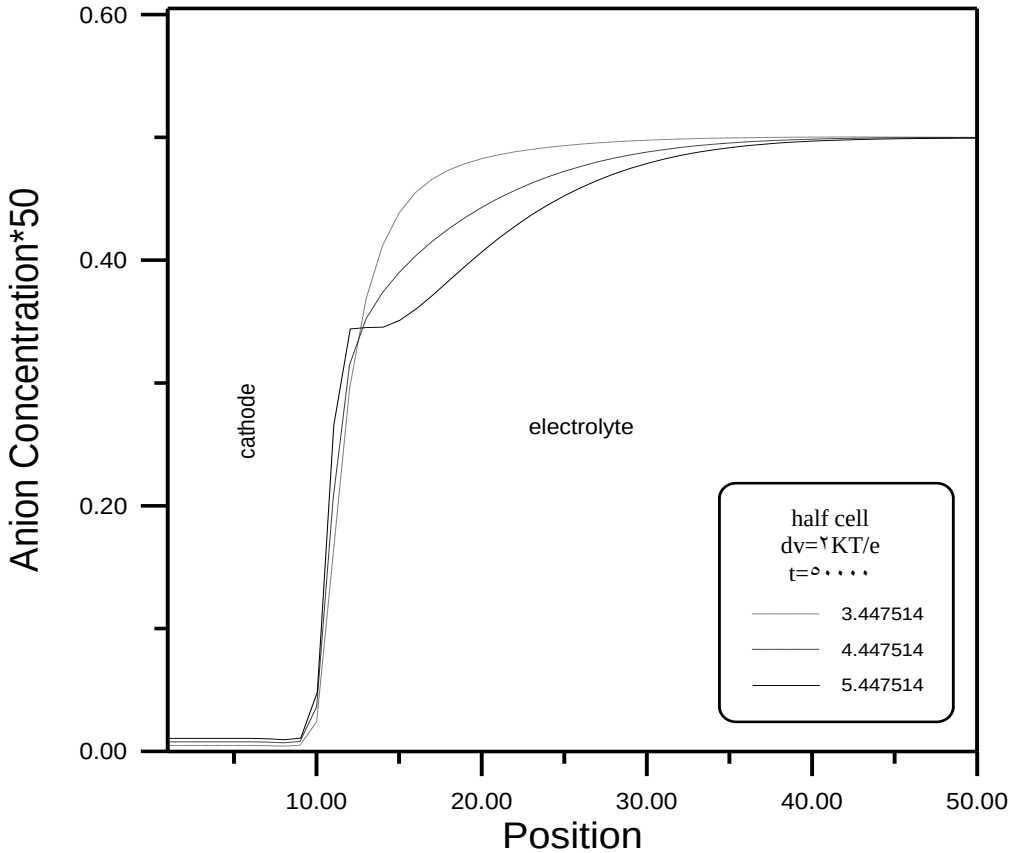

Figure (٥.٣٨) Anion concentration profiles across a ٥٠-site cell .

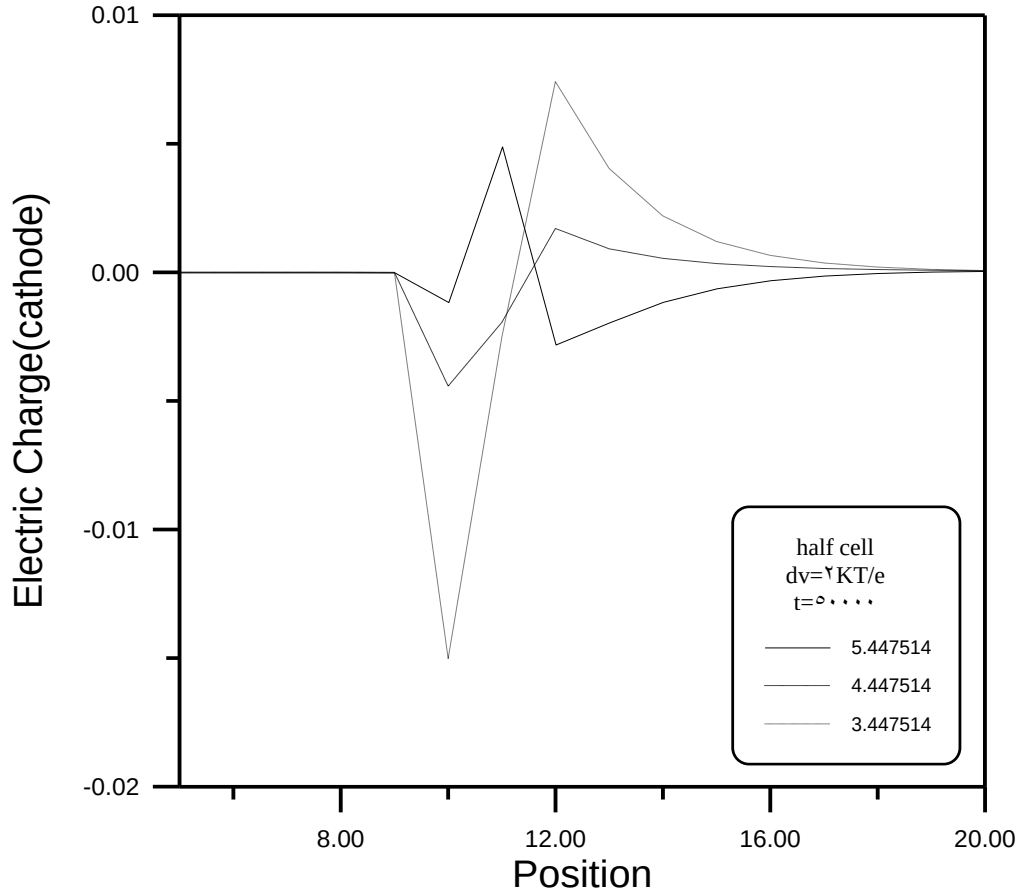

Figure(٥.٣٩) Electric charge(cathode) profiles across a ٥٠-site cell.

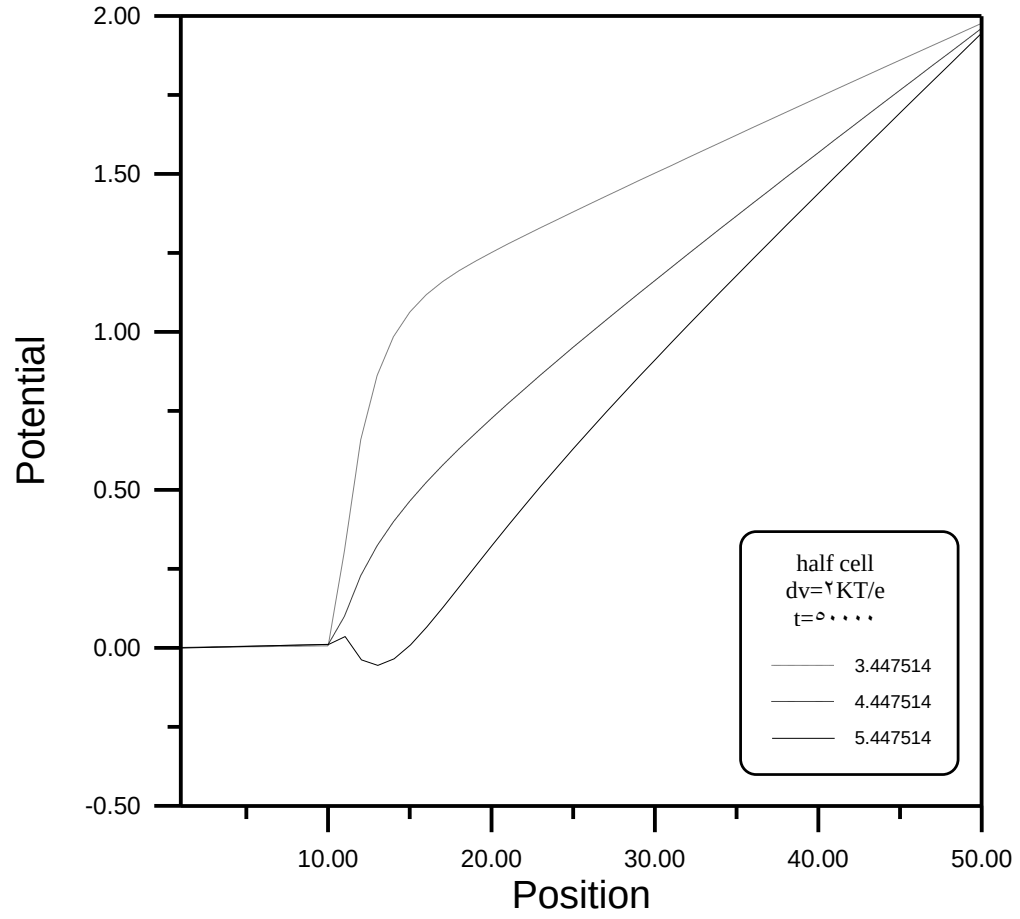

Figure (٥.٤٠) Potential profiles across a ٥٠-site cell.

٣. Electrodes spacing :-

Figure (٥.٤١) shows that the deposition at the cathode is decreased with increasing of electrodes spacing due to dropping of the electric potential across the cell sites and thus deceleration of the electrochemical reactions resulting in reducing the oxidization and reduction processes.

Figures (٥.٤٢ – ٥.٤٥) illustrate ionic concentration growth , charges distribution at the cathode and electric potential distribution across the sites (١٠٠ and ٥٠) for the half cell at t = 0.5×10^{5}.

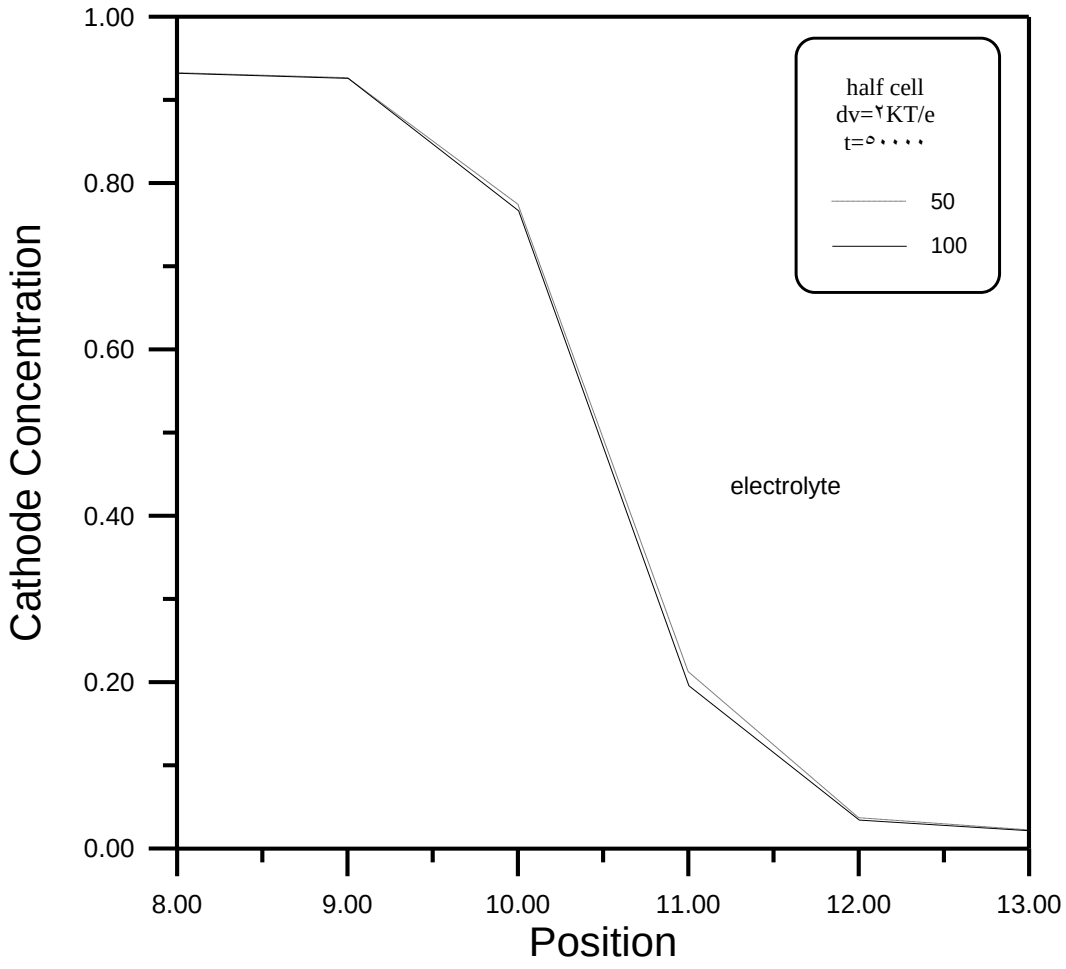

Figure(٥.٤١) Cathode concentration profiles across ٥٠- and ١٠٠-site cell .

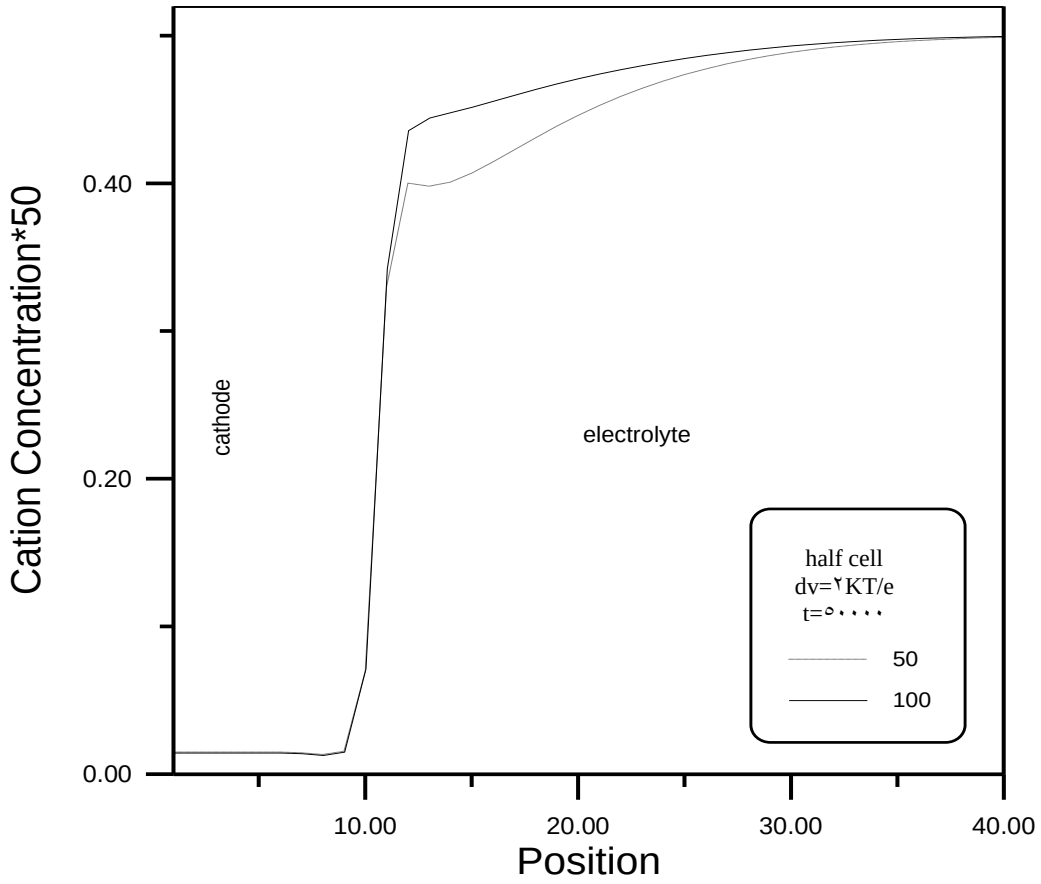

Figure (٥.٤٢) Cation concentration profiles across ٥٠- and ١٠٠-site cell.

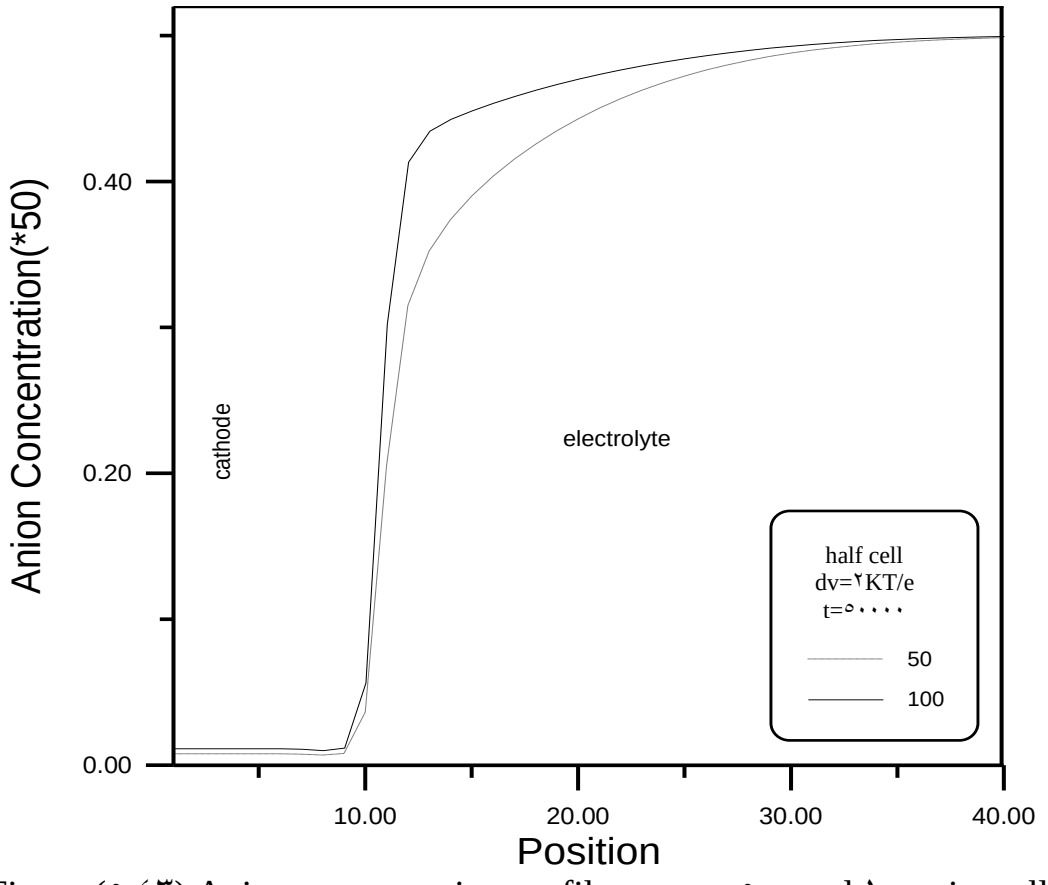

Figure (٥.٤٣) Anion concentration profiles across ٥٠- and ١٠٠-site cell.

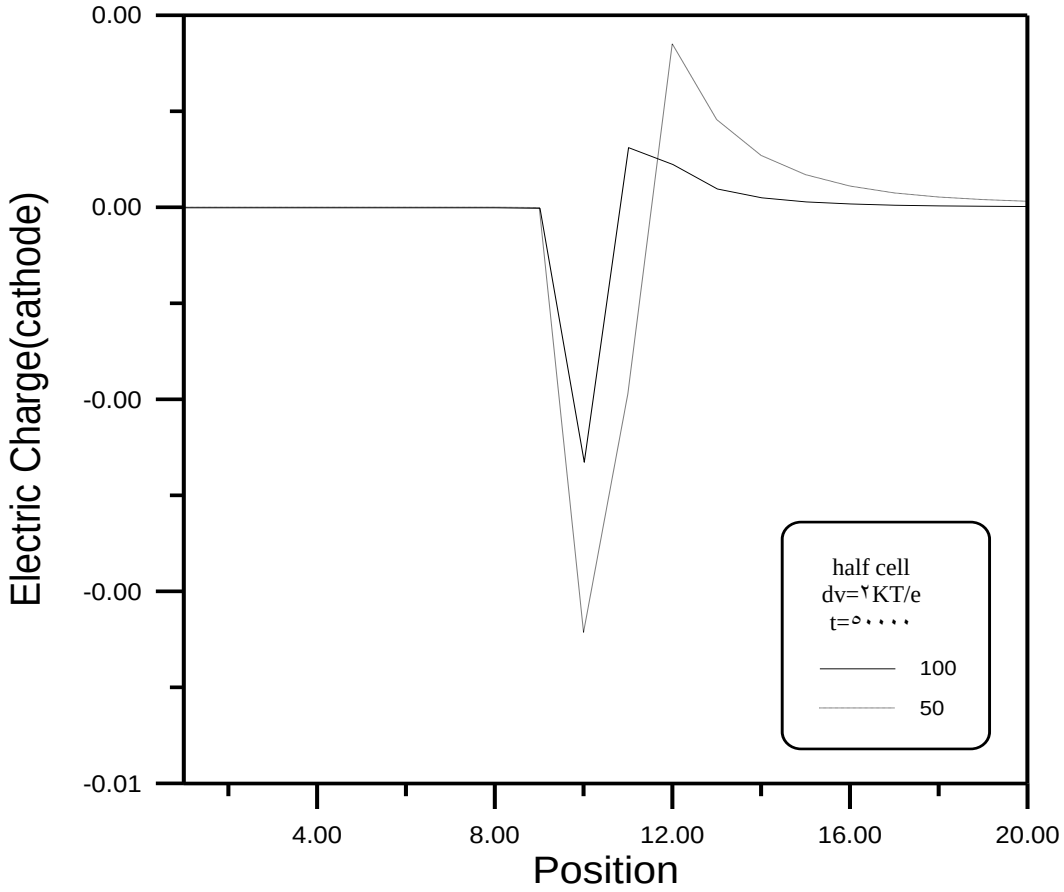

Figure (٥.٤٤) Electric charge(cathode) profiles across ٥٠- and ١٠٠-site cell.

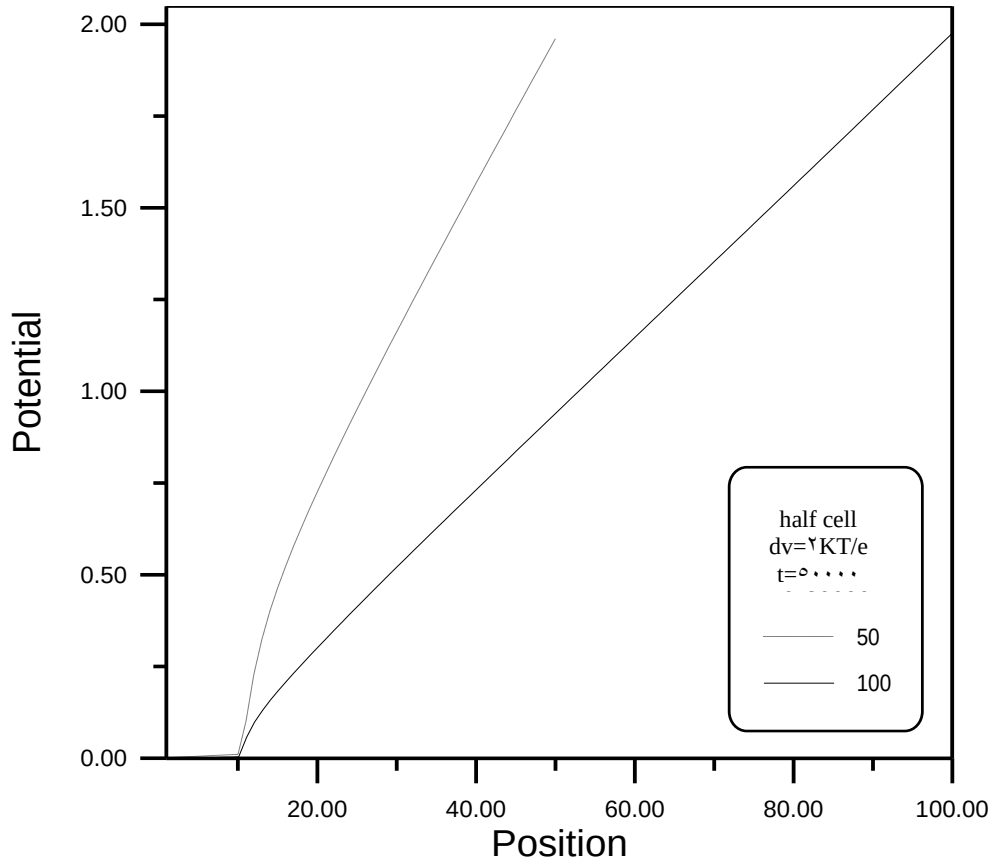

Figure (٥.٤٥) Potential profiles across ٥٠- and ١٠٠-site cell.

٤. Potential difference :-

Figure (٥.٤٦) shows that the deposition is increased with the applied potential increasing across the cell because of the increasing of the electrical potential for these sites , and hence accelerating the electrochemical reactions are leading to increasing of the processes of oxidation and reduction at the anode and cathode electrodes ,while figures (٥.٤٧ – ٥.٥٠) , illustrate the ionic concentration growth , charges distribution at the cathode and electric potential distribution across the sites ٥٠ for the half cell at t = 0.5×10^{5} for two values of potentials of (٢ and ١٠) KT/e .

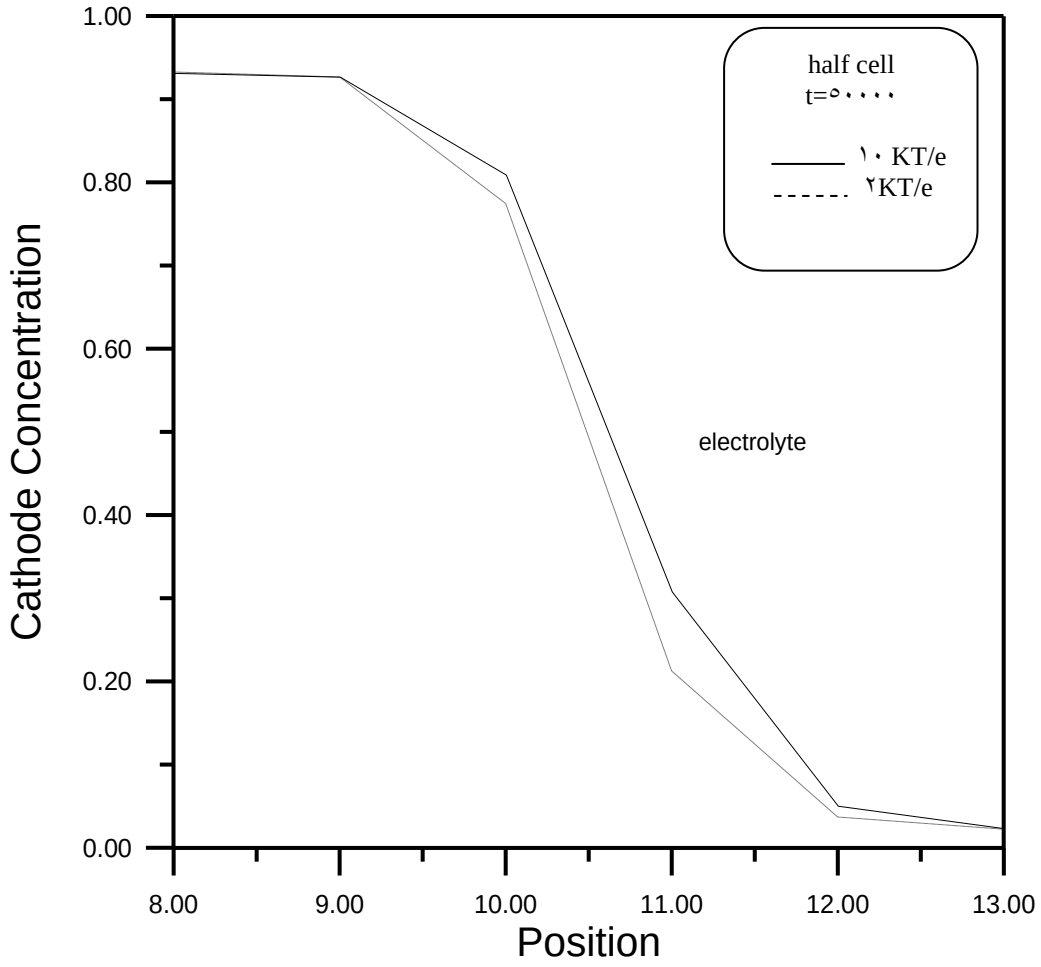

Figure(٥.٤٦) Cathode concentration profiles across a ٥٠-site cell.

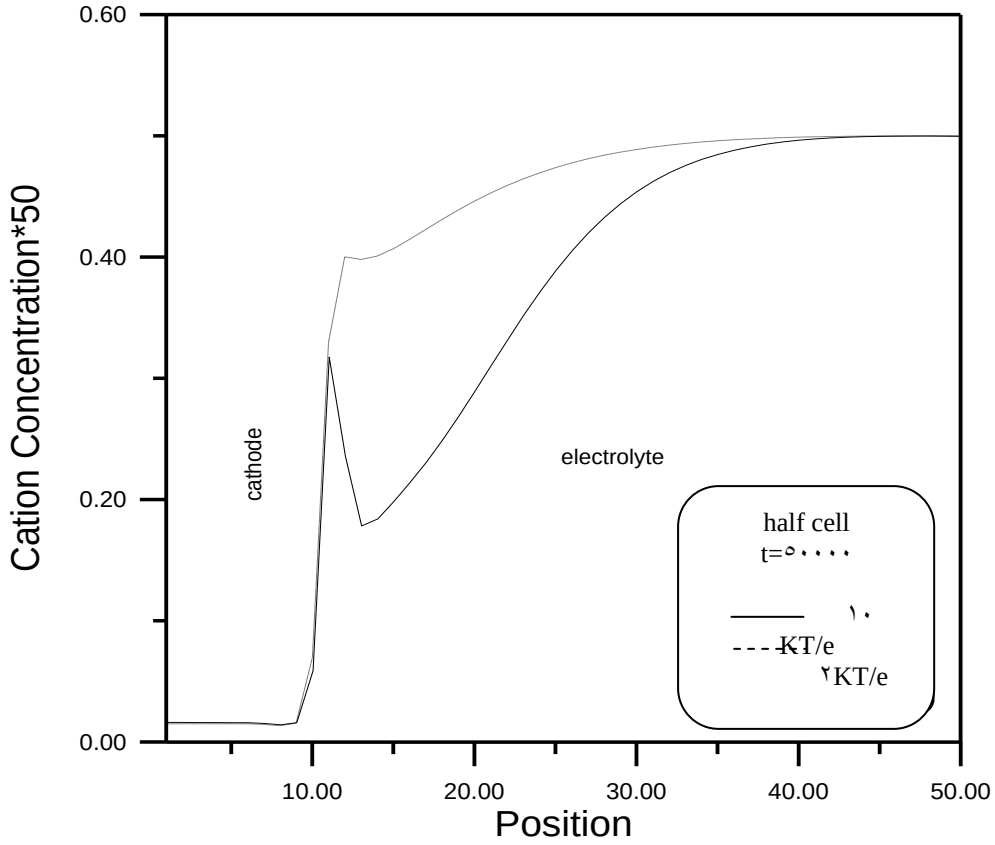

Figure (٥.٤٧) Cation concentration profiles across a ٥٠-site cell.

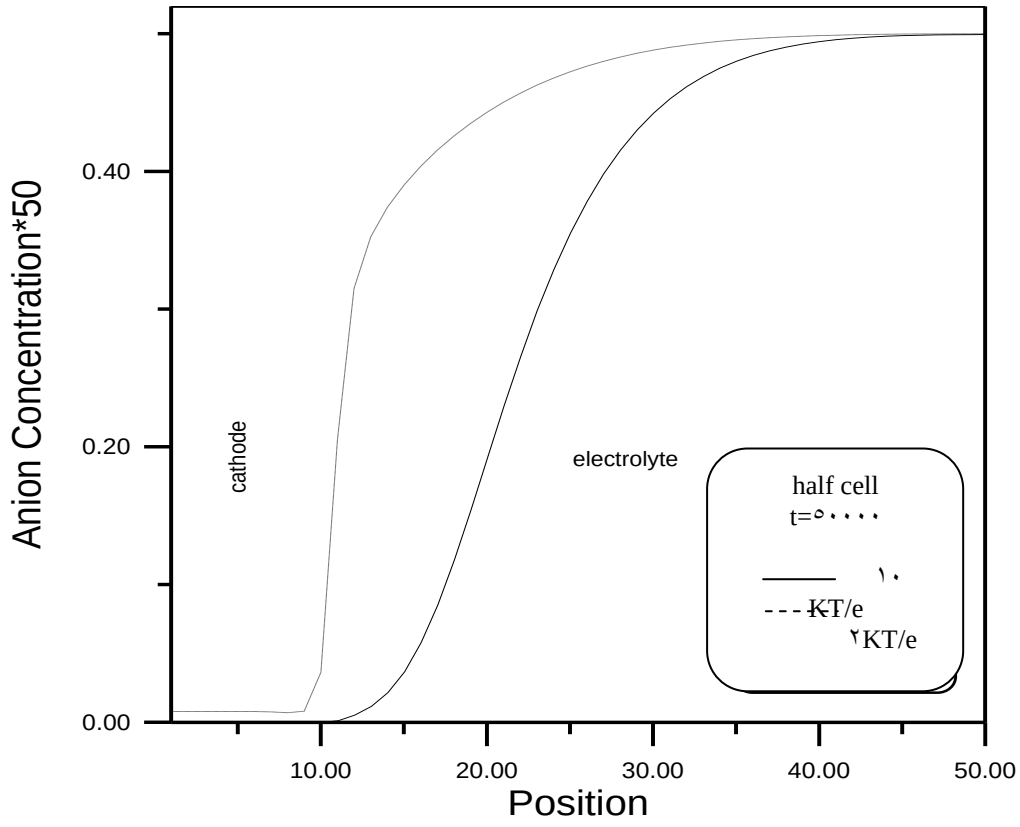

Figure (٥.٤٨) Anion concentration profiles across a ٥٠-site cell.

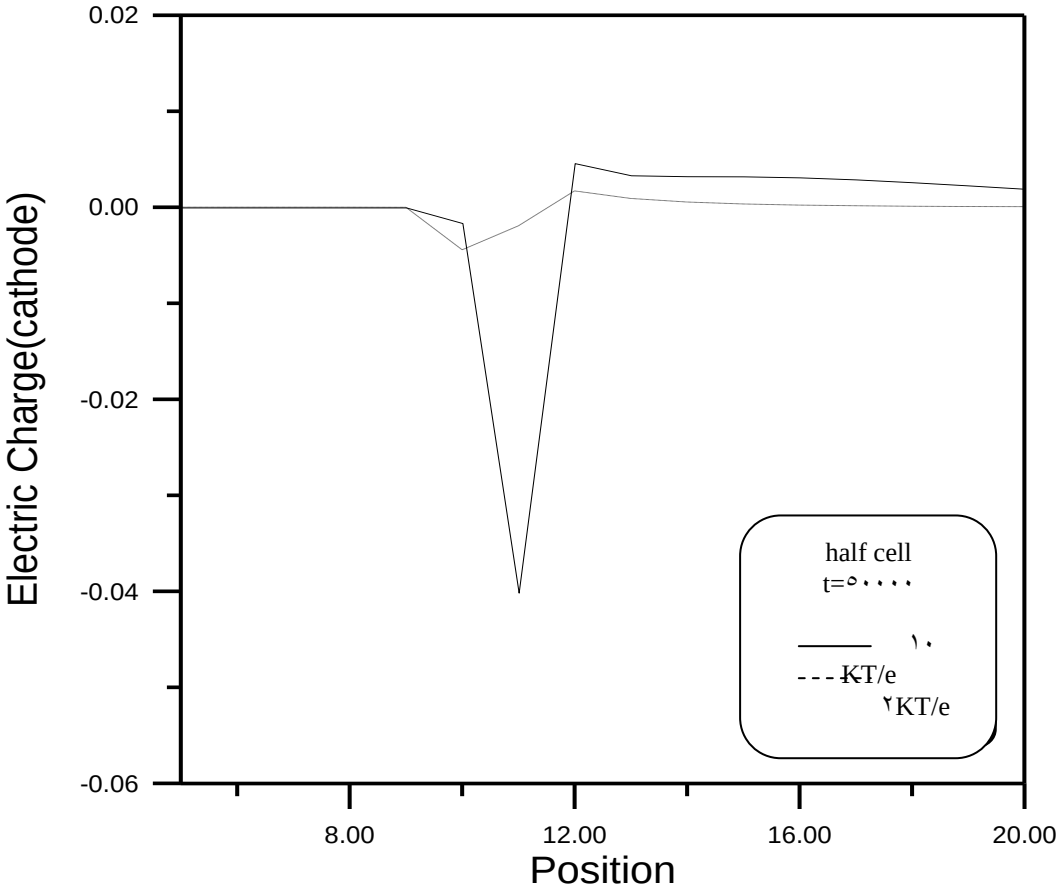

Figure (٥.٤٩) Electric charge(cathode) profiles across a ٥٠-site cell.

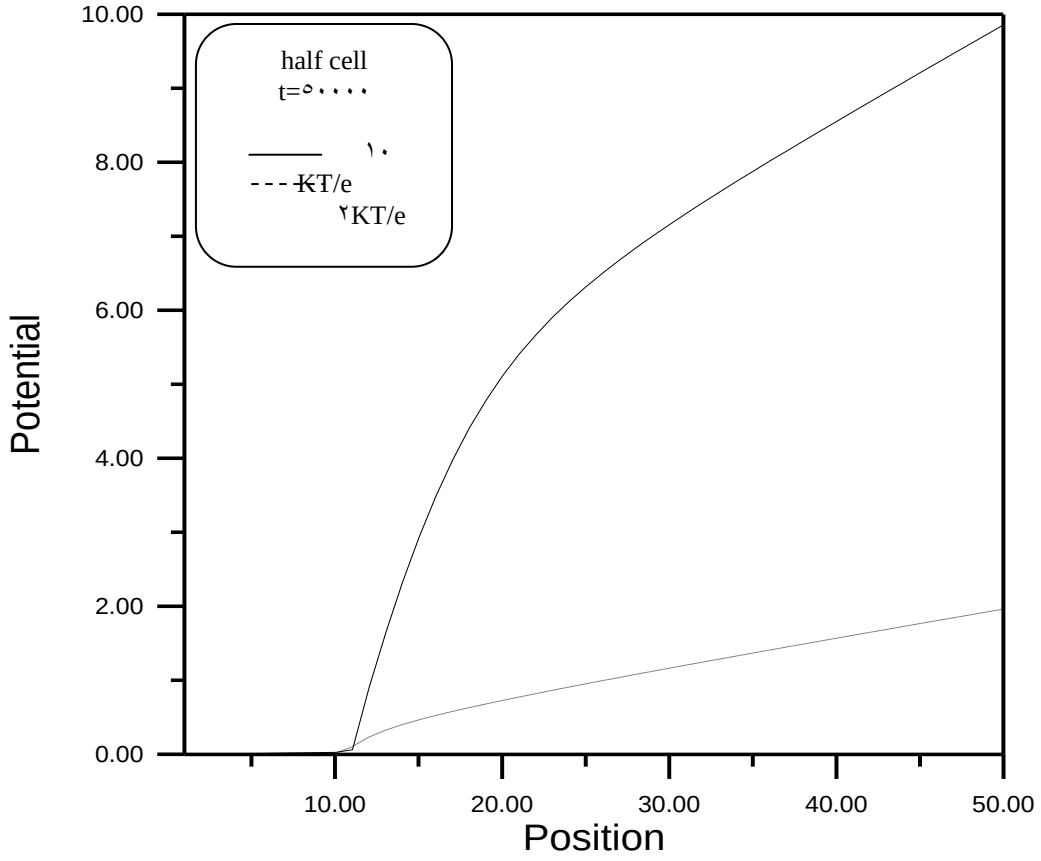

Figure (٥.٥٠) Potential profiles across a ٥٠-site cell.

٥.٥ The Time Rate of Deposition

Figure (٥.٥١) shows the deposition rate occurred at the cathode during the three time intervals t = $(1,3,5)\times10^{5}$ and it is observed that the deposition rate equal = ٠ out of the boundaries of the double layer . The highest deposite rates during these intervals mentioned above are (٠.٧٤٦١,٠.٧٧٩٩ and ٠.٨٠٣٩) respectively , these values are dropped as it is aparted from the electrode surface up to vanishing .

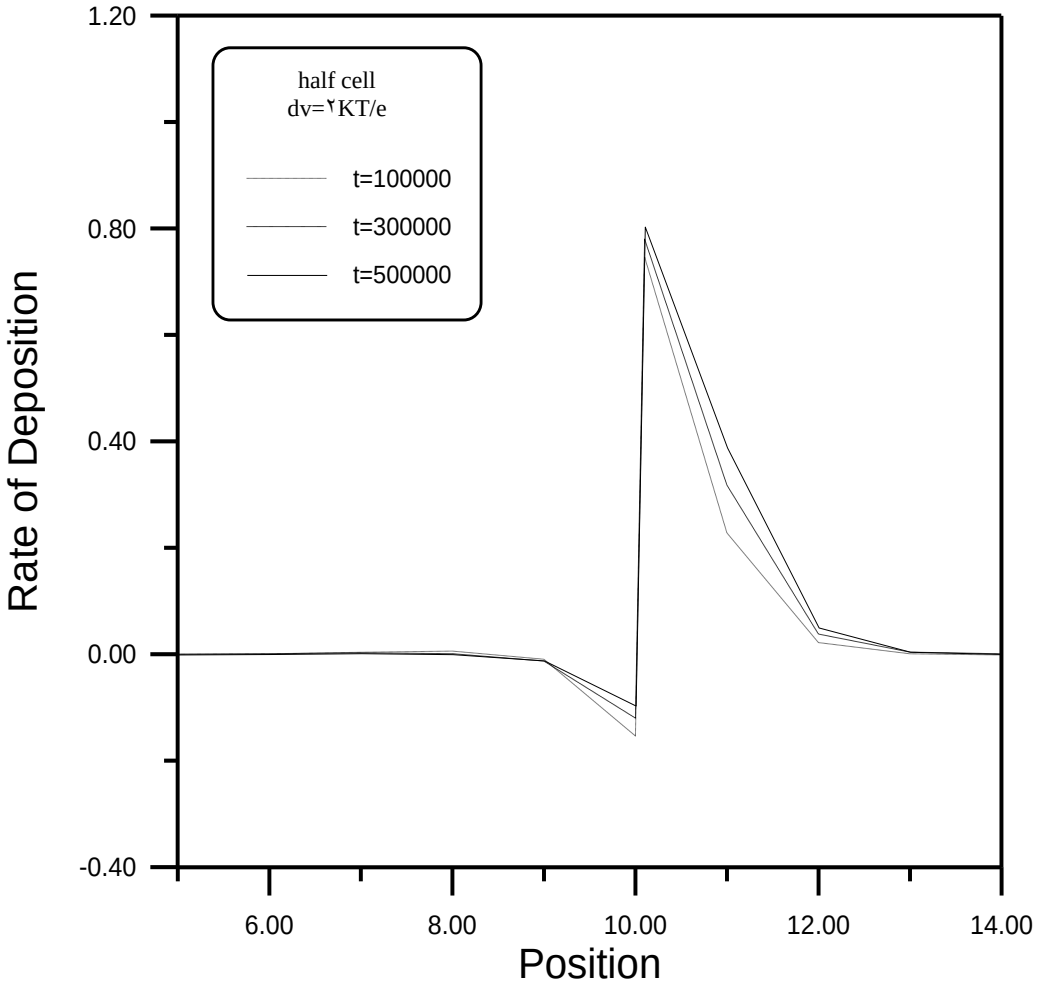

Figure (٥.٥١) Rate of deposition across a ٥٠-site cell.

٥.٦ The Second Method of Diffusion Current

There are two methods for the diffusion current used in the calculation of the concentrations (metal , cation , anion and solvent) . The first one is the equation (٣.٧) in which results were discussed in articles (٥.٢) and (٥.٣) .The second is equation (٣.٨) .

Figures (٥.٥٢) and (٥.٥٣) illustrate the simulation for the concentrations (metal , cation , anion and solvent) at time t = 5×10^5 , while figures (٥.٥٤) to (٥.٦٠) show each of growth and dissolution at the cathode and anode electrodes , the evolution of the ion concentration , charge distribution and electric potential a cross the sites at each of the cases (half and full) during the time intervals of t = $(1,3,5)\times10^5$ and what is said a bout results exploration and interpretation in section (٥.٣) holds for this section .

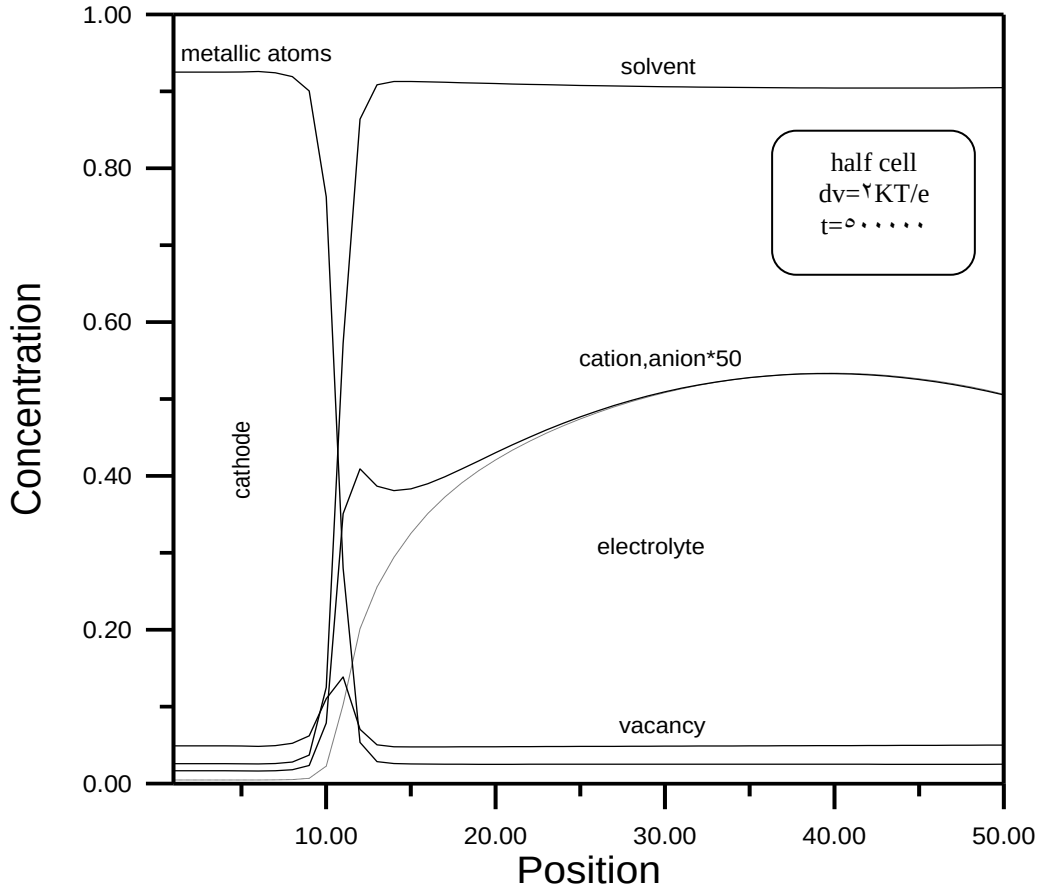

Figure(٥.٥٢) Concentration profiles across a ٥٠-site cell.

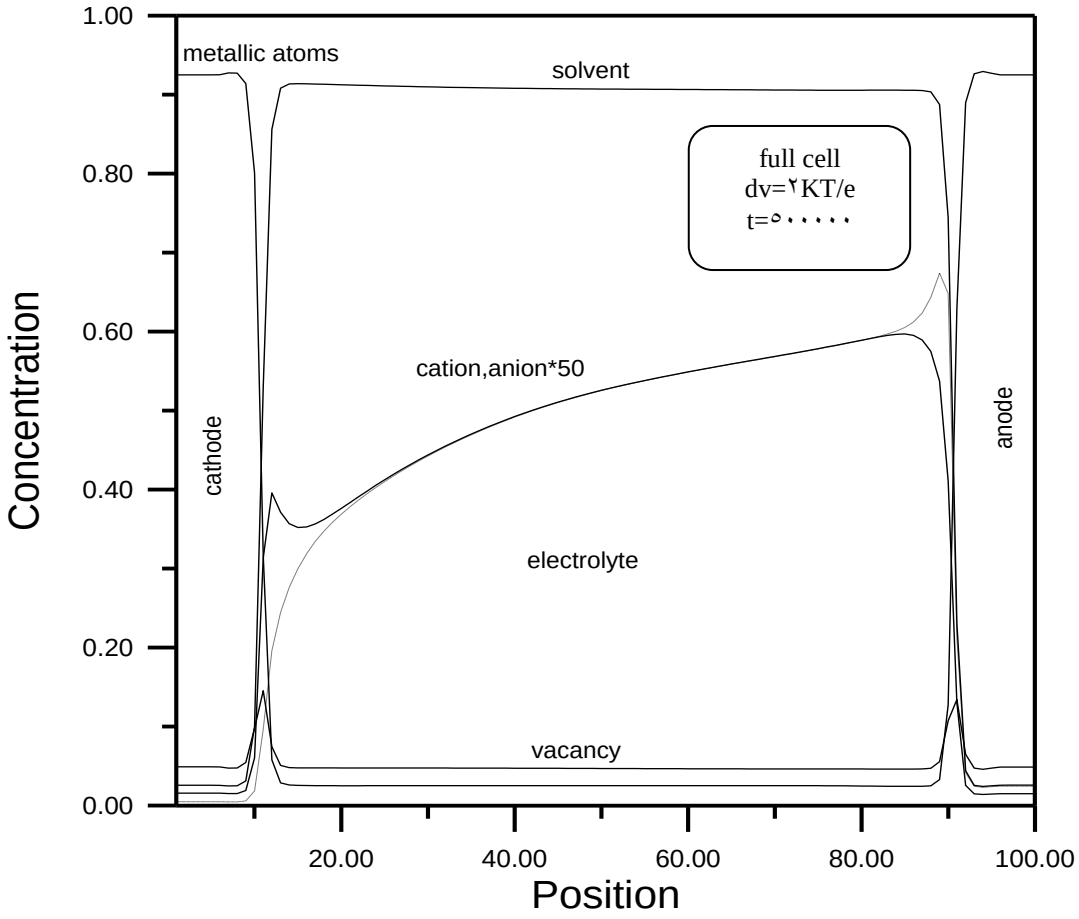

Figure(٥.٥٣) Concentration profiles across a ١٠٠-site cell.

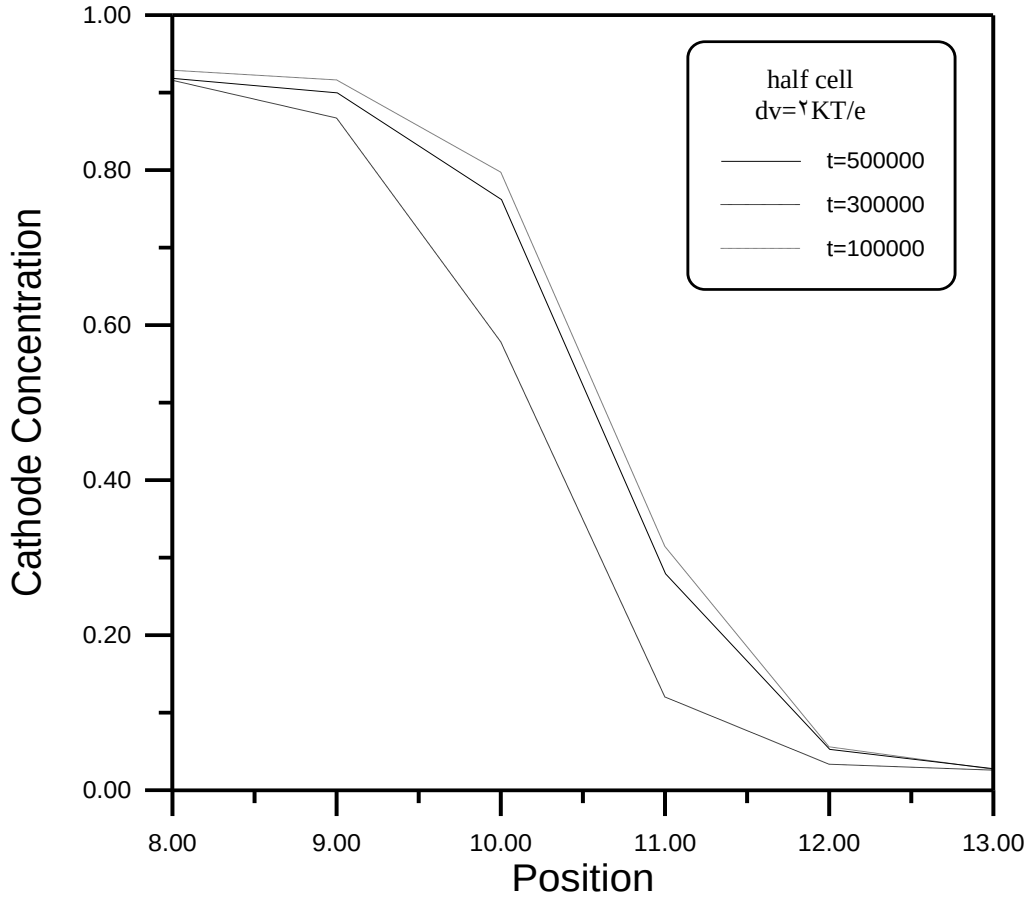

Figure(٥.٥٤) Showing the electrode position (reduction) at the cathode.

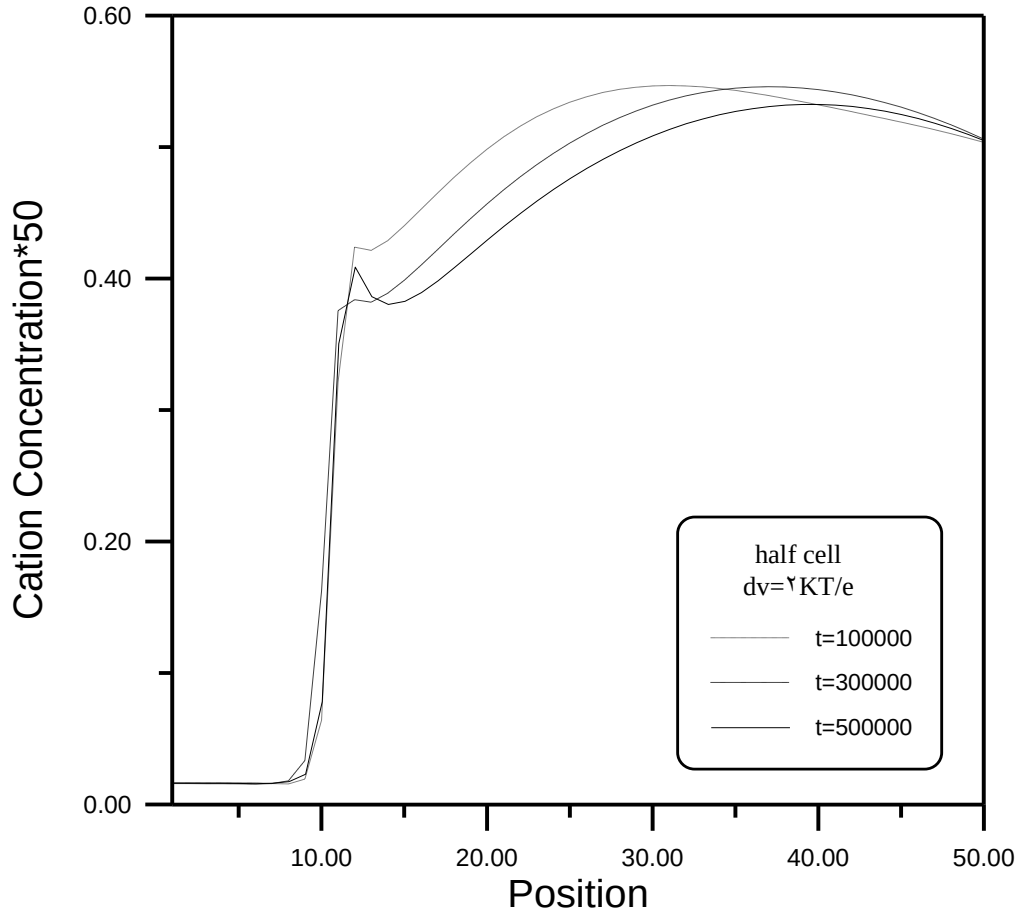

Figure(٥.٥٥) Cation concentration profiles across a ٥٠-site cell.

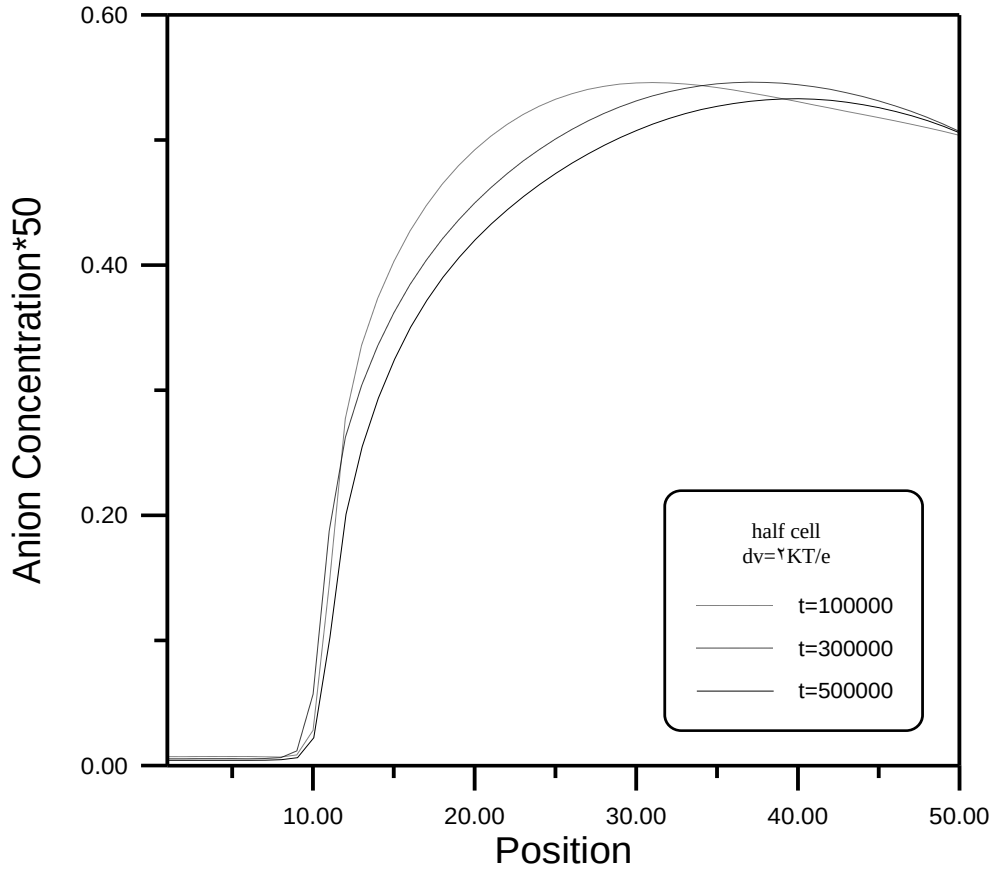

Figure(٥.٥٦) Anion concentration profiles across a ٥٠-site cell.

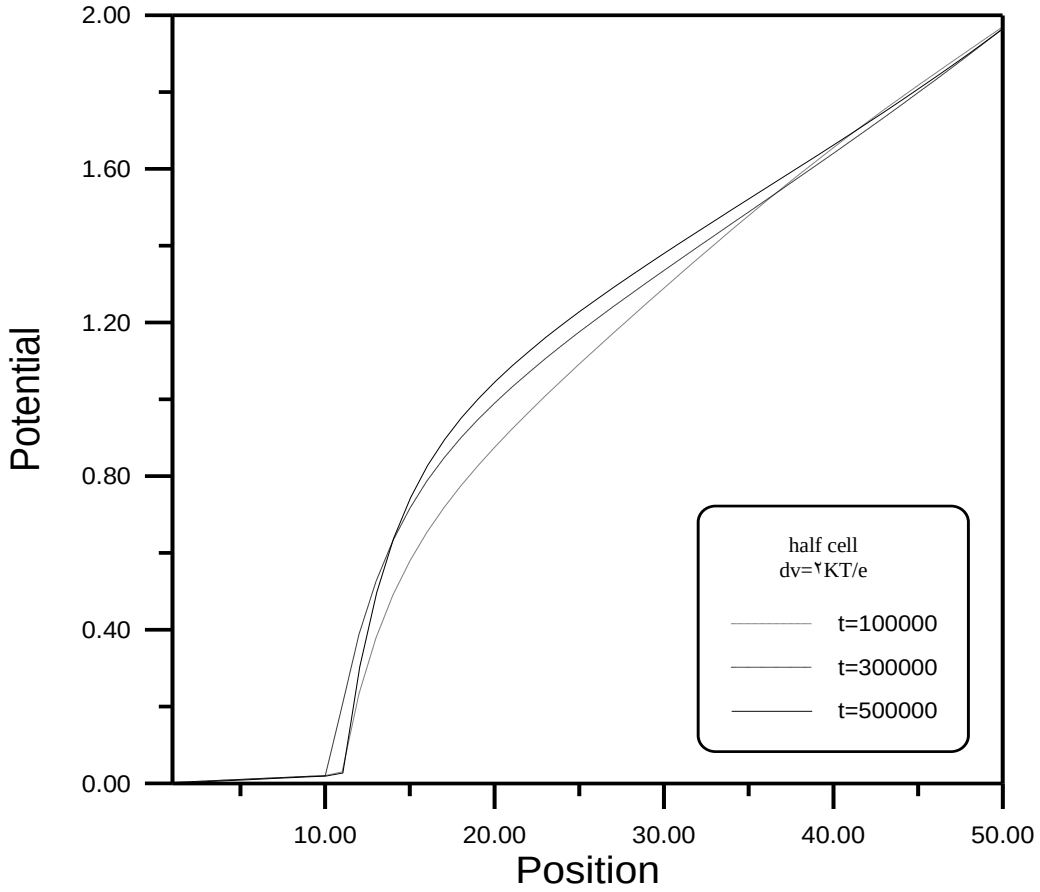

Figure (٥.٥٧) Potential profiles across a ٥٠-site cell.

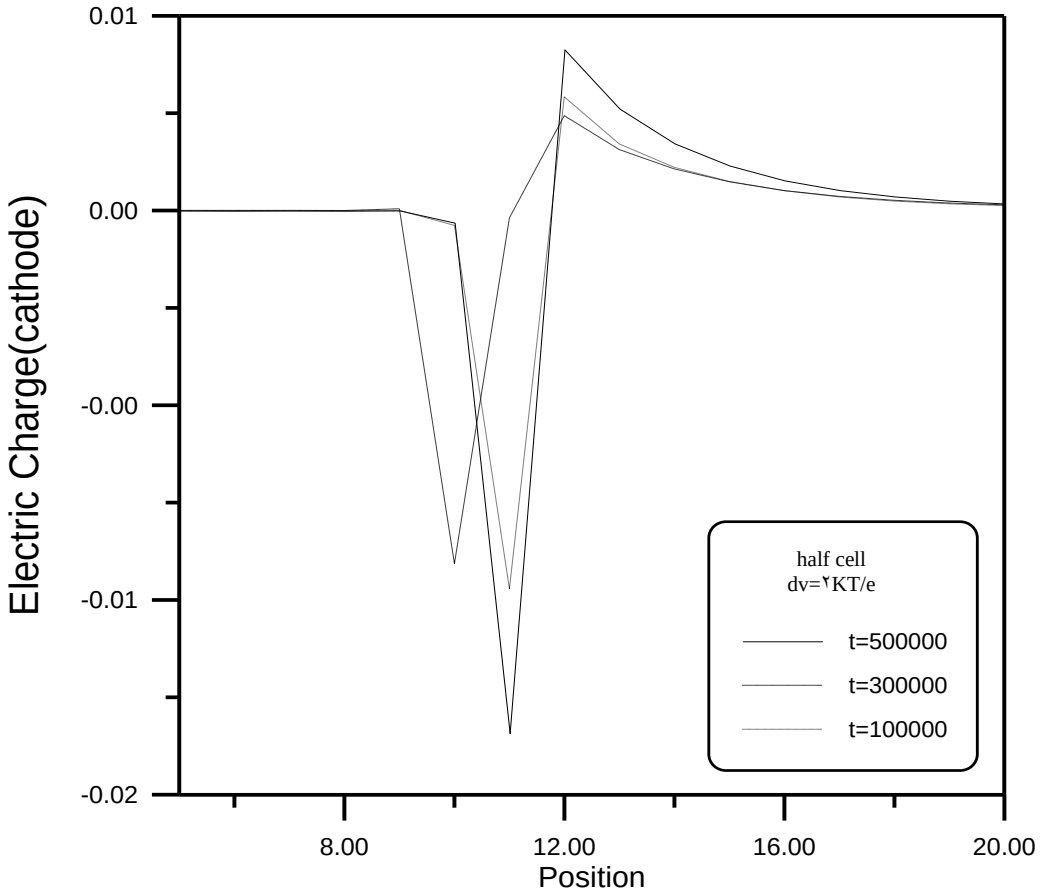

Figure(٥.٥٨) Charge distribution across a ٥٠-site cell.

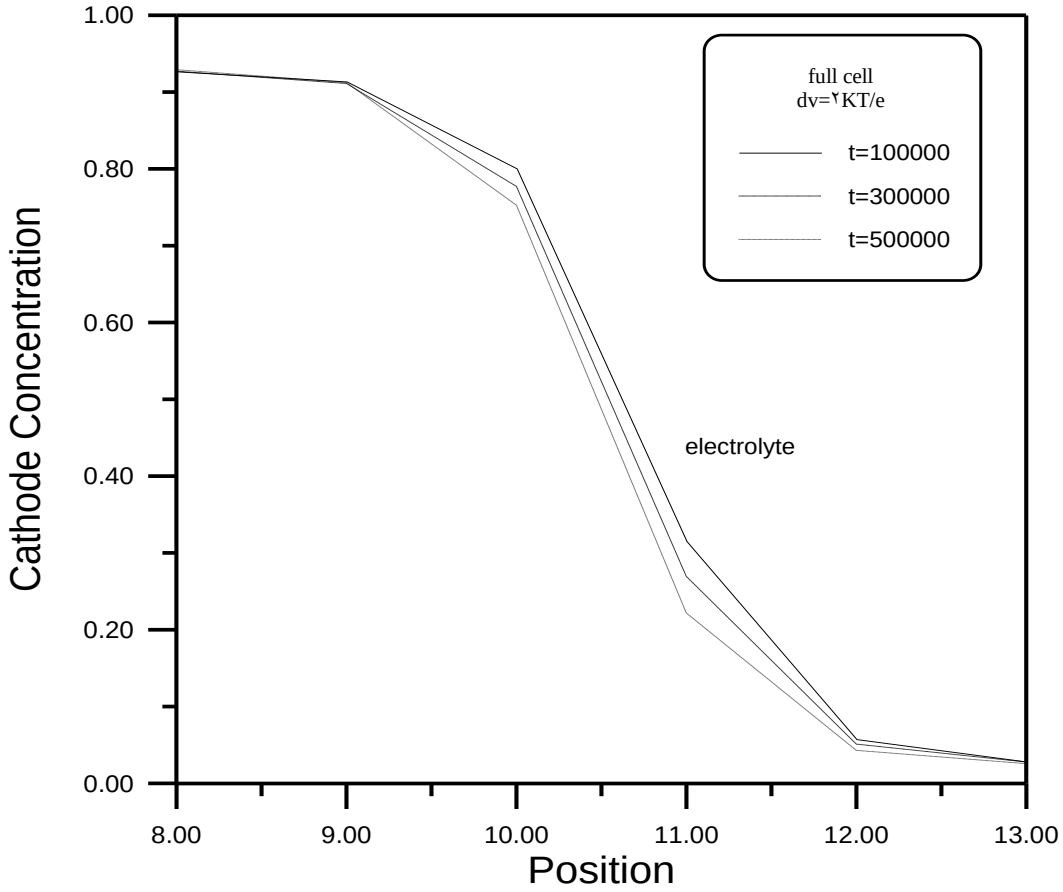

Figure(٥.٥٩) Showing the electrode position (reduction) at the cathode.

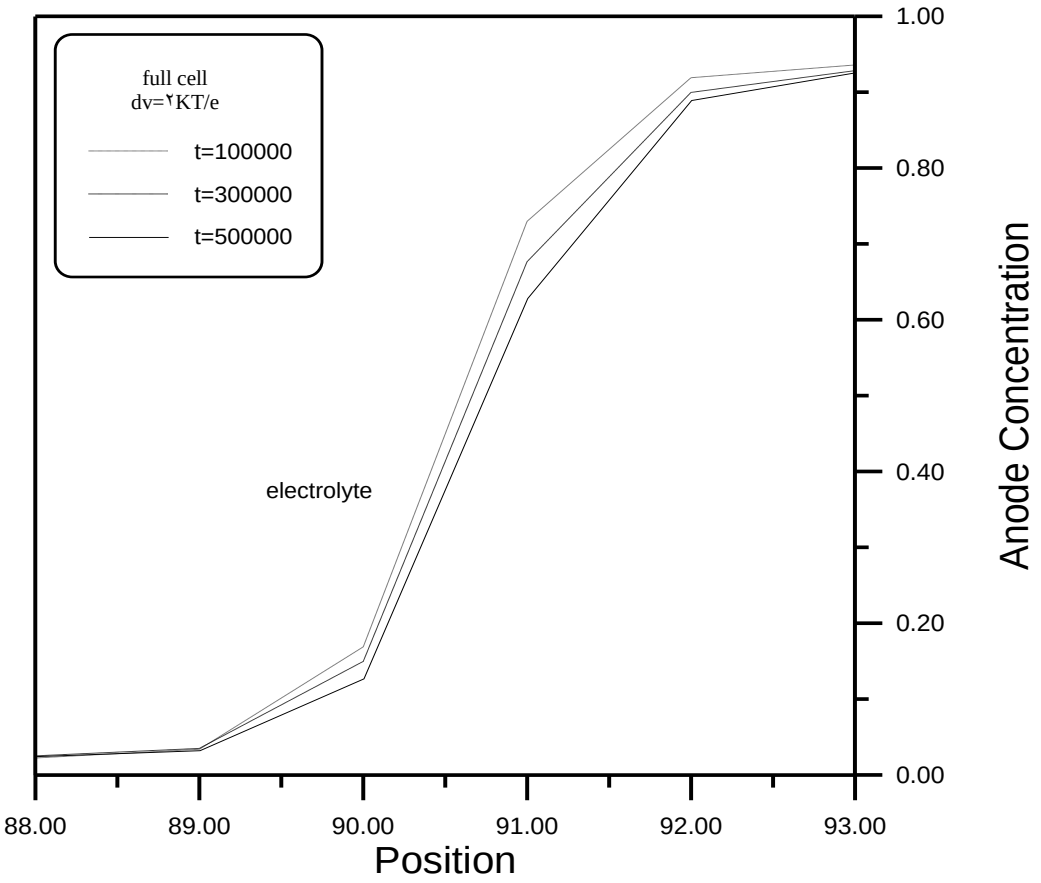

Figure(٥.٦٠) Showing the dissolution of metal at the anode .

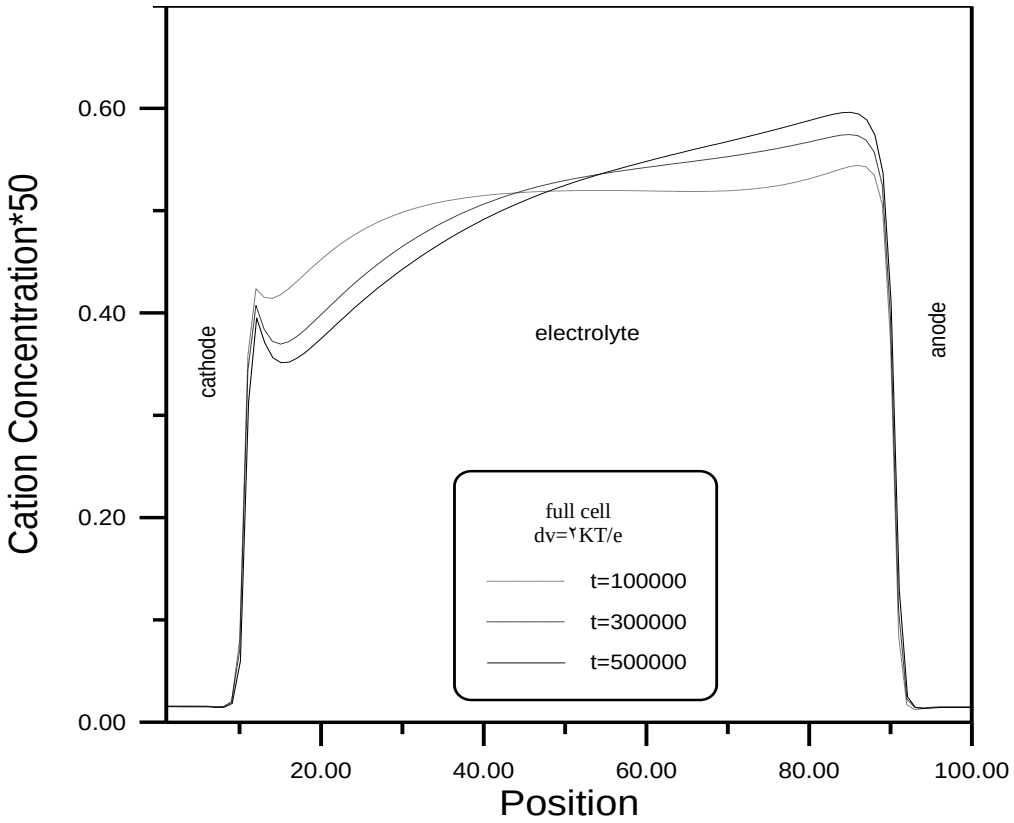

Figure(٥.٦١) Cation concentration profiles across a ١٠٠-site cell.

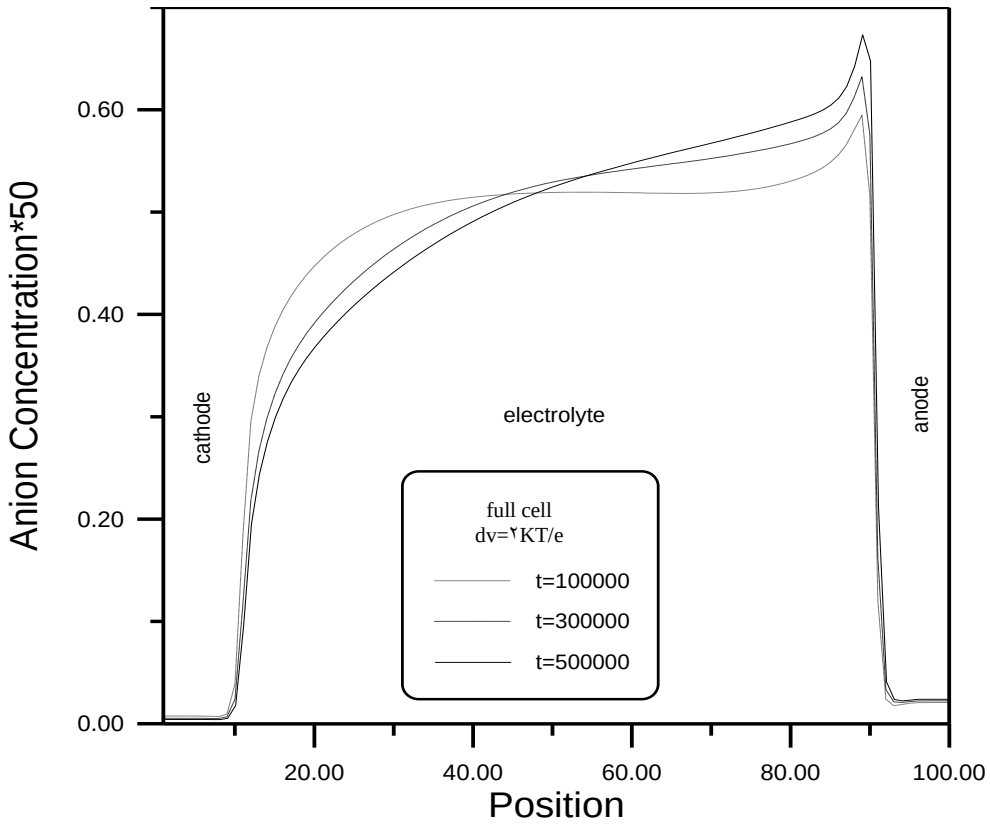

Figure(٥.٦٢) Anion concentration profiles across a ١٠٠-site cell.

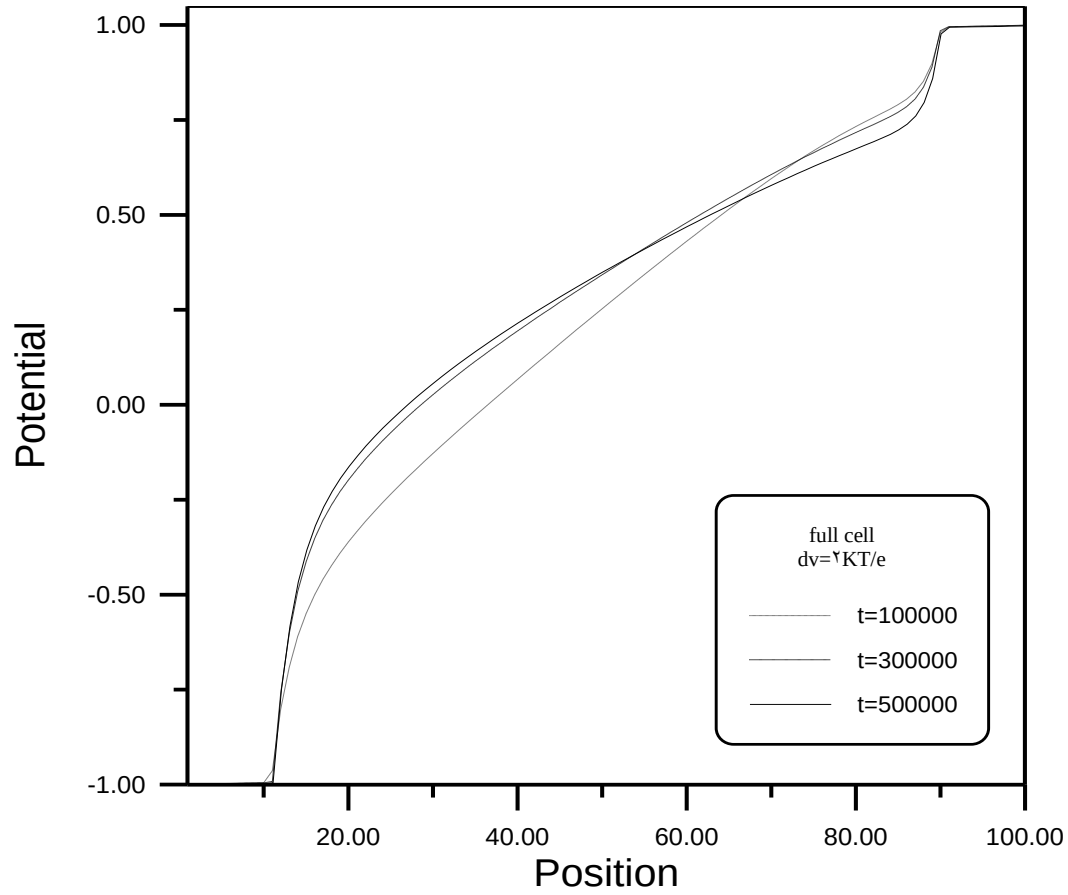

Figure (٥.٦٣) Potential profiles across a ١٠٠-site cell.

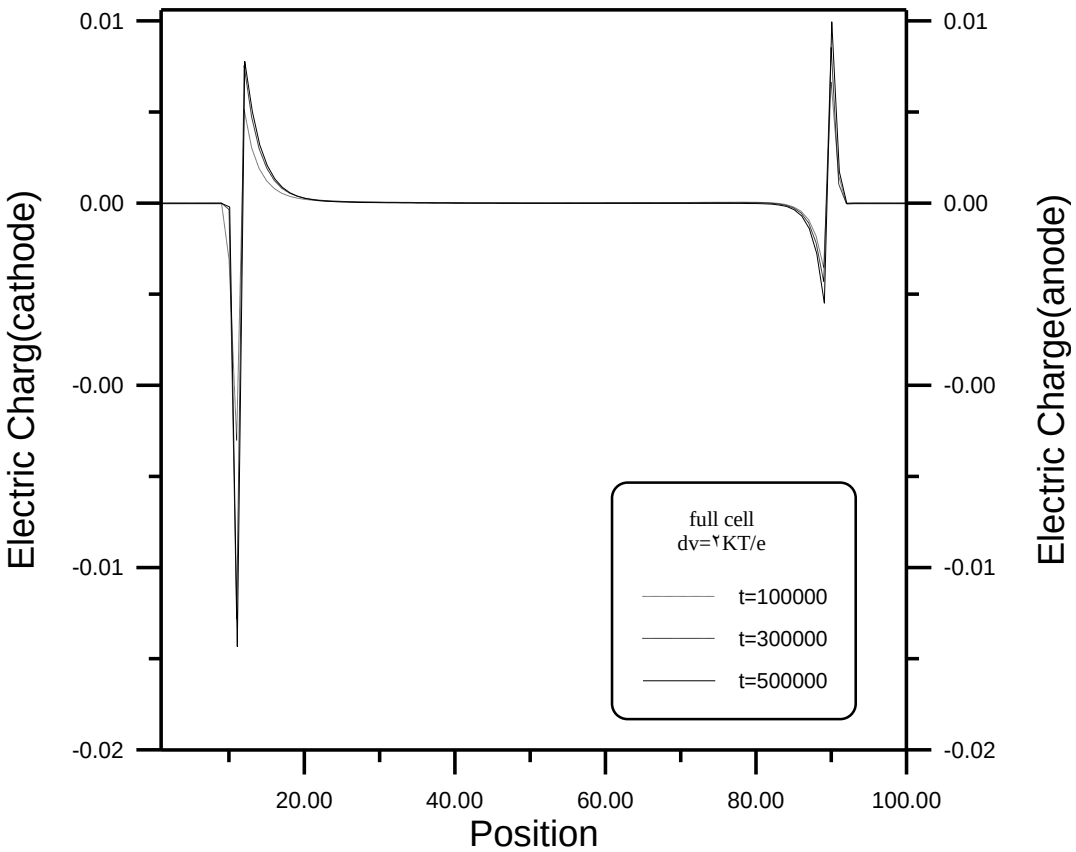

Figure(٥.٦٤) Charge distribution across a ١٠٠-site cell.

٥.٧ Comparison between the First and Second Method of the Diffusion

A comparison is achieved between the two methods from the view points of (deposition , ionic concentration growth , charge distributions and electric potential across the sites) in case of half and full cell subjected to a potential of ٢KT/e at time $t = 5\times10^5$.

a. Half cell :-

Figure (٥.٦٥) shows that the deposition of the first method of the diffusion is higher than that of the second one due to high reduction at the cathode of the first method. Figures (٥.٦٦) and (٥.٦٧) show that the ionic concentration growth of the first method is less than that of the second one . Figure (٥.٦٨) shows that the electric potential distribution across the sites is higher causing increasing electrochemical reaction speed . Figure (٥.٦٩) represents charges distribution at the cathode of the first method which extends over a larger space leading to the increasing of the growth velocity.

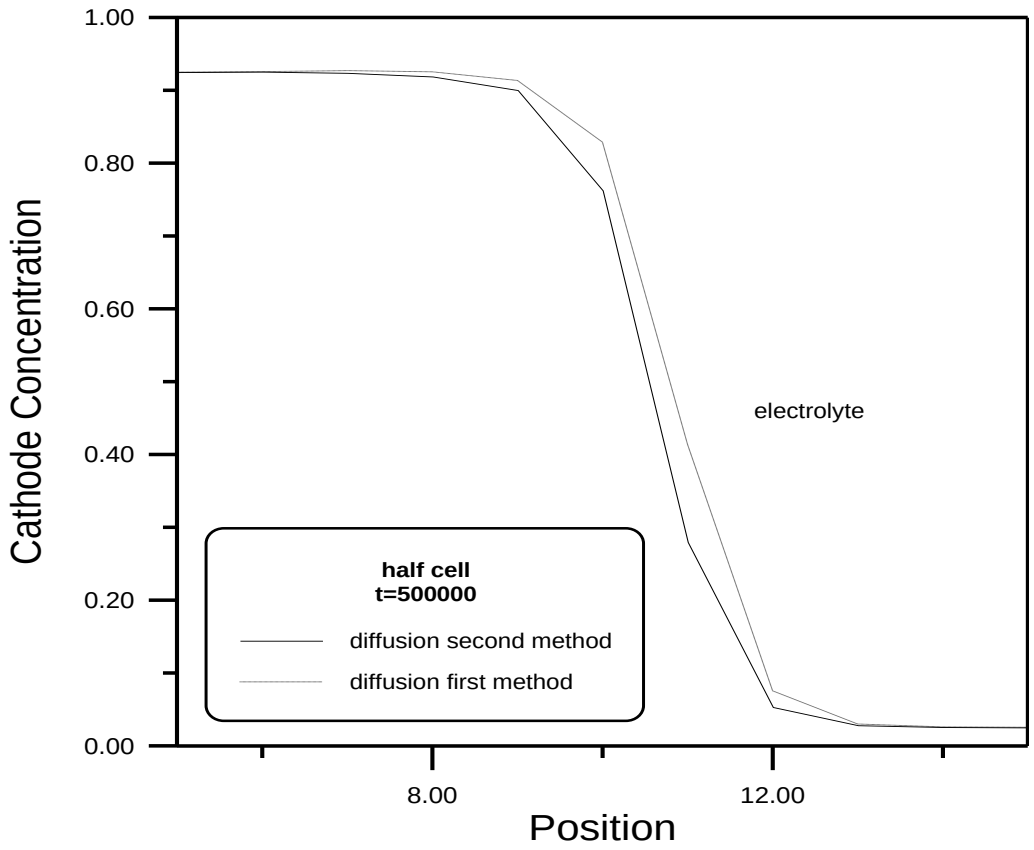

Figure(٥.٦٥) Showing the electrode position (reduction)at the cathode.

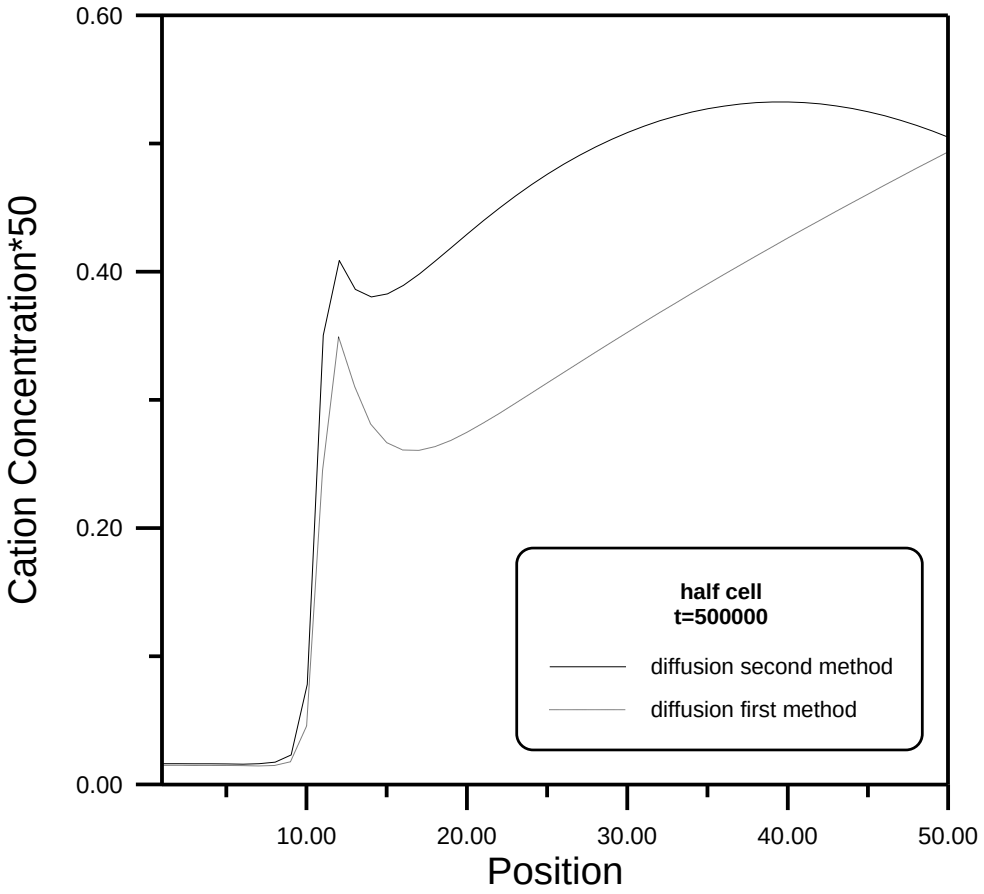

Figure(٥.٦٦) Cation concentration profiles across ٥٠-site cell.

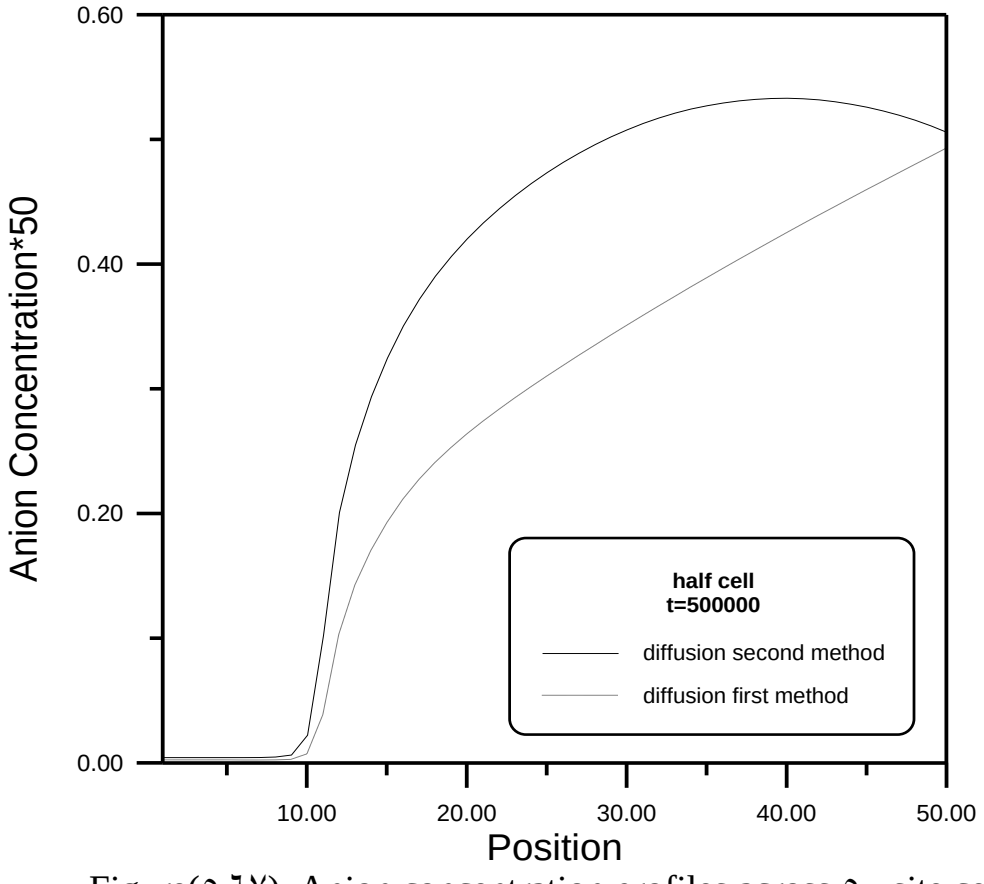

Figure(٥.٦٧) Anion concentration profiles across ٥٠-site cell.

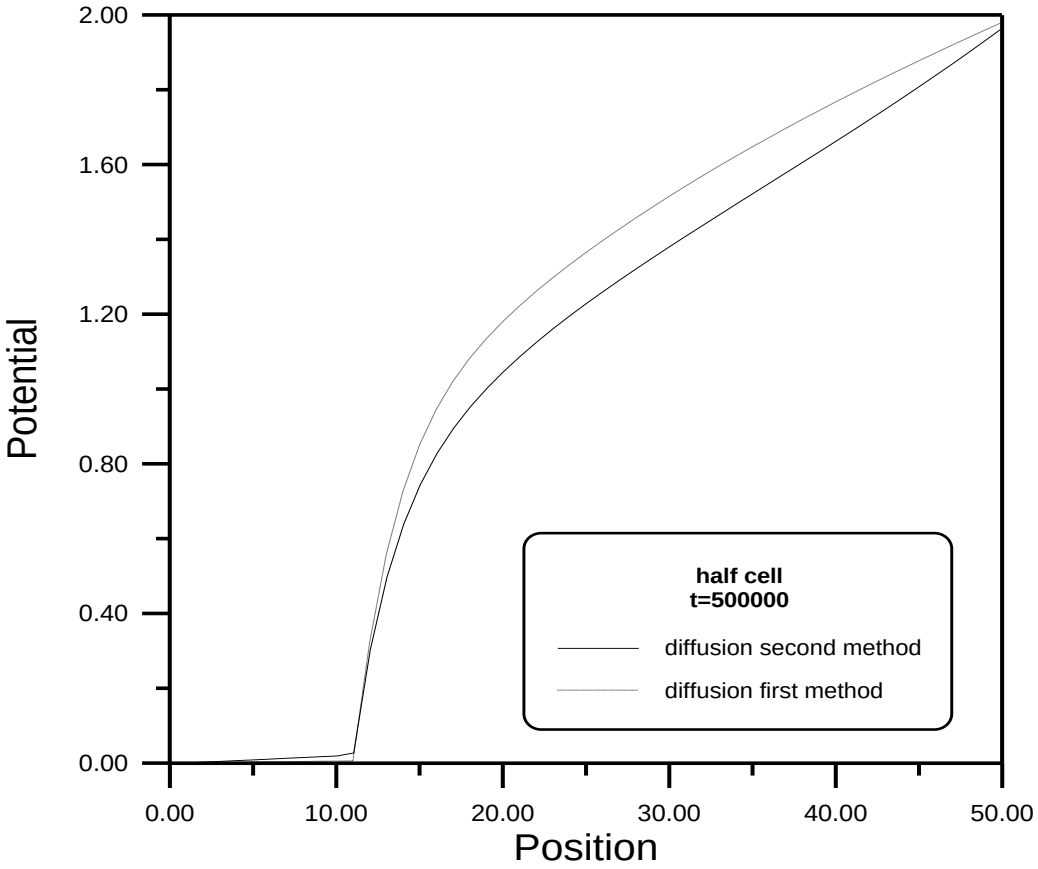

Figure (٥.٦٨) Potential profiles across ٥٠-site cell.

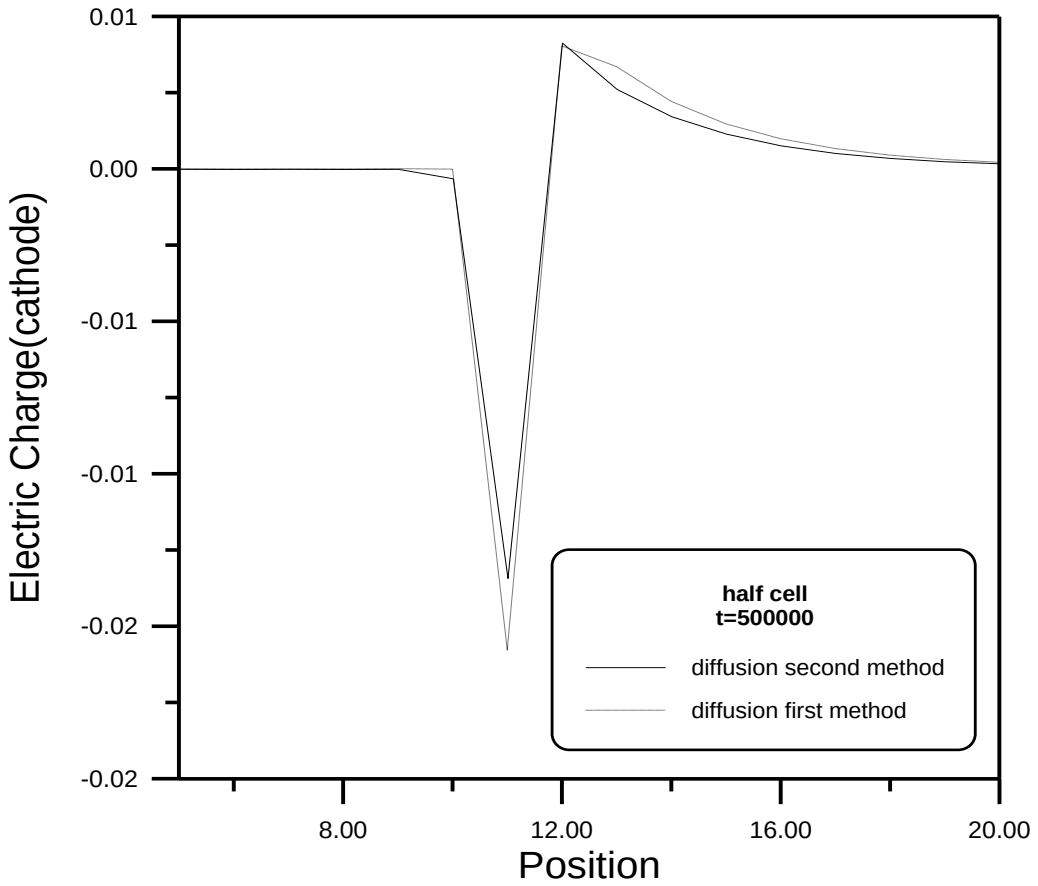

Figure(٥.٦٩) Charge distribution across ٥٠-site cell.

b. Full cell :-

Figures (٥.٧٠) and (٥.٧١) show that the second method diffusion deposition rate is higher than that of the first method because of higher reduction at the cathode of second method . Figures (٥.٧٢) and (٥.٧٣) represent the evolution of the ion concentration which is higher for the second method than that of the first method at the cathode . The reverse takes place at the anode . Figure (٥.٧٤) shows that the electric potential distribution across the sites for the second method is higher than that of the first method causing accelerating of the electrochemical reaction of the second method . Figure (٥.٧٥) illustrates the charges distribution at the cathode and anode electrodes. It is observed that the distribution area of the second method at the cathode is more – extended causing a higher growth velocity .

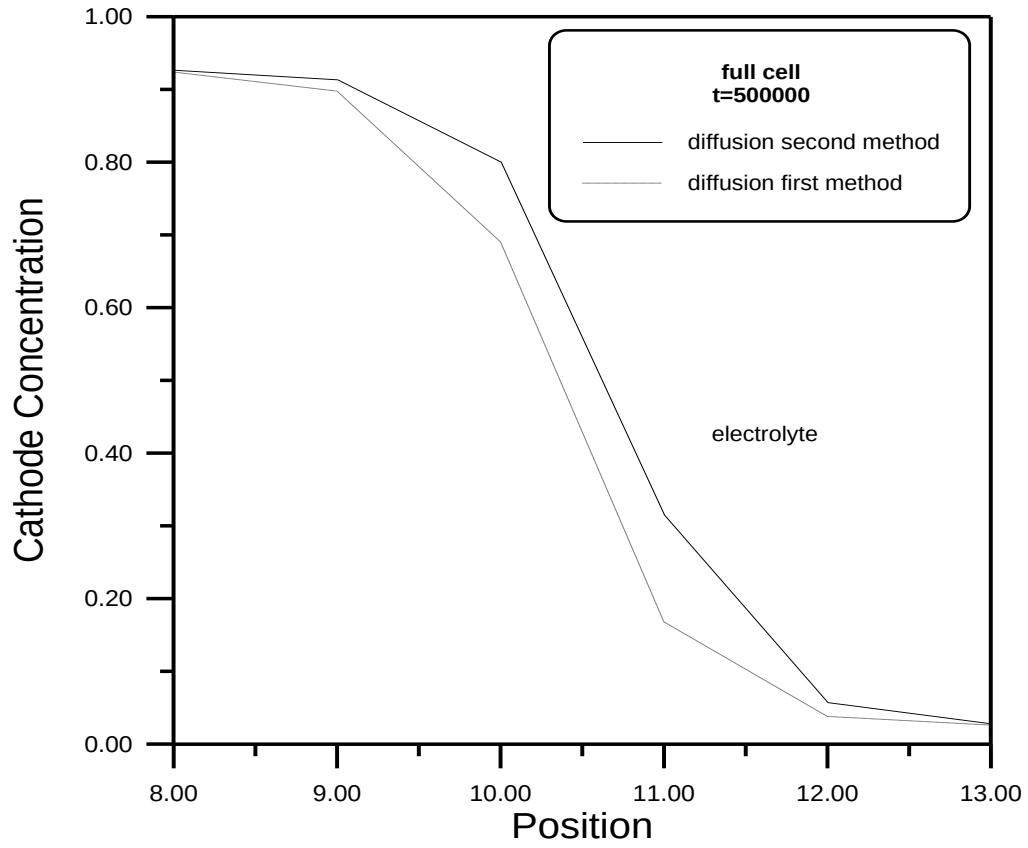

Figure(٥.٧٠) Showing the electrode position (reduction)at the cathode .

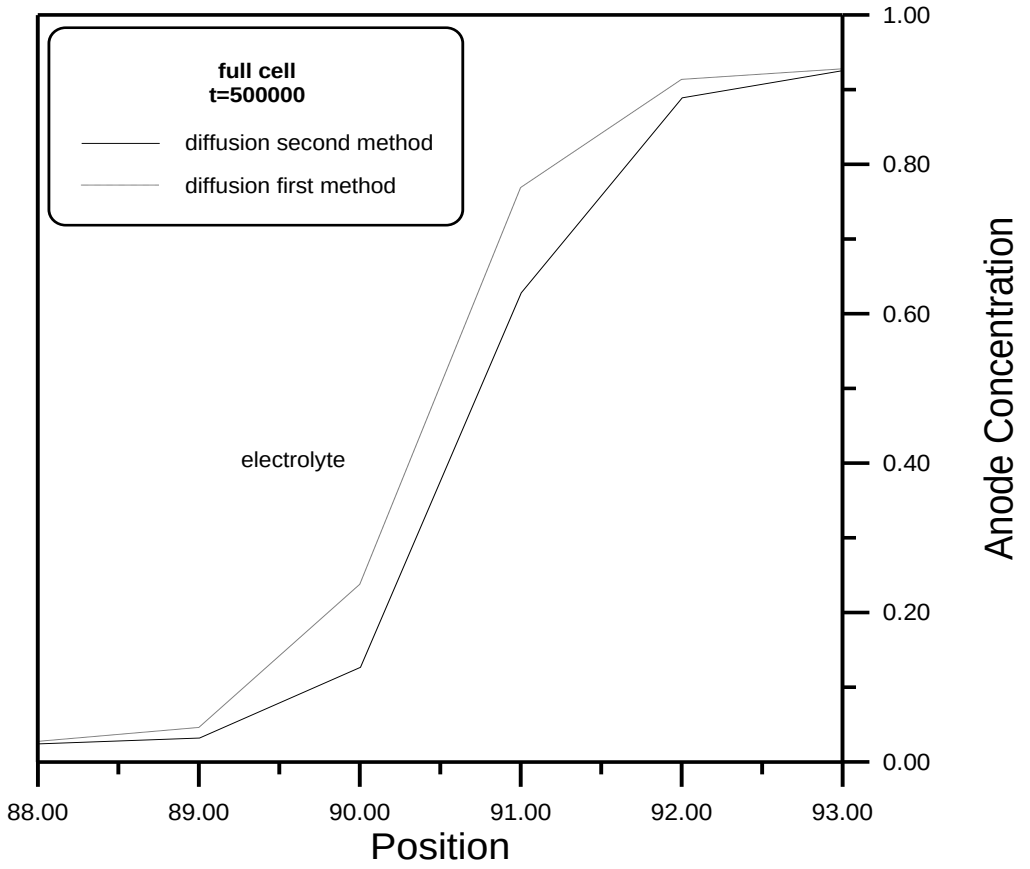

Figure(٥.٧١) Showing the dissolution of metal at the anode .

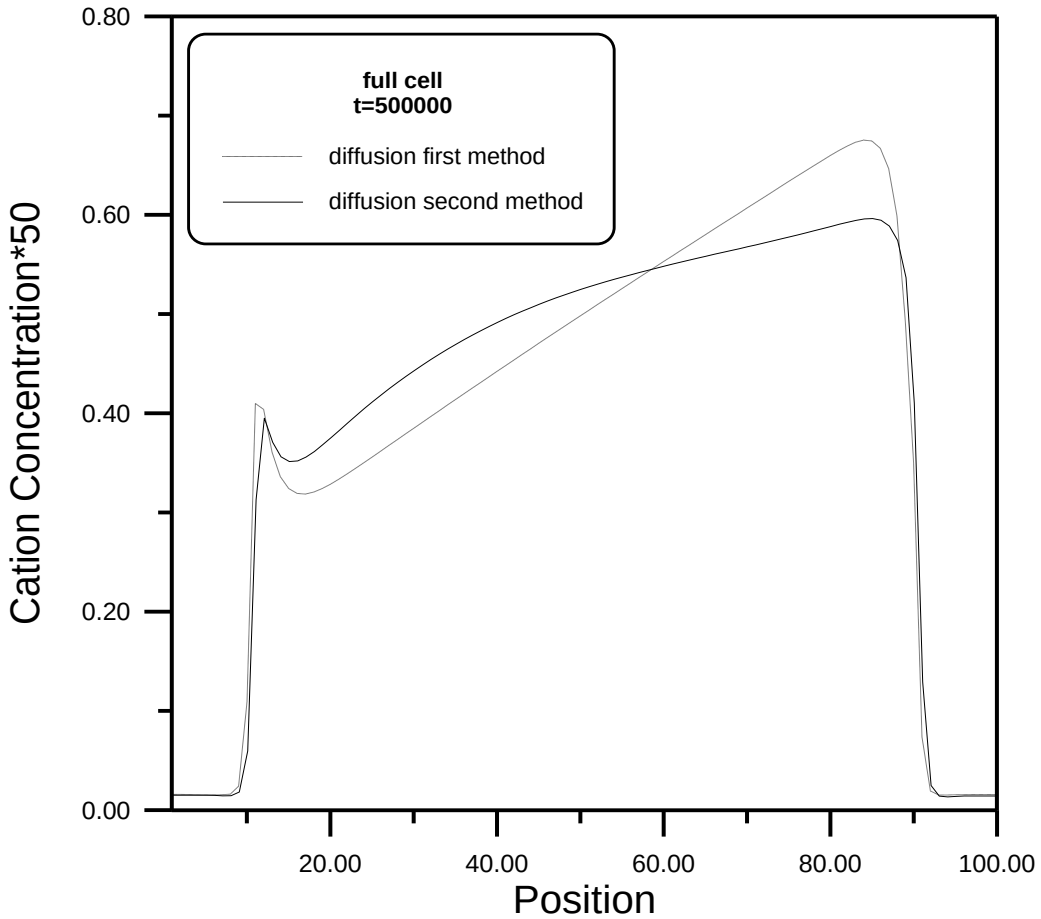

Figure(٥.٧٢) Cation concentration profiles across ١٠٠-site cell.

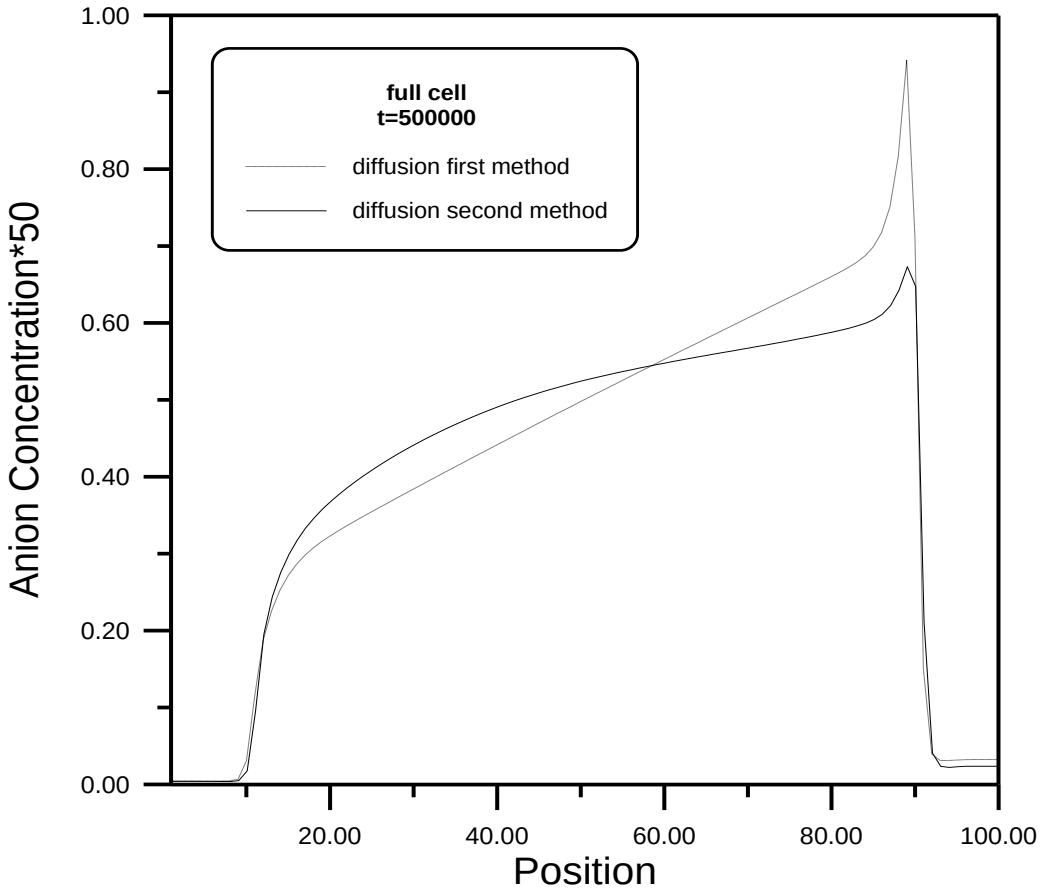

Figure(٥.٧٣) Anion concentration profiles across ١٠٠-site cell.

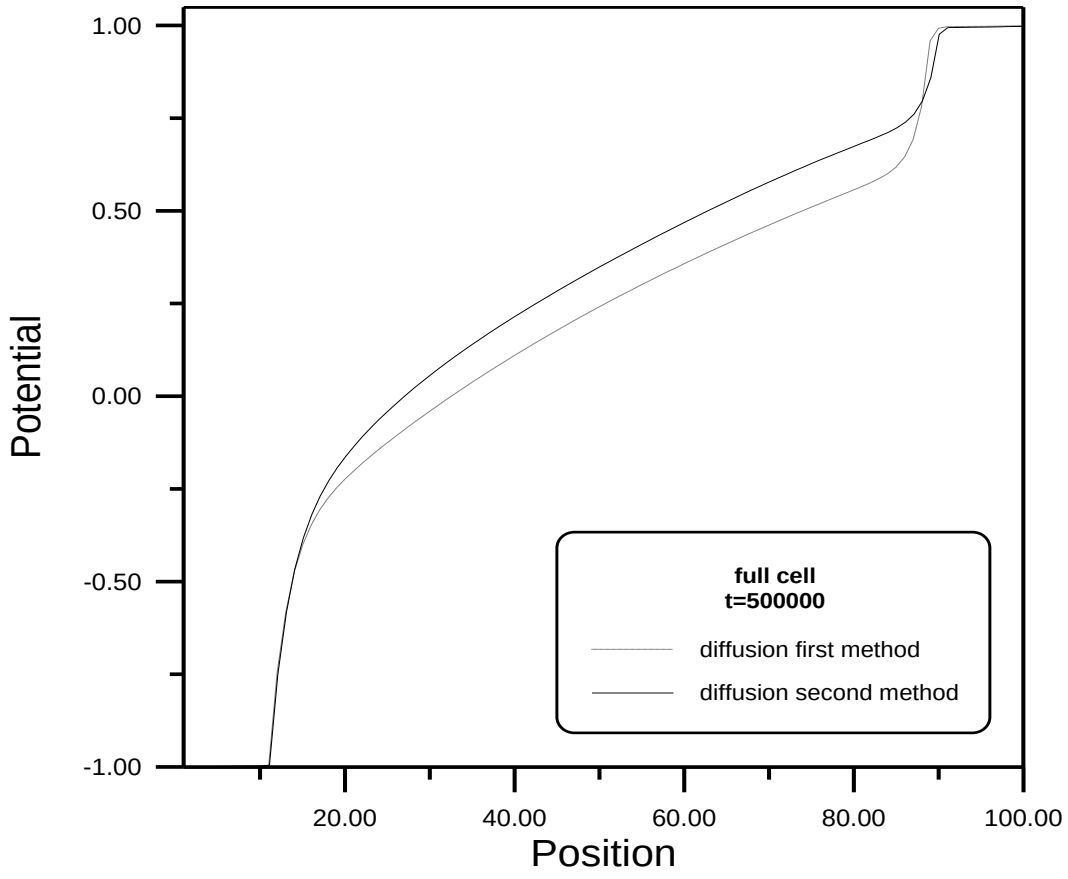

Figure (٥.٧٤) Potential profiles across ١٠٠-site cell.

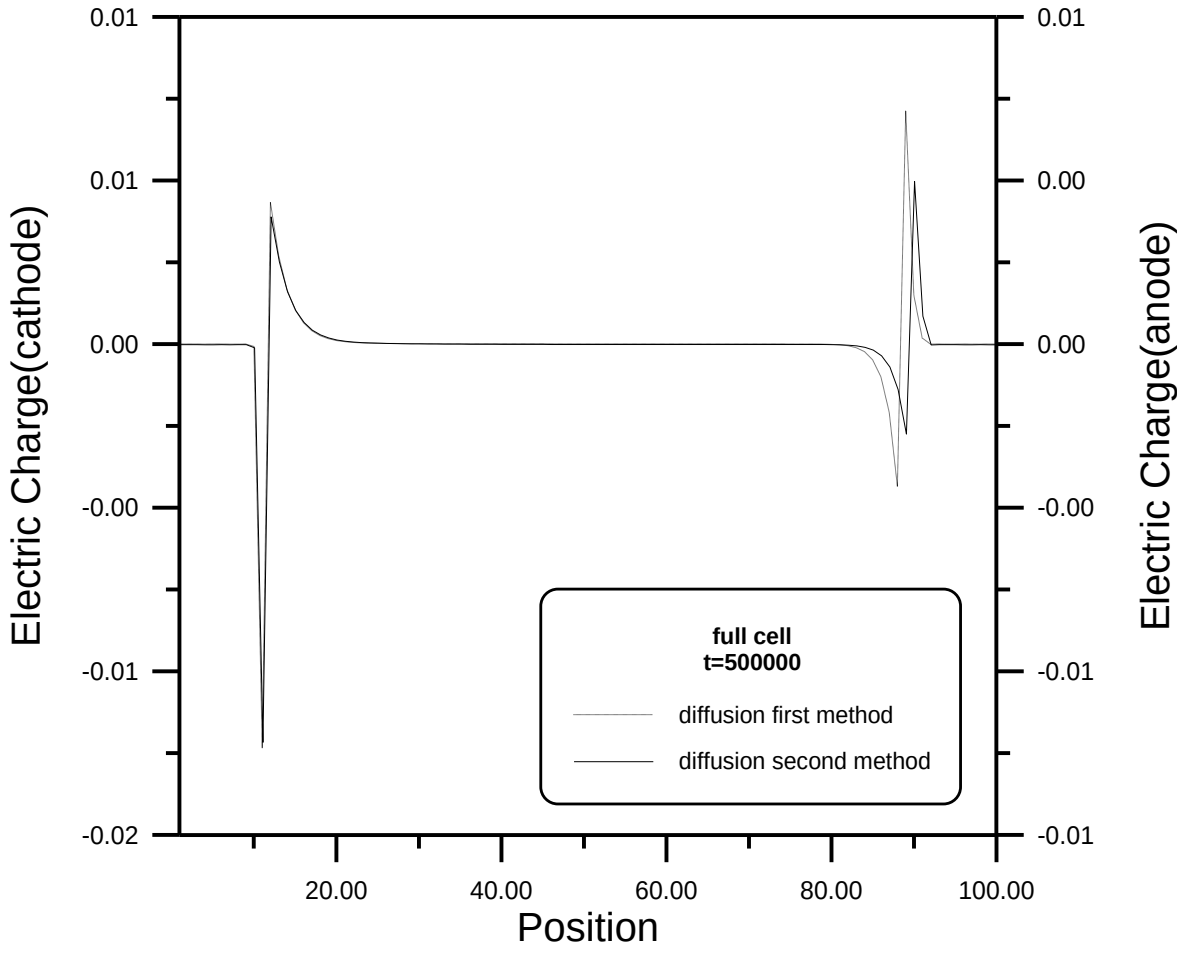

Figure(٥.٧٥) Charge distribution across ١٠٠-site cell.

REFERENCES

[١] Vincent C.A. and Scrosati B. , Modern Batteries (Edward Arnold Publishers, London, ١٩٩٧); see also the web site, <http://www.corrosion-doctors. org> for general information on Batteries , corrosion , and electrodeposition.

[٢] So R.M.C. and Sommer T.P.," On the Modeling of Homogeneous Turbulence in a Studly Stratified Flow " , Int.J.Heat Mass Transfer, ٣٩ , ٤٥٥(١٩٩٦) .

[٣] Stephen k. ," Chemical Reaction at an Electrode , Galvanic and Electrolytic Cells ", Simon Fraser University Press , PP(٣-٤٠) , ٢٠٠٤.

[٤] http://hyperphsics.phy-astr.gsu.edu/hbase/chemical/echemcon.html#c/ .

[٥] Bockris J.O'M. , Bonciocat N. and Gutmann F. , " An Introduction to Electrochemical Science",Plenum Press,New York,Vol.٢,PP(٣٤-٧٣),١٩٧٤.

[٦] Selim R. and Bro P. , " Influence of Initial Surface Condition of Lithium Metal Anodes on Surface Modification with HF ", J. Electrochem. Soc., ١٢١, ١٤٥٧ (١٩٧٤).

[٧] Bernard M.-O. , Plapp M. and Gouyet J.-F. , " A lattice Gas Model of Electrochemical Cells ", Physica A (to be published), ٢٠٠١.

[٨] Frank F. C., " The Kinetic Theory of Crystal Growth and Dissolution Processes ", Contemp. Phys., ٢٣, ٣(١٩٨٢).

[٩] Glicksmann M. E. , and March S. P.," in Handbook of Crystal Growth", Vol. ١,D. T. J. Hurle, editor (Amsterdam: Elsevier),١٩٩٣.

[١٠] Glicksmann M. E. and Huang S.-C. , " Interfacial Wave Theory of Solidification : Dendritic Pattern Formation and Selection of Growth Velocity", Acta Metall., ٢٩, ٧٠١(١٩٨١).

[١١] Schmickler W . , " Interfacial Electrochemistry ", Oxford University Press, PP(٥٨-٦٣),١٩٩٦.

References

[١٢] Rothman D. H. and Zaleski S. , " Computer Simulations of Domain Growth and Phase Separation in Two - Dimensional Binary Immiscible Fluids Using Dissipative Particle Dynamics ", Rev. Mod . Phys. , ٦٦ , ١٤١٧(١٩٩٤).

[١٣] Chazalviel J.-N. ," Coulomb Screening by Mobile Charges ", Phys. Rev. A ٤٢, ٧٣٥٥ (١٩٩٠).

[١٤] Barton J.L. and Bockris J.O'M. , " Structural Changes Dendrite Deposits During Galvanostatic Electroylysis:A calculation " , Proc.R.Soc.London, Ser.A.٢٦٨,٤٨٥(١٩٦٢).

[١٥] Diggle J . W. , Despic A.R . and Bokris J.O'M. ,"Experimental Evidence for Homoclinic Chaos in an Electrochemical Growth Process ", J. Electrochem . Sec. , ١١٦ , ٥٠٣(١٩٦٩).

[١٦] Mullins W.W. and Sekerka R.F.," Morphological Stability of a Particle Growing by Diffusion or Heat Flow", J.Appl.Phys.,٣٤,٣٢٣(١٩٦٣).

[١٧] Aogaki R. and Makino T. ," Early Stages of Ramified Growth in Quasi-Two-Dimensional Electrochemical Deposition ", Electrochim. Acta , ٢٦ , ١٥٠٩ (١٩٨١) .

[١٨]Chen C.and Jorne J.,"Morphological Instability During Electrodepoition", J.Electrochem.Soc.,١٣٧,٢٠٤٧(١٩٩٠).

[١٩] Harris R. , Jorgenson L. and Grant M. , " A Guide to Monte Carlo Sinulations in Statistical Physics " , Phys.Rev.A,٤٥,١٠٢٤(١٩٩٢).

[٢٠] Dobretsov V.Y.,Vaks V.G. and Martin G. , " Coupled Relaxation of Concentration and Order Fields in the Linear Regime ", phys.Rev.B , ٥٤, ٣٢٢٧(١٩٩٦).

[٢١] Chen L.Q. , " Phase - Field Models for Microstructure Evolution " , Acta Metall.Mater.,٤٧,٣٥٠٣(١٩٩٤).

[٢٢] Losert W., Shi B.Q., Cummins H.Z. and Warren J.A. , " Spatial Period

Doubling of Dendritic Arrays in Directional Solidification ", Phys. Rev. Lett . ٧٧ , ٨٨٩ (١٩٩٦).

References

[٢٣] Warren J.A. and Langer J.S. , " Prediction of Dendritic Spacings in a Directional Solidification Experiment ", Phys. Rev. E ٤٧, ٢٧٠٢(١٩٩٣).

[٢٤] Jean – Franqois Gouyet and Mathis Plapp , " Interface Dynamics in Mean Field Lattice Gas Model ", Northeastern University Press , ١٩٩٦.

[٢٥] Bernard M.-O., Garnier J., and Gouyet J.-F. , " Laplacian growth of parallel needles : A Fokker - Planck equation approach ", Phys. Rev. E , Vol.٦٤,٠٤١٤٠١(٢٠٠١).

[٢٦] Charles Monroe , and John Newman , " The Effect of Interfacial Deformation on Electrodeposition Kinetics " , J. Electrochem. Soc. , A٨٨٠-A٨٨٦,٢٠٠٤.

[٢٧] Suzuki M. and Kubo R.,"Statistical Mechanics of Finite Ising Model ", J. Phys.Sos.Japan,٢٤,٥١(١٩٦٨).

[٢٨] Binder K. , " On the Dynamics of a Layered Heisenberg Magnet Near the

Phase Transition ",Z.Physik,٢٦٧,٣١٣(١٩٧٤).

[٢٩] Binder K. and Frisch H.L. ,"Cluster – Flips in random Ising Models", Z.Phys. B,٨٤,٤٠٣(١٩٩١).

[٣٠] Mathis Plapp and Jean – Franqois Gouyet ," Spinodal Decomposition of an ABv model alloy : Patterns at Unstable Surfaces " , Eur. Phys. J. B٩ , ٢٦٧(١٩٩٩).

[٣١] Bernard M.-O. , Plapp M. and Gouyet J.-F. ," A lattice Gas Model of Electrochemical Cells : Mean-Field Kinetic Approach ", Fractal , ٢٠٠٢ .

[٣٢] Marc-Olivier Bernard, Mathis Plapp and Jean-Franqois Gouyet,"mean-Field Kinetic lattice Gas Model of Electrochemical Cells " , Phys.Rev.E٦٨,٠١١٦٠٤(٢٠٠٣).

[٣٣] Gouyet J.-F., Plapp M., Dieterich W. and Maass P. ," Description of Far-

From – Equilibrium Processes by Mean- Field Lattice Gas Models " , Adv.Phys.,Vol.٥٢,No.٦,PP(٥٢٣-٦٣٨),٢٠٠٣.

[٣٤] Spalart P.R.," Direct Numerical Study of Leading Edge Ontamination In Fluid Dynamics of Three – Dimensional Turbulent Shear Flows and Transition",Agard-Cp-٤٣٨,PP(٥.١-٥.١٣),١٩٨٨.

References

[٣٥] Spalart P.R. and Watmuf J.H. f. , " Shear – Free Turbulent Boundary Layers : Physics and Modeling ",J.Fluid Mech., ٢٤٩ ,٣٣٧(١٩٩٣) .

[٣٦] Franqois Gurniki , " Turbulent Convective Mass Transfer In Electrochemical Systems " , S-١٠٠ ٤٤ Stockholm , Sweden , ٢٠٠٠.

[٣٧] Allen J.B. and Larry R.F. ," Electrochemical Methods Fundamentals and Applications ", Second Edition , New York , ٢٠٠١.

[٣٨] Martin G. , " Kinetics of Surface Segregation and Phase Separation in

Nanostructures", Phys. Rev. B, ٤١, ٢٢٧٩ (١٩٩٠).

[٣٩] Gouyet J.-F. , " Probability Density of the ٢D Percolation Cluster

Perimeter " , Europhys. Lett., ٢١ , ٣٣٥ (١٩٩٣).

[٤٠] Plapp M. and Gouyet J.-F. ,"Surface Modes and Ordered Patterns during Spinodal Decomposition of an ABv Model Alloy " , Phys. Rev. E, ٥٥, ٤٥(١٩٩٧).

[٤١] Bockris J.O'M. ,"Modern Electrochemistry ",Vol.١, PP(١٧٥-٢٤٧),١٩٧٧.

[٤٢] Schmickler W. and Henderson D. , " New Models for the Electrochemical Interface , Progress in Surface Science ", Vol. ٢٢, No. ٤,

PP(٣٢٣-٤٢٠),١٩٩٥.

[٤٣] Fleury V. , Rosso M. , Chazalviel J.-N. and Sapoval B. ," Experimental Aspects of Electrochemical Deposition of Copper Aggregates " , Phys. Rev. A ,٤٤, ٦٦٩٣ (١٩٩١).